LAPPEENRANTA UNIVERSITY OF TECHNOLOGY

LUT School of Energy Systems

Master's Degree Programme in Electrical Engineering

Aleksei Mashlakov

SIMULATION ON DISPERSED VOLTAGE CONTROL IN DISTRIBUTION NETWORK

Examiners: Professor Jarmo Partanen

Researcher (M.Sc.) Tero Kaipia

Supervisors: Researcher (M.Sc.) Tero Kaipia

Researcher (M.Sc.) Ville Tikka

ABSTRACT

Lappeenranta University of Technology

LUT School of Energy Systems

Master's Degree Programme in Electrical Engineering

Aleksei Mashlakov

Simulation on dispersed voltage control in distribution network

Master's Thesis

2017

102 pages, 74 figures, 2 tables, 1 appendix

Examiners: Professor Jarmo Partanen

Researcher (M.Sc.) Tero Kaipia

Keywords: dispersed voltage control, renewable distributed generation, voltage fluctuation and rise, demand response, reactive power control, automatic voltage control

Renewable distributed generation (RDG) has become more accessible, affordable, and widespread than it was just a few years ago, leading to increasing number of connections to distribution networks. One of the technical challenges of such tendency is to maintain an acceptable voltage level that becomes inconsistent because of the inherent variability in the power output of RDG units. Therefore, it necessitates the development and implementation of effective voltage control strategies to reliably supply energy to the equipment of end users. To solve this problem, a modified automatic voltage control (AVC) algorithm that can operate utilizing a model of a controlling network and/or real-time measurements was proposed to keep the voltage within the acceptable limits. Also, the effectiveness of demand response (DR) algorithm for stand-alone voltage control was investigated to evaluate its perspectives. The cooperation of the modified real-time AVC algorithm with both reactive power control (RPC) of photovoltaic (PV) systems and DR was investigated to decrease the number of on-load tap changer's (OLTC's) operations. The effectiveness of the developed dispersed voltage control algorithms was tested in different simulation conditions on a verified model of a power grid that has been created in MATLAB®. The results of the research have proven the reliability of both versions of the modified AVC algorithm in distribution networks with RDG. Furthermore, the results also allowed evaluating the amount of controllable load for stand-alone voltage control based on DR algorithm. The cooperation of AVC algorithm with DR algorithm reduced the use of OLTC, while the combined actions with RPC of PV systems were less effective and resulted in the same number of OLTC's operations in comparison to the stand-alone performance of AVC algorithm in the same conditions.

ACKNOWLEDGEMENTS

This master's thesis was done at the Lappeenranta University of Technology (LUT), Department of Electrical Engineering between February and May 2017.

I would like to thank my supervisor, researcher Tero Kaipia, for his patient guidance, insightful and friendly replies to many questions that I struggled with during this thesis. It was a wonderful chance to investigate the proposed topic that has provoked in me an infinite interest in the coordination of distributed resources for the effective operation of a power grid.

I would also like to thank researchers Ville Tikka, Juha Haakana and LUT Helpdesk service that assisted me in technical questions during the implementation of this thesis and contributed to its accomplishment.

My gratitude is also sent to the LUT for the opportunity to study there within the framework of Double Degree Program. It was a beautiful possibility to gain so much experience getting to know Finnish people, education, customs and make friends with people all around the world. I thank all my fellow students in Lappeenranta for the amazing time that we had there.

Last but not the least, I would like to express my gratitude to my family, which always believed in me, supported, and contributed all their power and time to make me who I am now.

Mashlakov Aleksei

August 2017

TABLE OF CONTENT

LIST OF SYMBOLS AND ABBREVIATIONS

Roman symbols

C – capacitance;

C_{grid} – grid-side converter;

C_{rotor} – rotor-side converter;

$E[P(t)]$ – expectation value of the load;

F – wire cross-section;

I – current;

L – inductance;

M – motor torque;

np – exponent 1 controlling the type of the load;

nq – exponent 2 controlling the type of the load;

P – active power;

P_G – active power from generator;

P_{GMAX} – maximum active power from generator;

P_L – active power to load;

$P_{LOAD\_PROFILE}$ – initial active power at the initial voltage;

Q – reactive power;

$Q(t)$ – seasonal variation with 26 two week indices;

$q(t)$ – hourly variation for working day, Saturday and Sunday;

Q_G – reactive power from generator;

Q_{GMAX} – maximum reactive power from generator;

Q_L – reactive power to load;

$Q_{LOAD\_PROFILE}$ – initial reactive power at the initial voltage;

Q_n – breaker;

R – wire active resistance;

$s_p(t)$ – standard deviation of the load;

$s_{\%}(t)$ – percentage of the average load;

U_1 – voltage at the beginning of the feeder;

U_2 – voltage at the end of the feeder;

V – positive sequence voltage;

V_0 – initial positive sequence voltage;

V_{gc} – voltage command signals to grid side;
V_{lower} – network voltage lower limit;
V_{max} – maximum network voltage;
V_{mean} – mean network voltage;
V_{min} – minimum network voltage;
V_n – nominal voltage;
V_r – pitch angle command signals to rotor side;
V_{ref} – reference voltage of AVC relay;
$V_{reflower}$ – lower limit of the reference voltage of AVC relay;
V_{refnew} – new reference voltage of AVC relay;
$V_{refupper}$ – upper limit of the reference voltage of AVC relay;
V_{upper} – network voltage upper limit;
W_a – annual energy consumption of a customer;
X – wire reactance;

Greek symbols

ΔU – direct-axis voltage variation component;
ΔU – complex voltage variation along the feeder;
δU – quadrature-axis voltage variation component;
μ – mean value of normal distribution;
σ – standard deviation;

Abbreviations

AC – alternating current;
AMI – automatic metering infrastructure;
AMR – automatic meter reading;
AVC – automatic voltage control;
CC – central coordinator;
CIS – customer information system;
DB – dead-band;
DC – direct current;

DER – distributed energy resources;
DFIG – doubly fed induction generator;
DG – distributed generation;
DMS – distribution management system;
DNO – distribution network operator;
DR – demand response;
EES – electrical energy storages;
EV – electric vehicle;
GC – generation curtailment;
HV – high voltage;
IED – intelligent electronic device;
IGBT – insulated gate bipolar transistor;
LCOE – levelized cost of electricity;
LV – low voltage;
MAS – multi-agent system;
MV – medium voltage;
NIS – network information system;
OLTC – on-load tap changer;
OPC – object linking and embedding for process control;
PCC – point of common coupling;
PF – power factor;
PV – photovoltaic;
RDG – renewable distributed generation;
RES – renewable energy sources;
RMS – root mean square;
RPC – reactive power control;
SCADA – supervisory control and data acquisition;
SE – state estimation;
STATCOM – static synchronous compensator;
SVC – static VAR compensator;
TDD – total demand distortion;
VVC – volt/VAR control;
WT – wind turbine.

1 INTRODUCTION

The world energy sector is on the stage of the global transformation. Nowadays in many countries around the globe together with the development of centralized power supply, a tendency of extensive transition to distributed power supply is being actively supported [1].

Among various technologies of distributed generation (DG), renewable energy sources (RES) are showing the most rapid growth of the development, and they are one of the main factors for a modern power industry. The economic attractiveness of RES is increasing every year – according to the annual study of Lazard (2016) [2], over the last seven years the index of levelized cost of electricity (LCOE), presented in Figure 1.1, has decreased by 66% for the wind energy and by 85% for the solar energy.

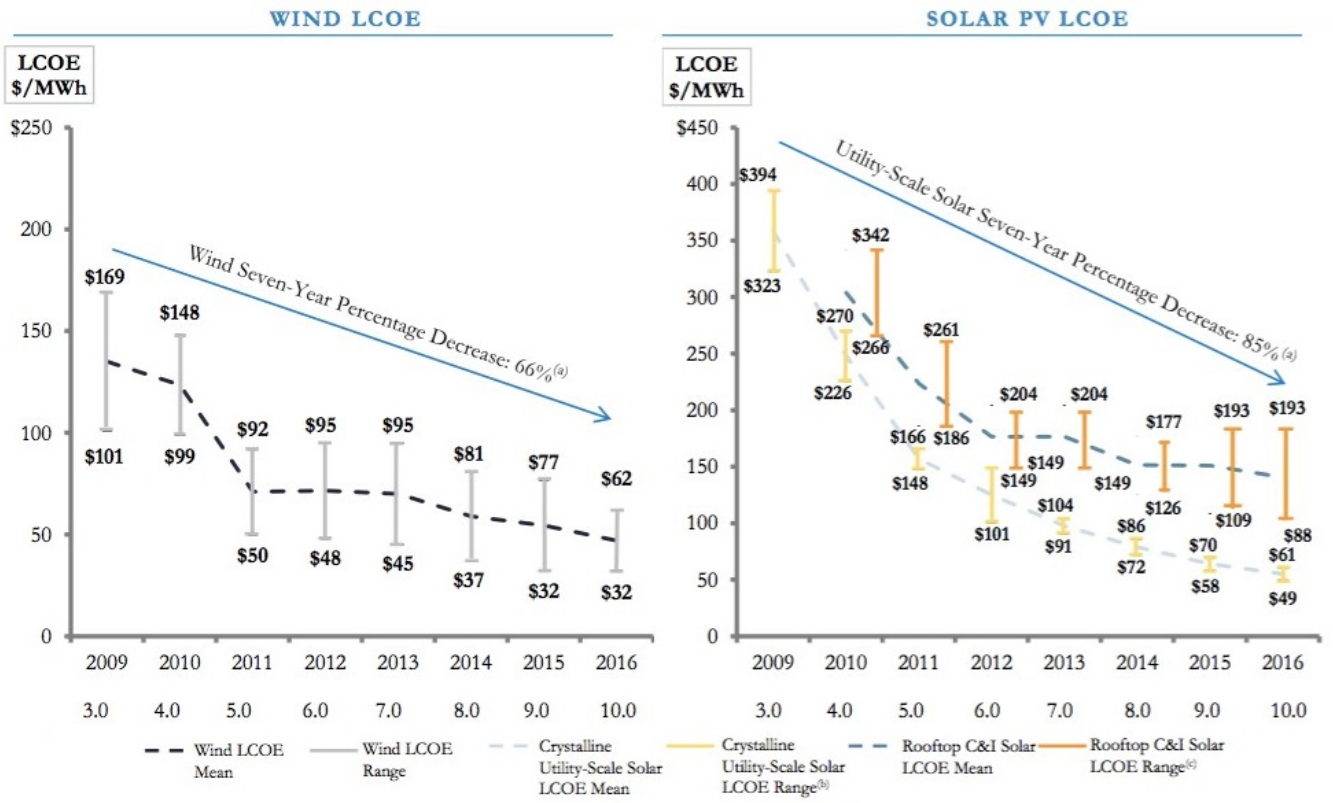

Figure 1.1. Unsubsidized LCOE - Wind/Solar (Historical) [2].

At the moment, the expenditures for the alternative energy generation are close to the traditional power generation and sometimes even lower. According to Figure 1.1, the cost of energy production for the most effective wind generators was about 32 $/MWh in 2016. In compliance to [2], the same indexes for the electricity obtained from conventional power generation varied from 48 to 281 $/MWh. The perspective of further RES' LCOE decreasing

will impact on the use of traditional energy sources. According to the Bloomberg New Energy Finance agency, a share of capacity addition of renewable distributed generation (RDG) has been exceeding the same share of traditional fossil-fuel power generation since 2013 [3]. The forecast data of power generation capacity addition illustrated in Figure 1.2 testifies that the priority of RDG's putting into operation in the world will grow in comparison with decreasing employment of traditional fossil fuel based power generation.

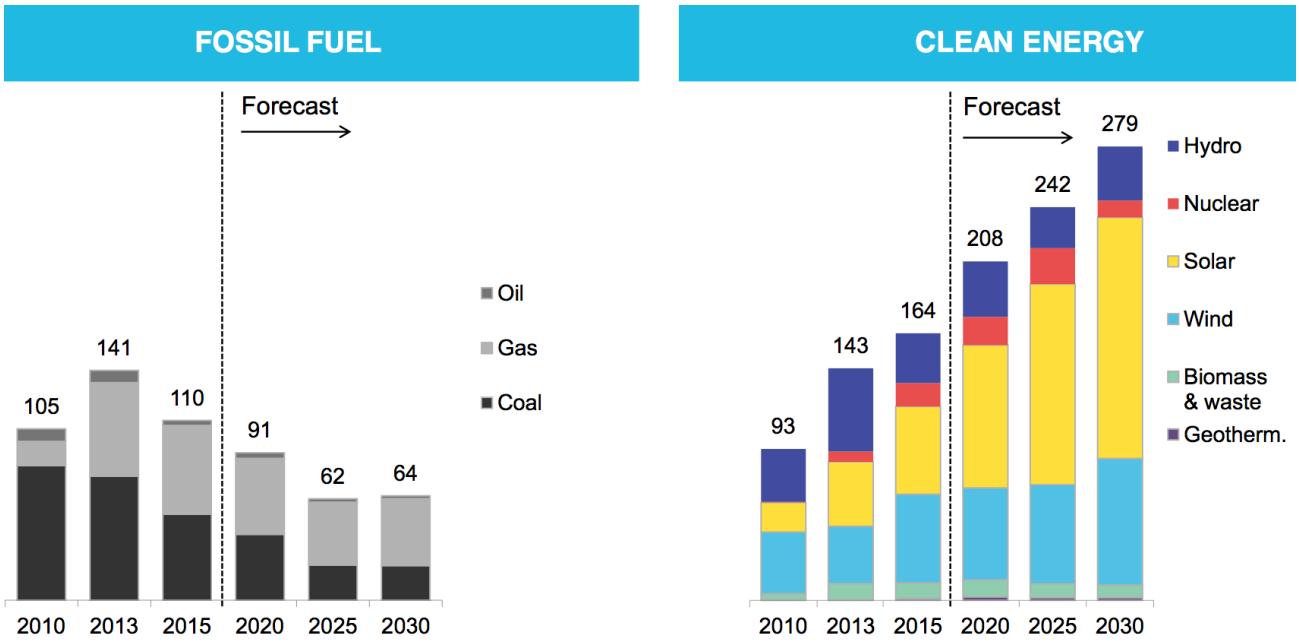

Figure 1.2. Power generation capacity addition (GW) [3].

The key factors of further DG's expansion are growing demand for the energy supply in the world, grid congestion, the necessity in power supply of remote areas, reduction on the construction of new power assets, and degradation of the power grid. While some of the benefits of RDG's integration, in addition to the economic attractiveness, include the reduction of pollution caused by fossil based energy generation, more competitiveness in electricity markets, highly reliable electricity supply, and curtailment of the mineral resources' usage [4]. Thus, the transition from the centralized grid to the integrity of centralized and distributed systems seems foreground scenario for the power industry.

1.1 Motivation and problem-setting

Despite the benefits of renewable distributed energy generation, the enlargement in its volume results in serious changes in the characteristics of the power grid. This is especially noticeable

for the level of low voltage (LV) and medium voltage (MV) networks, where the unidirectional nature of the power flows is altered, leading to arise of earlier unprecedented disturbances and challenges related to faults [5]. The growing penetration of RDG in distribution networks forces the distribution networks operators (DNOs) to employ new means to control the operation of the network, but also new opportunities to do so arise. This process is associated with the necessity to solve a broad range of scientific research problems; such issues are, for instance, voltage rise and voltage fluctuations that appear because of significant active, but often also intermittent power injections by RDG. If the mitigation of the effects is done with traditional operational principals, it limits the capacity to connect RDG into the network. However, the presence of distributed energy resources (DERs) in the network such as RDG units, controllable loads, and electrical energy storages (EESs) gives additional opportunities that can be used to enhance the voltage quality. The implementation of DERs to be a part of the voltage control system that enables providing adequate quality of voltage supply to customers is among the most important and interesting challenges.

1.2 Barriers to the implementation

A large amount of dispersed voltage control algorithms were proposed in the past decade with different complexity, data transfer needs, and for different kinds of conditions in the network [6]. Most of the publications focus on the principals of the algorithm without concerning about the time domain characteristics of the algorithms during the employment into real networks. A number of practical applications is still very low, and new ones are reluctantly introduced into the network by DNOs. A simulation is one of the possibilities to examine the behavior of the network in the presence of RDG. However, there are obstacles for the recreation of the real network's operation as well as for the adoption of voltage control algorithms as follows:

- Models of the networks seldom take into account a latency of the communications between the devices that can happen in real networks because of many reasons [7]. A duration of the latency is varying with time and depends on several factors. Even though these can be created artificially, an element of inaccuracy comparing with the communications in real networks will still remain.
- A simulation speed directly depends on the particularization of the model. The more factors and elements are considered in the model, the more time consuming the

simulation becomes. This sets constraints for the penetration of real hardware in the model and increases the actual time of the simulation. The existing models are usually simplified because of a limited number of components in the network. It allows them to use a very large simulation time periods. However, the results of such simulations are not trustworthy and not always could be applied to real cases because of the model's simplicity that is not correlated with real-life conditions. That is why it is important to find a compromise between the accuracy and time domain.

- A behavior of the real load is unpredictable, and the electricity load curves fluctuate much at an individual household level. The available data include average hourly demand. Load profiles with certain standard deviations have been defined in past based on hourly measurements, but these are not enough to evaluate the behavior of the loads on the level applicable in the now considered voltage quality studies. However, they allow approximating the mean consumption curve.
- Dispersed voltage control is still in developing phase. The entanglements are based on a variety of issues. One of them is the absence of such markets that would enable the DNOs to purchase and then use the customer owned resources in network management. This restricts the capabilities of these DG units to be involved in the centralized control of the power grid. The requirements of real-time information about the state of whole distribution network remain to be a stumbling block. Real-time measurement data are usually only obtained from the primary substations. More accurate state estimation (SE) could be made available by using an automatic meter reading (AMR) system, but at the moment these systems are not capable of real-time data collection. However, the hour-level AMR measurements enable improving the accuracy of network analysis by adding additional data measurements to the SE algorithm or by reviewing the load curves [8].
- Network planning tools need to be evolved since DG units are often described as negative loads in distribution network planning, not as true generating units. Only assumed worst-case scenarios are applied to estimate the capabilities of the network. This is not enough to evaluate network state and different control strategies.

To create the environment for real research of DG's effect in the network that could give an explicit evaluation of dispersed voltage control methods, all of these barriers have to be overcome, and optimal solutions are needed to be found.

1.3 Objectives and delimitations

The main objective of the work is to find a solution to the voltage rise and fluctuation problem in distribution networks with RDG and to develop a simulation model that enables studies of voltage control algorithms based on the exploitation of DERs and conventional voltage control means. The following tasks are set and solved to achieve this purpose:

1. To discuss an impact of DG on a power distribution network;
2. To review the voltage control problems and methods in distribution networks with DG;
3. To create a simulation model of a power grid with the penetration of RDG;
4. To develop dispersed voltage control algorithms that can be applied to the simulation model and to real networks;
5. To verify an efficiency of created algorithms in different conditions of the stochastic power output of RDG units.

The scope of the voltage studies is restricted by long-term dynamics due to smooth fluctuations in the power output of RDG. The simulation model and developed dispersed voltage control algorithms are not intended for the short-term stability studies, as well as fault studies.

1.4 Research methods and tools

In order to support the objectives, system analysis, theoretical electrical engineering and mathematical modeling methods were applied. Following licensed software was used to perform the work: Matrikon object linking and embedding for process control (OPC) Simulation Server, MATLAB® (Simulink®, SimScape™, OPC Toolbox™).

The object of the research is a part of a real power grid (110/20/0.4 kV) with the presence of wind turbines (WTs) connected into the MV network and customer-end LV network connected photovoltaic (PV) generating units. The subject of the research is a simulative investigation of dispersed voltage control algorithms.

1.5 Practical significance

The main achievements of the thesis can be formulated as follows:

1. The method of voltage control for distribution networks with RDG based on a modified automatic voltage control (AVC) algorithm with the employment of the network's model and/or dispersed real-time measurements.
2. The development and implementation of flexible simulation model on the basis of MATLAB® software to test the dispatching and managing of the networks with RDG.
3. The results of simulations and efficiency of dispersed voltage control algorithms based on demand response (DR) and reactive power control (RPC) of PV systems.

1.6 Outline of the thesis

Chapter 2 is dedicated to the analysis of DG's influence on the state of a distribution network.

Chapter 3 contains a description of voltage control in conventional distribution networks and networks with DG.

Chapter 4 examines different types of voltage control methods in the networks with DG.

Chapter 5 contains the description and operating principle of the developed dispersed voltage control algorithms.

Chapter 6 provides main characteristics of the power grid's simulation model with the presence of RDG. The technical data and way of implementation of the components are given.

Chapter 7 is dedicated to the simulations on developed dispersed voltage control algorithms in different conditions applied to the network to validate their operation and effectiveness.

Chapter 8 includes a summary of the work and conclusions on the obtained results. The aims of the further research are chosen.

2 POWER GRID WITH DISTRIBUTED GENERATION

This chapter starts by introducing a term DG, its technologies and types of interfacing with the grid. It then presents the possible ways and advantages of DG's integration in the existing power grid. Finally, it explains the influence of DG on a state of a distribution network.

2.1 Definition of distributed generation

There are different approaches defining DG based on the voltage level, generating capacity, location, and dispatchability [9]. In general terms, DG is the generation units with the power range from kW to MW that are connected to the grid on the level of distribution network with a short distance from an electrical user [10]. Distributed generation can be categorized as renewable and non-renewable.

Non-renewable technologies of DG consist of internal combustion engines, steam turbines, small gas turbines, small co-generation units and micro-turbines. Renewable technologies of DG include WTs, PVs, fuel cells, small hydro-power plants, biomass, and geothermal generating plants. [9]

The connection of DG to the network can be implemented with the use of an induction or a synchronous generator and by means of power electronics converters. Renewable energy sources such as PVs, fuel cells, and biomass apply power electronics to convert their output direct current (DC) power for interfacing with alternating current (AC) grid. The synchronous generator is employed by micro-turbines and small hydro-power plants. The induction generator is mostly used with WTs and some low-head hydro applications. Both generators cannot be directly connected to the grid due to power quality issues. Hence, they also apply power electronic converters for interfacing with the grid. [11]

Distributed generation units can operate synchronously with the traditional centralized electrical grid and independently in islanding mode, creating entire areas with different types of distributed sources – Microgrid. However, islanding operation is not possible for the induction generator among other interfacing technologies. [11,12]

2.2 Possible ways of integration to the power grid

Possible scenarios of DG's integration are depicted in Figure 2.1. The distributed generation units can supply energy to the centralized grid as well as to the particular customers (for instance, manufacturing plants) to create local islander power systems.

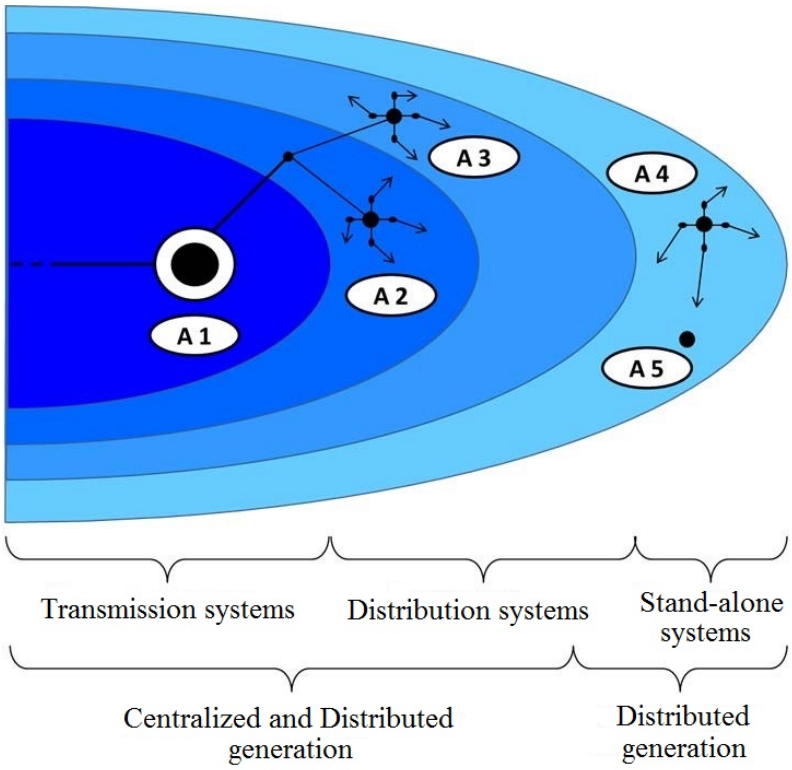

Figure 2.1. Possible scenarios of DG's integration to the power grid [13].

As it can be seen in Figure 2.1, the area of a centralized power supply is divided into two zones. The first zone consists of large power sources A1, working in transmission networks, and the second zone – from distributed sources A2, operating in distribution networks. Also, in the area of distribution networks, the sources of separate users A3 are running. They are different from A2 by the output power range, cost of generated power, and profile of its consumption. A4 represents the sources for separate and combined decentralized energy production in isolated networks. A5 is dedicated to the stand-alone energy production. Thus, there are three types of the user's power supply based on DG [13]:

1) Stand-alone energy supply, where small DG units are utilized independently (A4, A5) in isolated systems;

2) Peak and reserve energy supply on the basis of DG (A2) in the area of centralized systems;
3) Distributed energy generation in the area of centralized systems where DG units are used as the main source and their operation is coordinated with the centralized system.

The distributed generation units in the last two cases have some positive properties what allows considering them as one of the main elements of the future power systems. The following properties are specified [14]:

1) Increasing the customer's energy independence;
2) Decreasing the level of necessary power reservation;
3) Minimizing the energy sources' transport;
4) Cutting the transportation losses of secondary energy sources;
5) Enhancing the reliability of electric network;
6) Reducing the investments to the power grid.

2.3 Influence of distributed generation on state of distribution network

The generalized structure of the power grid with large centralized and small decentralized plants is displayed in Figure 2.2. The purpose of backbone (400 kV and above) and supplying networks (110 – 400 kV) is to unite energy systems and large power plants for parallel operation as integrated object and to perform functions of electric energy transmission to the supply centers of distribution networks. Because of the introduced functions, such networks usually have meshed grid configuration. Distribution networks (10 – 35 kV) are designed to transmit power from the supply centers to customers. These networks usually have a radial configuration with one side power supply. [15]

The integration of DG brings elements in the centralized system with new dynamic characteristics and control capabilities. The distributed generation leads to a complication of power-system protection as well as dispatching with an extended area of responsibility in the face of a distribution network. The distribution network acquires the traits of the transmission network with corresponding problems of power system's stability and demands the development of the relevant automation. The main changes in the state of the distribution system are represented below. [5]

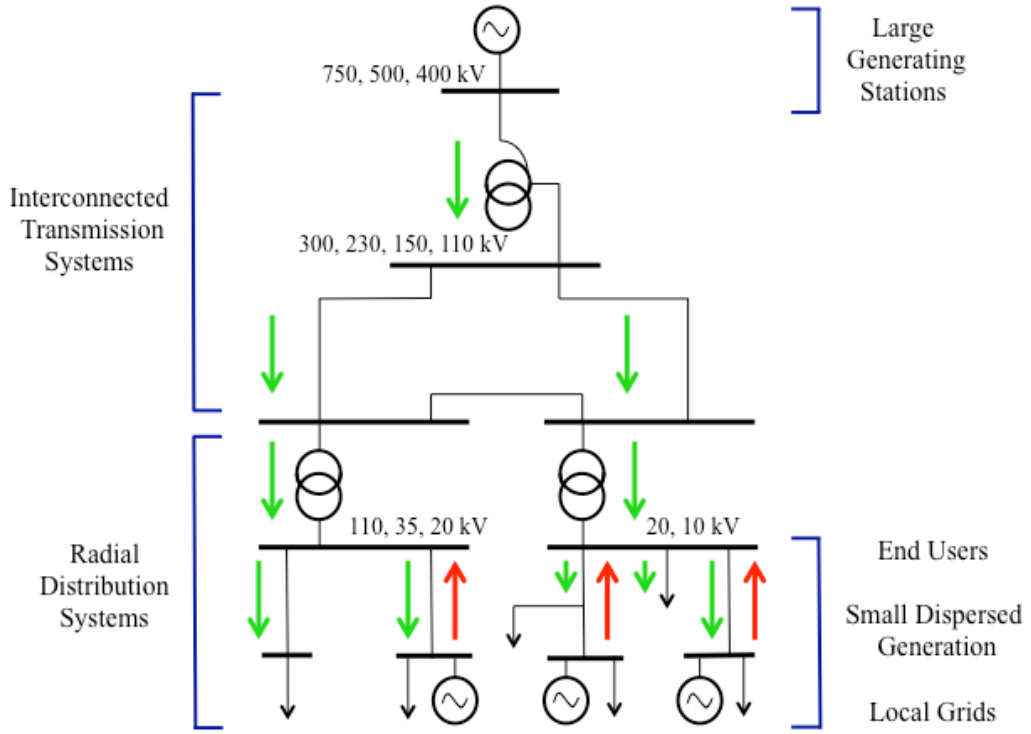

Figure 2.2. Generalized structure of power grid with distributed generation: green lines represent the power flow direction before the connection of DG; the red lines – after the appearance of DG in the network [15].

2.3.1 Steady - state response

1. The structure of traditional power grids assumes the unidirectional power flow from large generating power plants to customers. However, the appearance of DG makes possible the reversed power flows (highlighted by red lines in Figure 2.2) from distribution to transmission networks. This turns the "passive" distribution network into an "active" one where customers do not only consume electricity but also generate it. The stochastic direction and the level of power flows are mainly impacted by variable mode of RDG's performance.
2. The influence of RDG on voltage quality leads to the variation of the network's voltage level. It also can bring more frequent and large voltage fluctuations and change harmonic distortion [16]. However, RDG also allows more multifaceted approach for the voltage control in the nodes in comparison with traditional distribution networks without RDG. This is provided by the ability of RDG units to generate and absorb reactive power. [17]

2.3.2 Transient performance

1. Fault currents in the networks with DG can be supplied from multiple directions. what alters traditional current flows and fault levels. A small electrical distance of DG to network elements encourages a significant change of root mean square (RMS) values of short-circuit currents during the fault situation. The sinusoidal factor of short-circuit current is rapidly damping when short-circuit happens close to the point of DG unit's connection. [18]
2. Power system swinging and the asynchronous operation become possible in distribution networks. Even relatively short duration of fault can be enough to violate the synchronous dynamic stability because of small values of DG units' inertia constant. [5]
3. The tripping of a transmission line or other network elements connecting the DG with the external power grid can lead to unintentional island operation. In many cases, the generating power of DG is not enough to supply the local load. This situation results in the deficit of power and a significant decrease in frequency or/and voltage. It is possible to elude the violence of network's parameters by balancing the generating and consuming power.
4. However, the isolated operation of the DG demands the presence of necessary solutions allowing to mitigate the negative phenomena of islanding operation [5]:

   - asynchronous switching on by the means of automatic reclosing from the external power grid;
   - failing of automatic reclosing because of supplying current from DG unit not disconnected from the network during the autoreclosure open time;
   - significant decreasing of protection sensitivity to the faults in islanded part because of lowering the current values;
   - variation of the power grid's parameters out of the tolerance range and abnormal operation of the customer's equipment as its consequence;
   - possible tripping of the DG units whose protection is inappropriate to operate in the islanded mode.

2.4 Conclusions about chapter 2

The definition of DG was given and possible scenarios of its integration in different areas of the power grid were presented. It is noted that such advantages for the existing energy systems as increased reliability of power supply, reduced energy transport and minimized losses are only gained when the DG participates in the integrated control of the network as a supportive and main source of power.

New conditions of the power grid with DG were presented for steady-state response and transient performance. The role of distribution networks is increased: it begins to perform previously non-traditional for them functions of energy generation and power flow control. The main changes appeared in distribution networks can be described as violation of the traditional mechanism «generation-transmission-distribution-consumption»; the generation of energy becomes possible in close vicinity to the end users; the elements of the grid are beginning to work in the conditions of multidirectional supply; the levels and distribution of short-circuit currents are transforming; the probability of power system's swinging and asynchronous operation appeared.

3 VOLTAGE CONTROL

Voltage regulation is one of the main objectives of the DNOs since keeping the steady-state voltage within a tolerance range is essential in order to guarantee the performance and working efficiency of network components and supplying equipment [19].

The motivations of this chapter are to show the effects of voltage fluctuations on the equipment of end-users, demonstrate the influence of DG on voltage quality in distribution networks, compare voltage profiles in traditional networks and networks with DG, present voltage control methods based on the obtained characteristics of voltage profiles.

3.1 Importance of voltage quality

A real voltage waveform is not always sinusoidal because of the influence of many factors. It can be affected by the commutations of power equipment or by actions of grid automation as well as by the clearings of short-circuits or lightning overvoltages. The load itself can lead to voltage waveform distortion when it is a source of nonlinearity, unsinusoidality or intermittence of active and reactive power consumption. [20] All these factors result in the undervoltages, overvoltages, transient spikes and other voltage deformations shown in Figure 3.1.

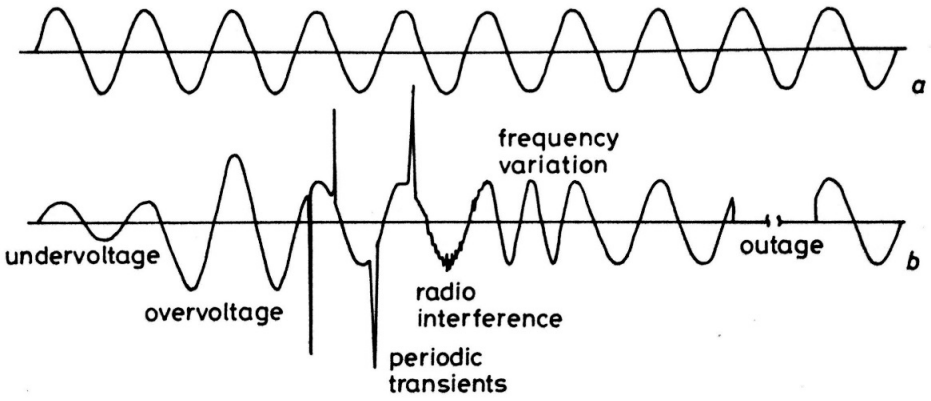

Figure 3.1. Ideal voltage waveform and voltage variations [21].

Voltage variation has a significant impact on the operation of load appliances. As an example, the characteristics of its influence on induction motor's operation are explained in Figure 3.2 a). Since motor torque is proportional to the square of voltage, the voltage fluctuation will

change the rotating torque-slip dependence. In this case, the large drop in voltage at the terminals of an induction motor, operating at full capacity, can lead to “breakdown” that is a full stall of the induction motor when the resisting torque exceeds the rotating torque. A light bulb is also sensitive to voltage variations. According to Figure 3.2 b), descending of voltage will be noticed when the light flux tarnishes, contrary the increasing of voltage will not only intensify the light flux, but it will also reduce the service life and lead to excess energy demand. [20]

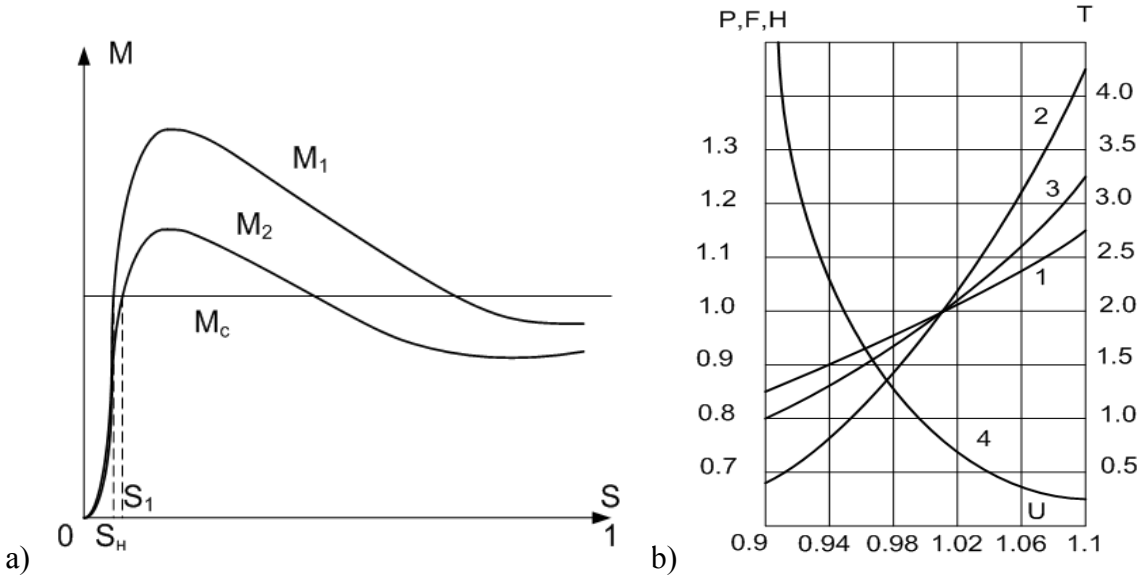

Figure 3.2. Effects of voltage variation: a) Speed-torque curve at nominal (M1) and lower voltage (M2); b) Dependence of a light bulb characteristics of voltage. 1- consuming power, 2- light flux, 3 - luminous efficiency, 4 - service life [20].

Voltage variation also adversely affects the quality of operation and service life of household electrical appliances. These include malfunction and breakdown of electronic loads. The most vulnerable loads are high-tech appliances such as personal computers, microwave ovens, TV sets, whose electronics is sensitive to voltage fluctuations [22]. A spike in voltage can result in an arc of electrical current within the appliance. The arc generates an excessive heat and causes damage to the electronic circuit boards and other electrical components. A harmful influence is also possible if smaller voltage surges repeat regularly, eroding the integrity of the electronic components and decreasing service life of appliances and electronics [23]. Also, the operational efficiency of the heating equipment is deteriorating due to considerable levels of voltage fluctuation [24]. That is why maintenance of supply voltage is so important to prevent harmful impact on the equipment.

The recommendations and standards exist in different countries that impose limitations on voltage quality to guarantee the normal operation of all network elements. Although, there is a large diversity of established voltage quality characteristics worldwide, most of them highlight magnitude, frequency, waveform, and the symmetry of the three-phase voltages. The European standard EN 50160 states that the range of variation of the 10 minutes RMS value of the supply voltage should be within ± 10 % for 95 % of the week [25].

3.2 Effects of distributed generation on voltage quality

It is known that DG can cause several potential issues to the quality of voltage in the network. The most common are introduced in the following subsections [26]:

3.2.1 Voltage rise

This situation happens in the weak networks when the generation exceeds the load. It predetermines the reversion of power flow that causes voltage rise along the feeder and may increase the voltage in LV networks beyond the tolerance range. Minimum load/maximum generation conditions are usually essential for the limits of the connected amount of DG units because in these conditions maximum voltage rise is obtained [27] as elucidated in Figure 3.3.

Often, the loads are low in sparsely populated areas. Moreover, the length of the feeders in these areas can be very long, leading to the remarkable line impedance. If a large DG unit is installed in such locations that are far from a primary or secondary substation, voltage rise problems may occur during the minimum demand. When considering residential loads, whose profile for a single customer of a detached house is illustrated in Figure 3.4, the highest probability of voltage rise will be at the noon of working day, when the load is minimum and experiences a downfall after the morning rise. It is provoked by the fact that the people from rural areas are usually working in towns and by the absence of significant industry in the rural areas. The situation in large cities is different with the lowest load at the weekends because many offices and factories are operating only during business week's mornings and days. The networks in cities, however, are strong and it is unlikely that DG can lead to voltage rise in this environment. Consequently, rural areas with DG are the most dangerous case.

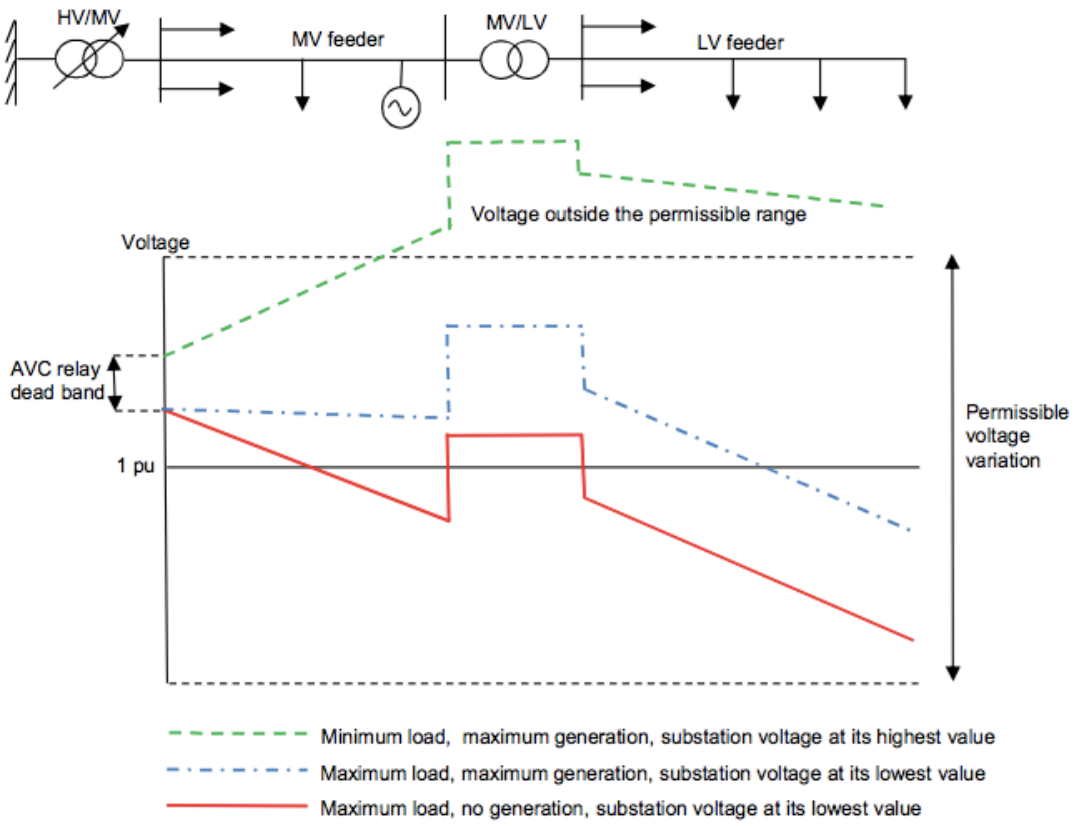

Figure 3.3. The effect of DG on the voltage profile of a radial feeder [28].

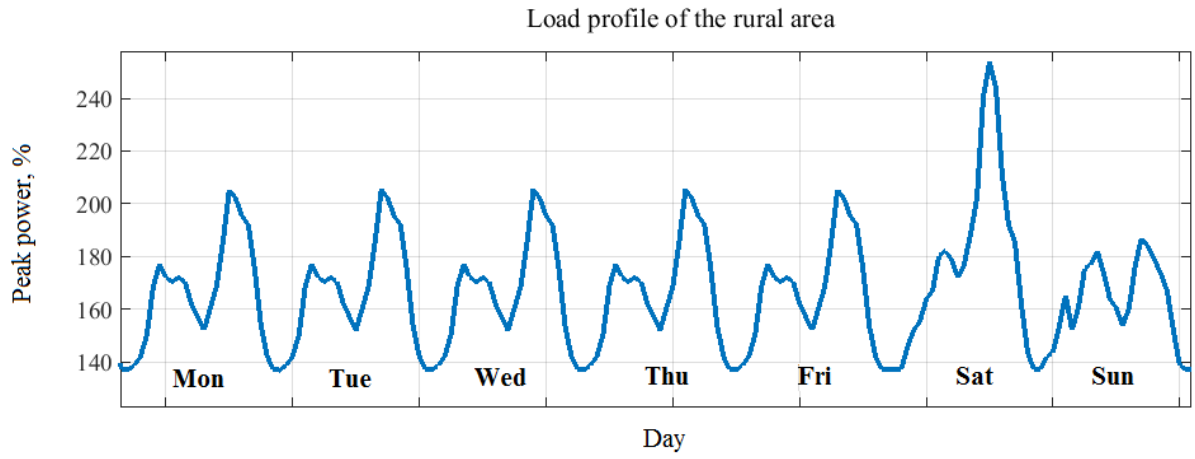

Figure 3.4. Example load curve of a rural area for a single customer [29].

The necessary factors for maximum generation are sunny and windy weather in case of PV systems and WTs, respectively. Therefore, it would be logical to consider the influence of PV generating units in southern regions where the activity of the sun is high, just as sea-coast or plain with good wind rose in the case of WTs. Thus, the ideal scenarios for voltage rise can be:

1) The sunny cloudless day in a rural area with the widespread installation of PV systems located in the southern region and connected to substation by a long feeder.
2) The windy day in sea-coast or plain rural area with the large WTs connected to the network.

These situations are already appearing in the existing networks. As displayed in Figure 3.5, sunny and windy weather in northern part of Germany led to excessive power generation, despite the fact that the load was at the average level. First, the extra power was generated by WTs in the morning and then with the influence of PV's power at noon. However, there is a good probability that the high load did not allow to violate 10 % range of voltage variation, but it is the prerequisite of future possibilities.

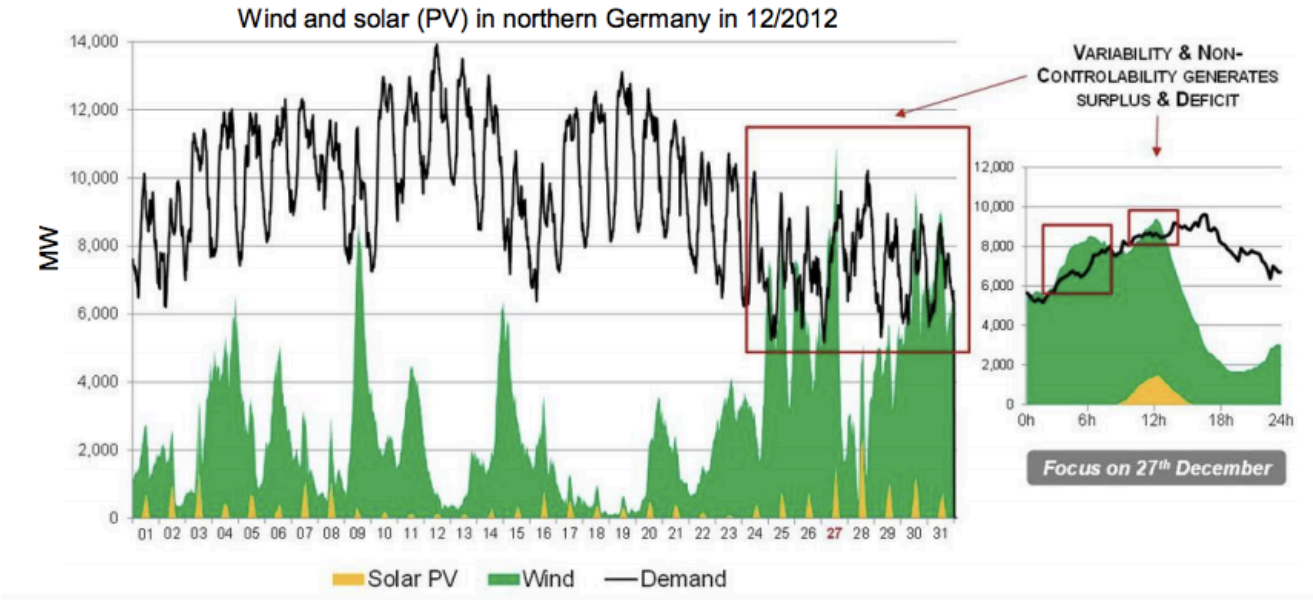

Figure 3.5. Excessive power generation in Germany [30].

3.2.2 Large and more frequent voltage variations

Voltage variation is created by load fluctuations in traditional networks. The presence of RDG units adds into the network additional voltage fluctuations because the power output of RDG is varying depending on the intermittency of weather conditions. There is a special term in power quality standards for such variations that depend on the source's type, network impedance and generator's characteristics called flicker. Voltage variations in steady-state are mostly caused by the change of prime source. Instability of solar radiation caused by rapid

changes of weather and passing clouds can lead to a variation of PV system's output power. Tower shadow, wind shear, and turbulence can cause flicker for WTs. [31] Fortunately, these changes are often smooth and do not cause to customers many problems as the voltage transients. They are provoked by the operation of connection or disconnection of generating units and can be the primary factor that limits the capacity of connected DG in addition to voltage rise. [28]

3.2.3 Harmonics

The presence of power converters in the interface of generating units implies the existence of harmonics in output current. To prevent the insertion of harmonics into the network and unacceptable network voltage distortion, the output current of the converter should be filtered [32]. This is often done by passive filters. Moreover, some synchronous machines can also generate harmonics into the network [33]. IEEE Standard 1547 defines the limits for the harmonic performance of DG units at the point of common coupling (PCC). The standard assumes that the output voltage is harmonic free and specifies only allowable output harmonic current injection presented in Table 3.1. The limitations are set for the percentage of harmonics in output current and for total demand distortion (TDD).

Table 3.1. Harmonic current injection of DG at PCC [34].

Harmonic order	h<11	11≤h<17	17≤h<23	23≤h<35	35≤h	TDD
Percent (%)	4	2	1.5	0.6	0.3	5

3.3 Voltage profile of the feeder in conventional distribution network

The stability of voltage in every node of the network is provided by the reactive power flow balance. It is vital to mention that reactive power flow balance should be considered for every node of the system, only then the voltage, as a local parameter, will be held within a tolerance range. However, reactive power flow balance of the whole system, which can be excessive in one part of the system and unprocurable in the other, does not ensure the absence of voltage oscillations. Therefore, the necessary voltages can be achieved by direct control of the voltage or by the control of the reactive power flow [35].

The existing distribution networks and the corresponding voltage control equipment have been designed to operate in the conditions of planned centralized generation. It implies the radial topology with a unidirectional power flow from the high voltage (HV) substation to the MV system, and then to LV customers [36]. A one-line diagram that is applied to analyze the voltage drop in the distribution network is demonstrated in Figure 3.6.

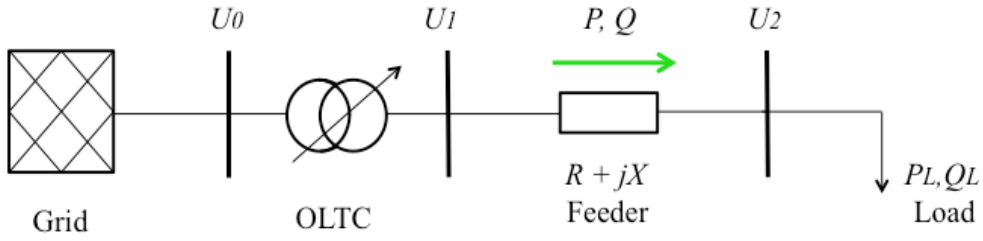

Figure 3.6. One line diagram of the distribution network [35].

In such system, voltage is decreasing towards the end of the feeder, and the voltage drop along the feeder can be defined as [35]:

$$\Delta \underline{U} = \underline{U}_1 - \underline{U}_2 = \underline{I} \cdot (R + jX) \tag{3.1}$$

where $\underline{I}$ is the vector of the feeder's current. The power from the grid can be formulated as [35]:

$$P + jQ = \underline{U}_2 \underline{I}^* \tag{3.2}$$

Therefore, by determining the current, flowing through the feeder, from the Equation (3.2) and inserting it in the Equation (3.1), the voltage variation between $\underline{U}_2$ and $\underline{U}_1$ can be presented as [35]:

$$\Delta \underline{U} = \frac{R \cdot P + X \cdot Q}{\underline{U}_2} + j \frac{X \cdot P + R \cdot Q}{\underline{U}_2} = \Delta U + \delta U \tag{3.3}$$

From Figure 3.7 it can be seen that the voltage drop can be resolve into a direct-axis ΔU and quadrature-axis δU components.

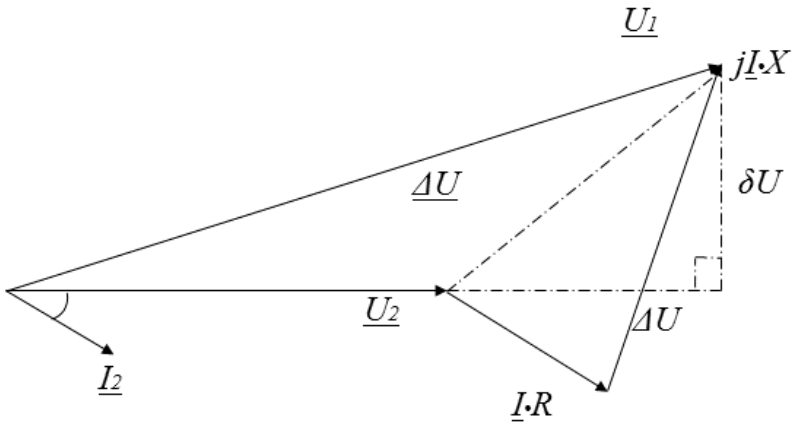

Figure 3.7. Phasor diagram of the voltage drop along the feeder [37].

The voltage angle between $\underline{U}_2$ and $\underline{U}_1$ is defined by the power flow. When it is small, the quadrature - axis component δU can be neglected, and voltage variation can be approximated by [37]:

$$\Delta \underline{U} = \frac{R \cdot P + X \cdot Q}{\underline{U}_2} \tag{3.4}$$

Thus, it can be deduced that in conventional distribution systems due to the impedance of the feeder, the load current causes the decreasing in the voltage profile along the feeder. According to the Equation (3.4), the drop of the voltage can be reduced by decreasing the numerator and increasing the denominator. In the conventional distribution network only the following measures are taken into account [37]:

1) $\downarrow R$ by means of $\uparrow F$, where F is a wire cross-section, which is chosen according to the conditions of providing the required quality of voltage;
2) $\downarrow Q$ by compensating the reactive power demand using shunt capacitors and thereby boosting the voltage;
3) $\uparrow \underline{U}_2$ by adjusting the voltage ratio of the transformer to keep the voltage at the secondary side of the transformer within acceptable limits.

3.4 Voltage profile of the feeder in distribution network with distributed generation

The voltage variation in a distribution system with DG units can be also analyzed by the one-line diagram. In Figure 3.8 the load and DG unit are represented by the active and reactive powers P_L, Q_L and P_G, Q_G, respectively.

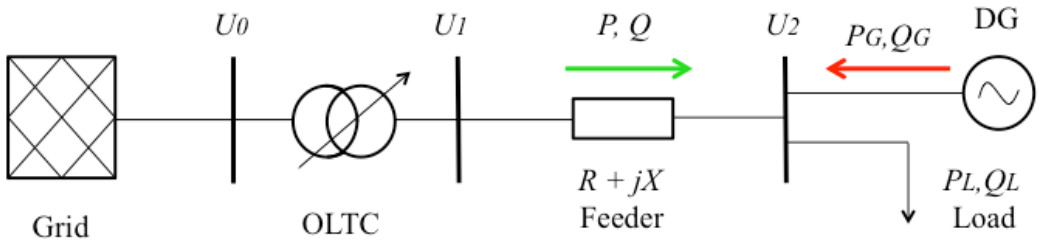

Figure 3.8. One line diagram of the distribution network with the presence of DG [35].

The voltage variation along the feeder can be calculated by the following equation [35]:

$$\Delta \underline{U} = \underline{U}_1 - \underline{U}_2 \approx \frac{R \cdot (P_G - P_L) + X \cdot (\pm Q_G - Q_L)}{\underline{U}_2} \tag{3.5}$$

According to the [35], the power is marked positive (+) if it is generated and negative (-) if it is consumed. Often, the opposite signing is used in the works. As it can be seen from the Equation (3.5), loads consume both active (- P_L) and reactive (- Q_L) power, but generators can supply active power (+ P_G) as well as absorb or generate reactive power (± Q_G). The injecting of active power by generators increases the voltage variation along the feeder, and if it is more than load active power, the power flow will reverse its direction.

Distributed generation units connected to the grid can be managed to help the system by regulating its power factor (PF) with regard to the voltage control if it is allowed by the regulating rules. For example, according to the studies presented in [38], an output PF of PV systems connected to the MV network can be changed in five steps: 0.95_{ind} - 0.97_{ind} - 1 - 0.97_{cap} - 0.95_{cap}. In the capacitive mode, the reactive power flows from the DG to the load. Conversely, during the inductive mode, the reactive power flows from the network to the plant that consumes reactive power. Thus, to support voltage growth reactive power should be injected into the grid in the capacitive mode. On the other hand, the inductive mode or consumption of reactive power will lead to voltage fall.

Therefore, the voltage in different sections of a distribution network with DG can be controlled by applying the following methods [28]:

- Assigning a dedicated connection point from an existing feeder for DG connection;
- Using on-load tap changer (OLTC) of HV/MV transformers;
- Altering the position of the MV/LV transformers' off-load taps;
- Utilizing step voltage regulators on feeders;
- Reactive power absorption by generators;
- Generation curtailment (GC);
- Installation passive or active reactive power compensators on feeders;
- Employment of EESs.

3.5 Conclusions about chapter 3

The importance of voltage stability was explained by the examples of such loads as a light bulb, induction motor, and household appliances, whose service life can be reduced by the effect of voltage variations. The influence of power generation by RDG units on voltage rise, harmonic distortion, and voltage fluctuation was shown. The requirements for voltage levels in the network according to the European standard EN 50160 were presented.

The main characteristics of voltage profiles in traditional networks and networks with DG were analyzed with the use of the one-line diagram. Possible voltage controls approaches in traditional networks and the networks with DG were listed.

4 VOLTAGE CONTROL METHODS WITH DISTRIBUTED GENERATION

At present, the existing voltage control methods in the networks with DG could be divided to centralized and decentralized. The centralized methods are exploiting developed communication for voltage control that allows evaluating the state of the network from substation to the rest of the network. The decentralized methods use local information and a limited number of devices for voltage control. The purpose of these methods is to weaken the voltage rise and fluctuation problem in distribution networks with DG. This chapter includes a literature review of these methods.

4.1 Centralized voltage control methods

4.1.1 Distribution management system based control

The distribution management system (DMS) is at the core of decision making for the control of distribution network operations. There are two types of DMS systems known as basic and advanced DMSs. The basic type is related to control actions connected with secure operation of the distribution system in case of faults. The advanced type applies more comprehensive regulating strategies that require the technical and market information about a state of the network to obtain the optimal decision. [39] In further review, the advanced DMSs are examined.

The modification of DMS with the use of GC presented in [40]. The generation curtailment is only applied in the case of all other possible DMS operation's failure that are available for voltage control. However, to minimize the amount of curtailment power, the sensitivity analysis is embedded in [41]. The optimized algorithm finds the most appropriate DG units to trim their generation.

Coordination scheme tested on MV network that utilizes DMS for online voltage control is described in [42]. The effective voltage control is provided by the wide range of devices in use. The main factor for control actions is the priority of these devices that is defined based on the electrical distance from the point of voltage control to the place of DG unit's installation. Such structure reduces the operational conflicts and increases the effectiveness of voltage support by the DG.

In [28] an optimization control algorithm is designed to be a part of the DMS that has already found application in the networks. The control parameter for substation voltage is the set point of the substation AVC relay. Additionally, the real and reactive powers of DG units can be controlled within the allowable range. The advantage of this method is that a lot of elements participate in the control operations such as DG units, reactive power compensators, controllable loads, and LV networks. Information about SE is employed as input data for the coordinated voltage control. The exchange of the control commands and measurements is performed by supervisory control and data acquisition (SCADA) system.

4.1.2 Coordination of distribution systems components

This method controls the voltage at the substation terminals based on measured or estimated upper and lower voltages in the network. To keep the voltage in a distribution system within the tolerance range, different control devices are applied. Here [43], a control method involves coordination of different devices such as the OLTC transformers, step voltage regulator, shunt capacitor, shunt reactor, and static VAR compensator (SVC).

The generator's AVC relay is one of the progressive methods used to enhance voltage control and contribute to further growth of DG's installations. The method of control described in [44] possesses a SE technique. It is created by the combined operation of the AVC relay of the transformer and DG units. Voltage control is provided by constraint of real power exported by generators, adjustment to the import (or export) of reactive power by generators, and control of OLTC at primary substations.

Coordinated voltage control scheme that involves the operation of static synchronous compensator (STATCOM) during contingencies is explained in [45]. This approach allows reducing the loading of OLTC in the case of a wide range of voltage altering. Most of the capacity of STATCOM will be employed during the accidental situations when the voltage will leave the dead-band (DB) region specified for the OLTC operations in normal conditions.

4.1.3 Intelligent centralized methods

Advantages of intelligent techniques allow providing voltage control taking into consideration a lot of parameters and conditions. It can be applied to define the location and capacity of possible installation of DG units as well as to integrate the operation of different devices for voltage control and even to provide islanding operation of power systems with DG. However,

the disadvantage includes complicated work to ensure successful implementation methods of programming with more input data.

One example of an intelligent system is a multi-agent system (MAS) elucidated in [46]. The term "agent" can be described as an entity (software or hardware) that is able to solve defined problems depending on the state of the environment individually and by means of cooperation with other intelligent agents [47]. A group of intelligent agents is forming the MAS concept. In this research, the MAS detects the best solution for the OLTC by comparing the number of control actions in each feeder and manages reactive and active powers of DG units to control voltage within each feeder. The test results show that this approach can help to increase the number of DG units and cope effectively with the voltage variation.

Here [48], a method to dispatch DG units in accordance with voltage control devices by the means of tabu search algorithm is described. Tabu search is a meta-heuristic algorithm that works by the principle of finding the best solution from the closest available moving gradually through neighborhood regions. The solution is found when the algorithm has achieved the stopping criteria. The method determines the appropriate size of DG unit that would not violate voltage level in the network. The optimization condition is the less number of switching operations for regulating devices.

4.2 Decentralized voltage control methods

4.2.1 Reactive power compensation

The voltage stability in the node of the network is defined by the amount of the reactive power generated or consumed by the devices in the network. In the worst-case scenario that is minimum load and maximum generation ($P_L = 0$, $Q_L = 0$ and $P_G = P_{G\max}$, considering unity PF of DG unit) by using Equation (3.5) with reactive power compensation we can write [35]:

$$\Delta \underline{U} = \frac{R \cdot P_{G\max} + X \cdot (\pm Q_{G\max} \pm Q_C)}{\underline{U}_2} \tag{4.1}$$

From Equation (4.1), it is seen that to reduce the second part of the numerator, the compensator must import/export the amount of reactive power that should be equal or even larger than the reactive power of the generator. Different types of distribution flexible AC transmission systems devices can be included in reactive power compensation such as

STATCOM, SVC, and capacitor banks [49]. In [50], a comparison of such devices has been performed. The simulation results have shown the effectiveness of SVC and STATCOM for voltage control. This is supported by the results achieved in the study presented in [51]. It has confirmed that these devices yield good results when used in terms of voltage stability.

4.2.2 Cooperation of power factor and voltage control

This approach created as a combination of two algorithms known as power factor control and voltage control [52]. When the measured voltage is within a tolerance range, the generator operates with constant power factor in PF control mode. Often, a constant value of PF is set to unity, but if it is not – then the reactive power follows the active power, keeping a constant ratio between them. However, if there are voltage deviations above or below the statutory limits, the PF is changed in order to control the voltage. In other words, reactive power compensation is provided in voltage control mode. One example of such strategy is implemented in [53].

4.2.3 On-load tap changer control

On-load tap changer alters its tap position through an AVC relay that detects if the secondary voltage is outside of the tolerance range. Distributed generation interferes the AVC relay's performance and reverses the power flow, leading to a voltage rise and fluctuations occurring at the PCC, and requires more tap operations.

The control method with the use of the AVC relays in OLTC is proposed in [54]. It improves the inaccuracy of load drop compensation technique when DG is presented. In [55], the fuzzy logic controllers are involved to regulate the operation of OLTC and capacitor banks. Every device in the system is prioritized in terms of control. The OLTC controller gets the voltages from the feeder to evaluate possible tap operation.

4.2.4 Generation curtailment

This approach allows trimming off the active power generation to enable further penetration of DG. The easiest method to implement such curtailment is to disconnect the DG unit. For WTs, it can be done continuously changing the blade angle of wind generators and, in the case of PVs, by controlling the power point tracking algorithm of the inverter. Regarding renewables, the challenge is created by the acceptable amount of power curtailment at the moment of excessive generation during low load periods. The trimming of renewables over a

certain threshold is unreasonable and makes the construction of renewables too costly. It exposes the inflexibility to the grid and signals that the electric power system needs large changes [56].

The generation curtailment strategy is proposed in [57]. This scheme will trim the output power generation on a given percentage if the dual mode of PF and voltage control was not sufficient enough and the voltage is still out of the limits. To prevent the "hunting effect", which is a continuous increase or decrease of the DG's output power during the short-time voltage rise, there is a time delay before allowing the DG to increase its output by one step back to the previous level. [57]

A simple battery storage strategy proposed in [58] operates as a source of active power in case of voltage variations. When the grid voltage exceeds the upper limit, batteries will absorb active power as well as inject active power in the grid when grid voltage falls below the lower limit. Between the upper limit and the lower limit, a DB is introduced to minimize the possibility of the hunting effect. [58]

4.2.5 Intelligent decentralized systems

Distributed methods based on MAS with the architectural particularity of centralized method have been proposed in [59]. Each controllable device has its own agent that plays for own hand to achieve optimization. Control agents of the distributed control structure try, through communication and consultation with other control agents, to [59]:

1) define the present and future state of the system;
2) take actions to meet their aims and satisfy the constraints.

The network planning of DG's integration can be implemented using artificial neural network based on decision support system as presented in [60]. The neural network explores the contribution of DG units' reactive and active powers on voltage profile by analyzing the slope of voltage curve in different places of DG units' installations. In [61], the tabu search algorithm is created to provide reactive power compensation for wind farms. The utilized in this algorithm sensitivity analysis considers the technical and financial constraints.

4.3 Conclusions about chapter 4

Different centralized and decentralized voltage control methods were reviewed and categorized into groups according to their functionality. The centralized voltage control methods require a high level of security and reliability of transmitted data between the elements. However, this type of voltage control management proved to be more systematic and robust in comparison with the decentralized methods. On the other hand, the decentralized voltage control methods are based on local data. They are more simplified, limited, and not able to guarantee the voltage control of the whole network, but still can be useful for local control in the frameworks of centralized methods.

The integration of DG does not alter the voltage control principle dramatically. It is still mostly based on the conventional elements such as OLTC and reactive power compensation. It even makes it more diversified introducing DG itself as the controlling component. The main changes are connected with the enhancement and complication of power grids while the modernization in voltage control methods is the accompanying effect.

5 DEVELOPMENT OF VOLTAGE CONTROL ALGORITHMS

This chapter presents the three voltage control algorithms that have been designed and simulated during the thesis work. The developed voltage control algorithms are demand response (DR), modified automatic voltage control (AVC), and reactive power compensation (RPC) of PV systems. These are all based on a control structure that assumes either distributed location of measuring points (modified AVC algorithm) or the distributed location of controlled sources (DR and RPC of PV systems). In proposed algorithms based on DR and RPC of PV systems, all measured data are gathered through smart meters and/or remote terminal units in central coordinator (CC) that evaluates the state of the system and then sends the command signals back to the intelligent electronic devices (IEDs) of controlled sources [62]. The communication structure of such algorithms is clarified in Figure 5.1. The command signal of modified AVC algorithm is only transmitted to the OLTC's mechanism of the corresponding transformer.

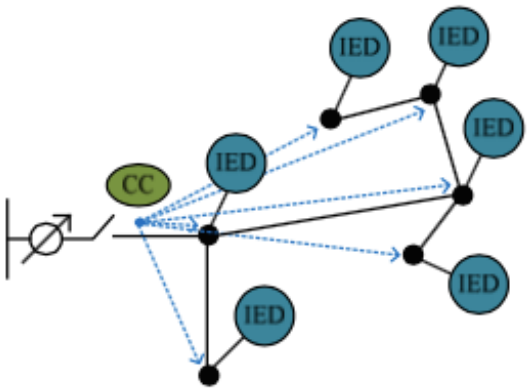

Figure 5.1. The communication structure of dispersed algorithms [62].

5.1 Demand response algorithm

The development of communication infrastructure provides new opportunities for the consumers to be engaging in the operation of the power grid as well as for the electric system planners and operators to take advantage of new approaches and tools for the control of the power grid. One of such perspectives is DR that controls the customer's electricity usage for balancing supply and demand.

Control of the load is carried out by two-way communications that are often considered to belong to smart grids and which are already available to some extent through the automatic metering infrastructure (AMI). The most crucial factor in such method is the time since the speed of DR should be quite fast for reliable operation of this method. The residential loads are controlled by direct load control programs employed by the power companies to manage the operation of the large electric systems in houses such as air conditioning systems, hot water heaters, and pool pumps. It turns them on and off in exchange for financial privileges and lower electric bills [63]. Unfortunately, the current capacity of controllable appliances is low and if electric heating loads and industrial (including agriculture) loads are excluded, many of the devices considered for DR control cannot emulate efficiently the behavior of reserve-power loads [64]. The situation can be changed in future when the charging stations of electric vehicles (EVs) and EESs can also be used in DR as ones of the main elements.

Among all the benefits of DR, the flexibility of load demand gives possibilities to cope with the voltage rise and variation problem. According to the [65], it allows to decrease the employment of the active power curtailment of DG and even make unnecessary the investments in grid reinforcement. In accordance with the Equation (3.5), its impact is even more significant on voltage than RPC because of the relatively high ratio of the resistance and reactance in distribution networks. Since the local consumption is increased it reduces the reverse power flow, power losses, and peak load power [66]. Two more conditions for DR implementation are the presence of controllable domestic loads that should be used on a daily basis and enough consumption of such loads during peak generation periods of DG. These factors are difficult to attain and they do not allow DR to be the main tool in voltage control at that moment. However, the combination of DR with other methods already now can give more reliability for voltage control [67].

The demand response algorithm was implemented in this thesis to investigate the possible effect on the mitigation of the voltage problems in networks with DG. The purpose is to define how much load should be controllable for proper voltage regulation in conditions of voltage rise and fluctuations. Voltage control is done by altering the load enlargement from its current consumption, provoked by the customer's behaviour and considered to be 100 %, to the predefined limit of available equipment capacity (additional 50 % of current consumption) for DR operation. Thus, a total capacity of the load is 150 % of the current consumption.

The input parameters to the algorithm are the per unit voltages of all nodes in 20 kV network. The operation of the algorithm is elucidated in Figure 5.2. The algorithm is activated when the maximum voltage from measuring nodes exceeds the upper limit during a specified delay. Then, the signal is sent by CC to the controllable loads to increase its consumption. If after the delay voltage is still above the limit, then the consumption is increased again. As soon as the voltages come back to the tolerance range, the algorithm is deactivated after the increased delay.

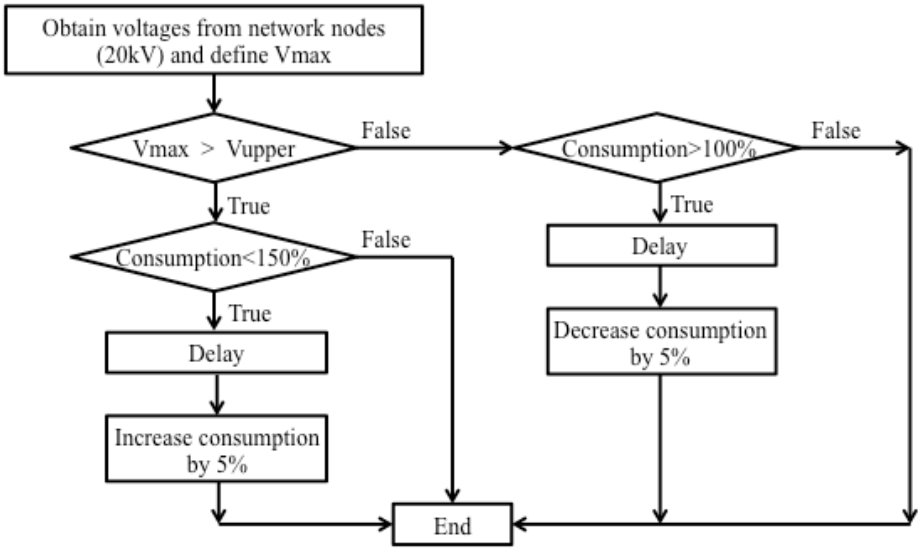

Figure 5.2. DR algorithm.

The step of enlargement for the consumption is 5 %. The delay before increasing the consumption is equal to 2 s to prevent activation caused by short variation of the voltage. The maximum voltage limit is 1.05 per unit voltage. The mechanical delay for the response of controllable appliances operation is set to 5 s. The delay for decreasing the consumption is set to 10 s.

The algorithm implies some assumptions as follows: the response of the load operates with small mechanical delay; all dynamic loads are available for control; the delay in communication is low; monetary questions, such as cost of switching, utility or inconvenience are not considered; the service time for a device is unlimited; the AMI is well developed and allows to obtain voltages from all nodes of the network. The assumptions related to the technical part are the matter of time because in near future they will be accessed for the power grid operation.

5.2 Automatic voltage control algorithm

One version of the modified AVC algorithm is designed to perform altered voltage/VAR control (VVC) as a part of the DMS that is achieving the optimal operation point of the network, minimizing the overall costs and keeping the system within the technical constraints. As a component of DMS, VVC calculates the optimal set of control actions while optimizing voltage violations, power losses, and lines limits. Traditional centralized VVC is based on the SE solution as an input data and power flow as an internal tool for what-if scenarios, but they have some drawbacks. [68]

The basis for distribution network's SE is the real-time and pseudo-measurements. Most of the SE methods were developed for transmission systems with higher possibilities for real-time measurements. However, the situation in the distribution networks is not so positive, and the number of AMR is at the low level. Therefore, the accuracy and the quality of estimation are incomparable with the transmission systems and can seriously affect the system management. [69]

Although power flow gives the possibility to a wide variety of optimizations with high mathematical accuracy, the power flow model remains to be a compound and tedious problem. Eventually, it leads to the utilization of limited VVC strategies by the majority of medium/small size utilities. [70]

The implemented VVC has elements of two known control strategies: SCADA Controlled VVC and Integrated VVC or Model-based VVC that are applied to the online and offline parts of the designed AVC algorithm, respectively.

The basis of the algorithm's offline part is the model of the controllable network that recreates the behavior of all components in the network and management systems including voltage control. The purpose of that part is to form a reference voltage signal for the online part. The input data for the model includes the prognosis of the wind conditions in the places of WTs' installation, static information obtained from the integration of the DMS with the network information system (NIS) and customer information system (CIS), as well as information from SCADA. The content of static network information includes the network parameters stored in NIS database and load information obtained from hourly load curves and CIS

(annual energies and customer types). The SCADA collects the information about the reconfiguration of system elements and the network operator also can enter it directly to the DMS.

Assumptions are made for the model that all components are modeled with high similarity to the real objects, but the model can have some level of uncertainty that is decreasing in the case of small forecasting time. Thus, the model's data allow evaluating possible consumption and generation in the network.

The input parameters for the offline part of AVC algorithm are the maximum, minimum, and mean voltages in the model. Mean voltage is calculated as the arithmetical average of maximum and minimum voltages. State estimation of the offline part is implemented assuming that voltages from all nodes are available.

The offline part of AVC algorithm depicted in Figure 5.3 operates in the following way: it is activated if network maximum or minimum voltage exceeds feeder voltage limits that are equal to ± 5 % of the basis voltage (20 kV). Then three conditions are verified. The first condition is that the opposite voltage (maximum/minimum) is not exceeding its limit after one OLTC's operation to prevent "hunting effect" that is continuous set point changes and operations of the tap changer. The second is that the new reference voltage does not exceed its limits, and the third one is that the difference between the new reference value and current mean voltage exceeds the DB. The allowance is made that the OLTC's operation modifies the voltages in the whole network for the value that is equal to the tap step. However, this is not exactly valid for the real network because of the losses.

After the new reference voltage is determined, the signal is transferred to AVC relay and the new reference voltage is set for the OLTC within the offline part if the signal remains during the delay time, which is equal to 3 s. Additional 2 seconds are required for tap's selection and transition. Nothing is done if the voltage control is unable to improve network state because the tap changer operation exceeds the determined limits. After the model stalls the simulation, the resulting dependence of reference voltage is communicated as an input reference data to the online part of the AVC algorithm. Then the online part of the AVC algorithm operates exploiting obtained dependence of reference voltage and real-time measurements of voltage from the PCC of DG units and at the substation node. It changes tap position of the

transformer if the real-time mean voltage value of the feeder differs from the reference voltage more than DB during the specified delay as shown in Figure 5.4.

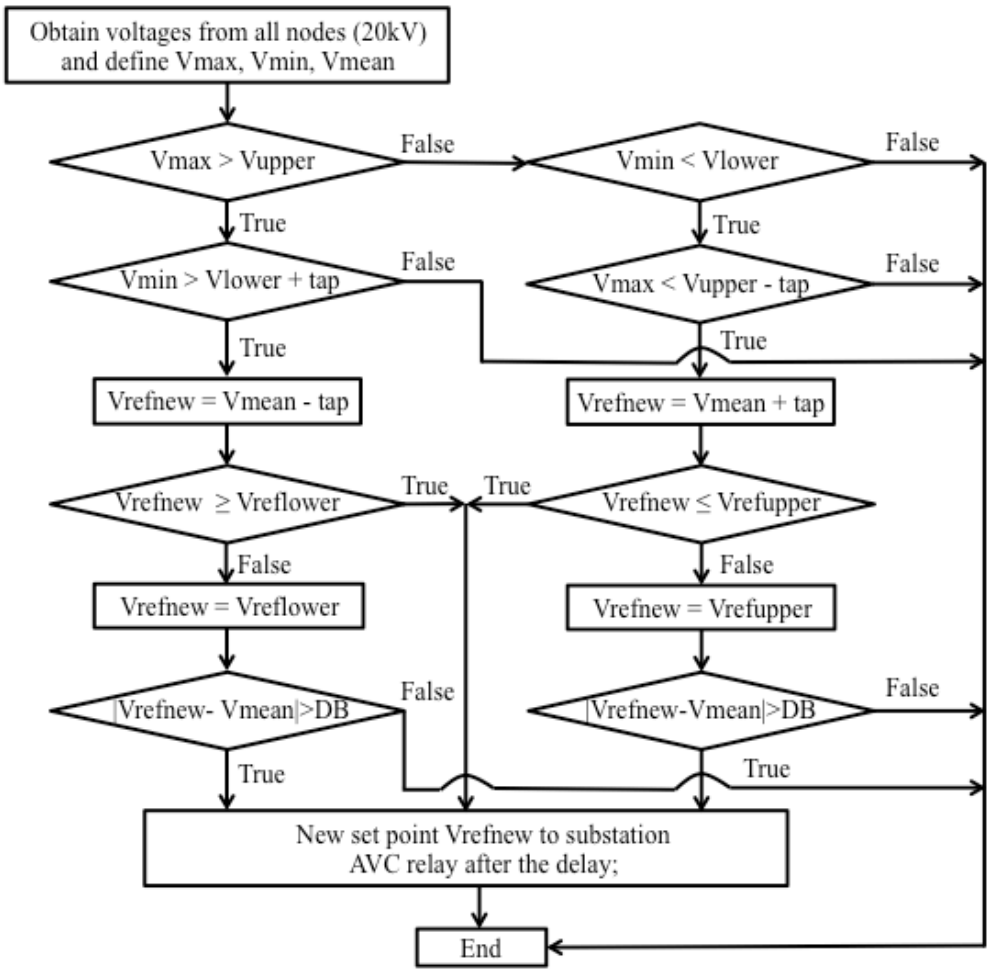

Figure 5.3. The algorithm of AVC for the offline model of the network.

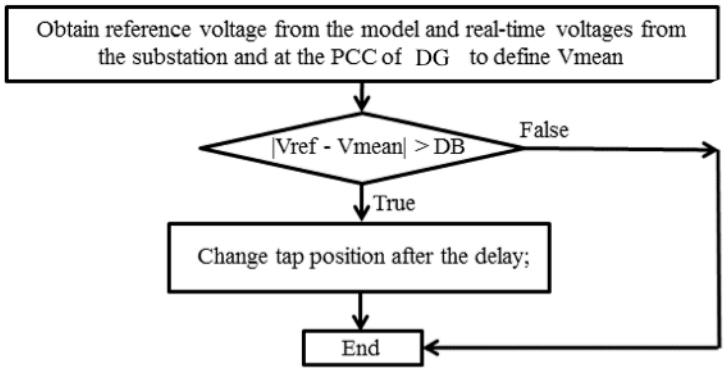

Figure 5.4. The algorithm for the online part of the AVC control.

The same control algorithm as in Figure 5.3 can also operate independently in real-time without the model of the network. This is the second version of modified AVC algorithm that will be investigated and compared with the efficiency of the model-based algorithm. The difference between the offline AVC algorithm applied in the model and real-time AVC algorithm, operating without the model, is only in the input parameters. They consist of the voltages at the substation and at the PCC of installed DG units as illustrated in Figure 5.5. The available real-time data could give a good estimation about the boundary voltages in the feeder but the negative part of the real-time control could be the constraint of information about the state of the whole network.

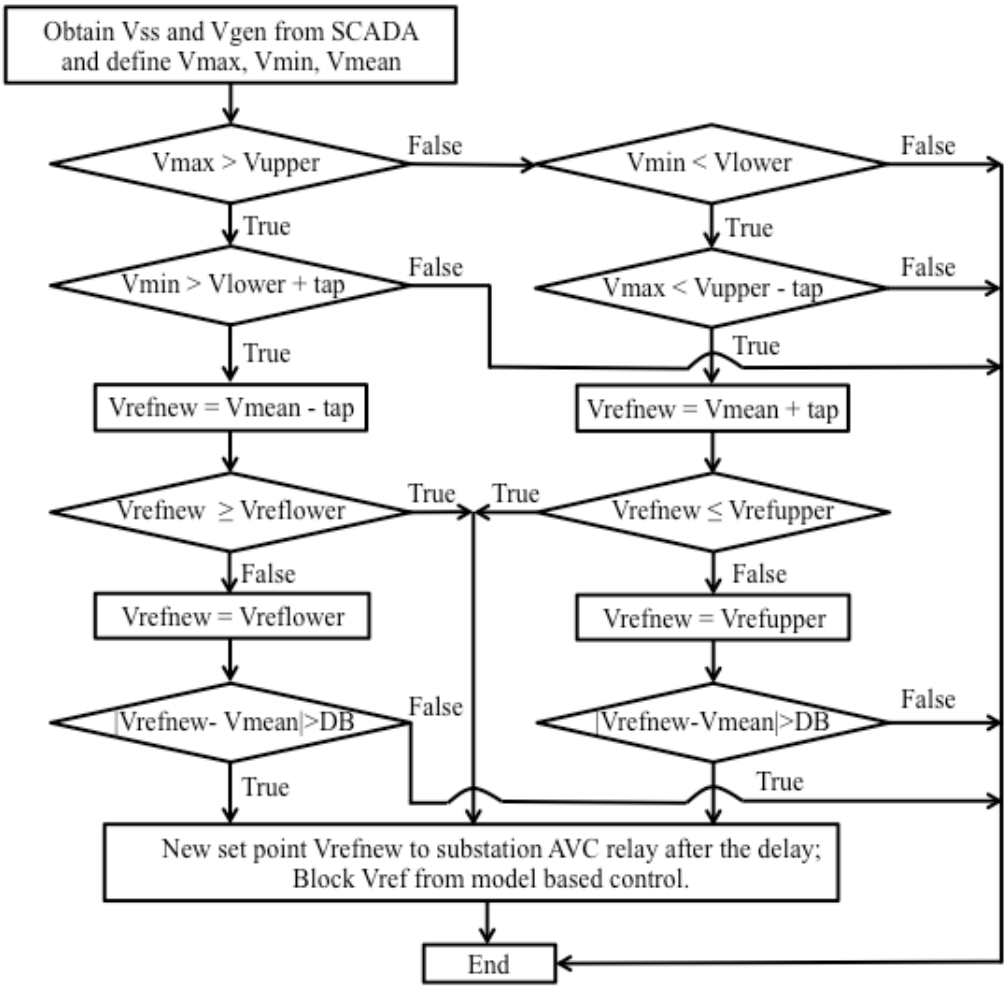

Figure 5.5. Stand alone real-time AVC.

The main advantage of the designed AVC algorithm within VVC is that the model-based part mitigates the problem of adaptability to feeder reconfigurations by monitoring the status of devices in the field and updating the dynamic operating model. Moreover, the model includes

the DG units and considers its influence. The only additional equipment's installation is the AMR at the PCC of DG units. The main disadvantage of the algorithm is that the increased number of taps changes provoked by DG units' stochastic operation leads to the additional maintenance service as the consequence of the deterioration of the tap changer's mechanism. It also causes voltage transients to the distribution network.

5.3 Reactive power control of photovoltaic systems

The created algorithm is the rule-based version of the voltage dependent reactive power control *Q(U)*. It works according to the dependency described in Figure 5.6. The algorithm was constructed with the analogy of DR algorithm to evaluate the possibilities of the household PV systems for voltage control and compare its performance with DR approach. The assumption is made in this thesis that DG units can participate in voltage support.

The algorithm operates in the following way: if any voltage from the measuring points exceeds the upper or lower limits, then the control command to PV systems is sent to start changing its PF, consequently, changing reactive power at the PCC. It is continuously altering PF up to the limit value until the voltage returns to the tolerance range. After the voltage returns into the predefined values, the PF is decreased with enlarged delay.

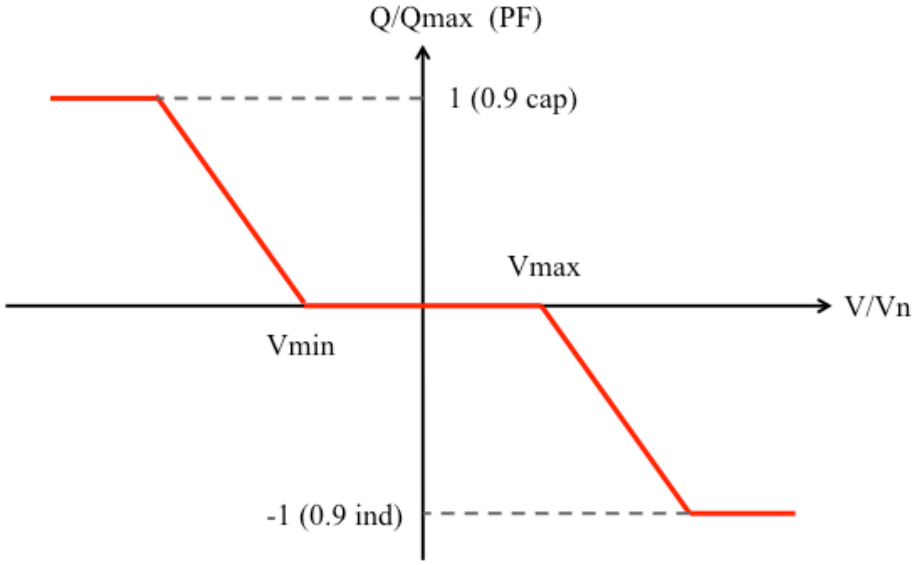

Figure 5.6. Rule-based voltage dependent reactive power control.

There are two modes available for the RPC. The inductive mode is decreasing the voltage, consuming the reactive power, while the capacitive mode is increasing the voltage, generating

reactive power. The functioning scheme of the algorithm's inductive mode is depicted in Figure 5.7. The capacitive mode operates in the same way with minimum voltage. The limit value of PF is 0.9 for both modes. The dead-band for voltage variation corresponds to the tolerance range from 0.95 to 1.05 per units. The step of PF's changing was chosen to be 0.01 per units. The time delay for every step when the voltage is outside of the DB is set to 1 s, while the delay to decrease the PF is set to 10 s. There is also a delay in operation of PV system and possible latency in communication that is equal to 5 s.

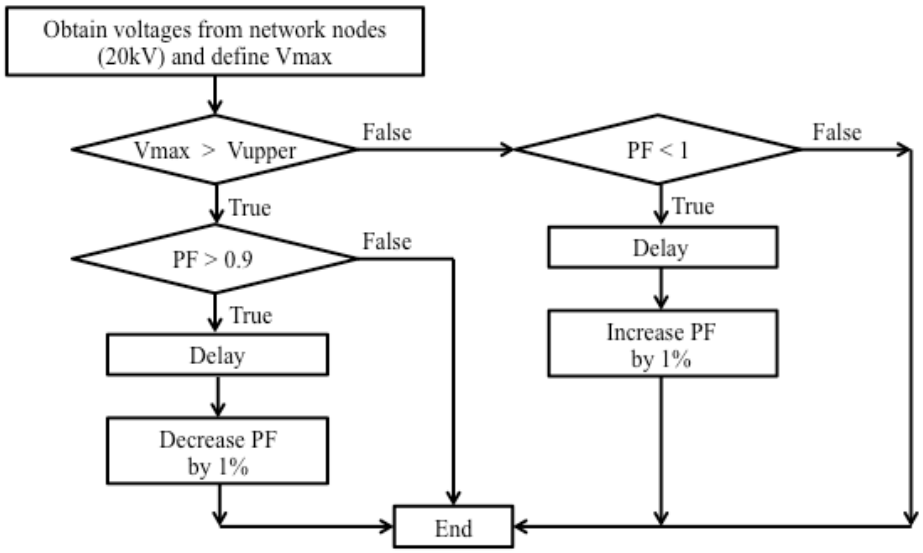

Figure 5.7. The inductive mode of the reactive power control algorithm.

The negative influence of the algorithm is that the consumption of the reactive power by PV generating units increases the power losses. However, it can serve as a positive effect if there are lightly loaded cables in the network that produces reactive power, and PV units can eliminate this production [71].

5.4 Conclusions about chapter 5

Three voltage control strategies were designed in order to mitigate the voltage rise and fluctuation problem in the networks with RDG. The DR algorithm increases the level of the customer's consumption to reduce the voltage. The modified model-based version of AVC algorithm can be used as a part of DMS performing VVC. The AVC algorithm can also work without the model of the network utilizing only real-time measurements. The RPC is based on the opportunity to vary the PF of the household PV systems. The advantages and disadvantages of the algorithms were also discussed.

6 TECHNICAL DATA OF UTILIZED POWER GRID MODEL

This chapter demonstrates the implementation of a simulation model of a power grid with RDG in MATLAB® environment. The purpose of this chapter is to provide insight into the model with a description of its possibilities and available applications. Time domain and general structure of the model are initially discussed. HV transmission network is then presented, followed by the description of MV and LV networks. Finally, the verification of the model is illustrated and aggregated model's data are represented.

6.1 Time domain and general structure of the model

MATLAB® software allows developing models that are relevant for simulation studies ranging from µs-ms accuracy for capturing power electronic switching to hours or days for investigating customer behavior and/or variable energy profiles over an extended period of time. There are three solvers available in MATLAB® with two step types demonstrated in Figure 6.1.

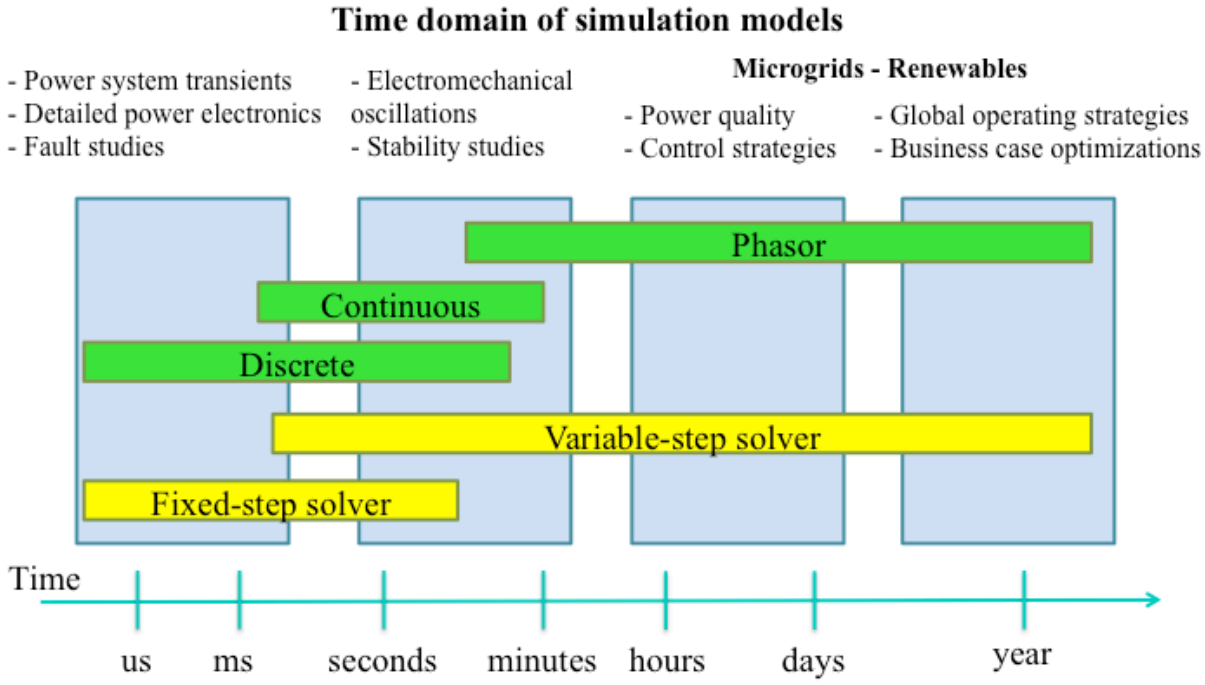

Figure 6.1. Time domain of the models in MATLAB®.

Initially, the purpose of the thesis was to investigate the possibilities of MATLAB® environment for the real-time simulations that in future would include some real hardware or/and software and validate its operation by applying different voltage control strategies to

the created grid. That is why at the beginning of the thesis to achieve that purpose there were two MATLAB® models implemented in the Discrete mode with the fixed-step solver and in the Phasor mode with the variable-step solver. The Discrete model was planned to be used as a physical model of the grid with a high level of the specification, while the Phasor model would represent the model of this physical system with an average level of specification. The Phasor model development was initially dictated by the necessity of power flow simulations that were inaccessible in the Discrete model, and later when power flow simulation was decided to substitute by the model-based voltage control algorithm. However, during the first simulations of the Discrete model, it became obvious that such level of modeling accuracy does not allow investigating the voltage rise and variation problem, leads to very time-consuming simulations, and sometimes results in crushing the MATLAB® because of the singularity issue that appeared in the network. Even though, the singularity problem remained in the later versions of the Phasor models but only in the face of warnings as shown in Figure 6.2.

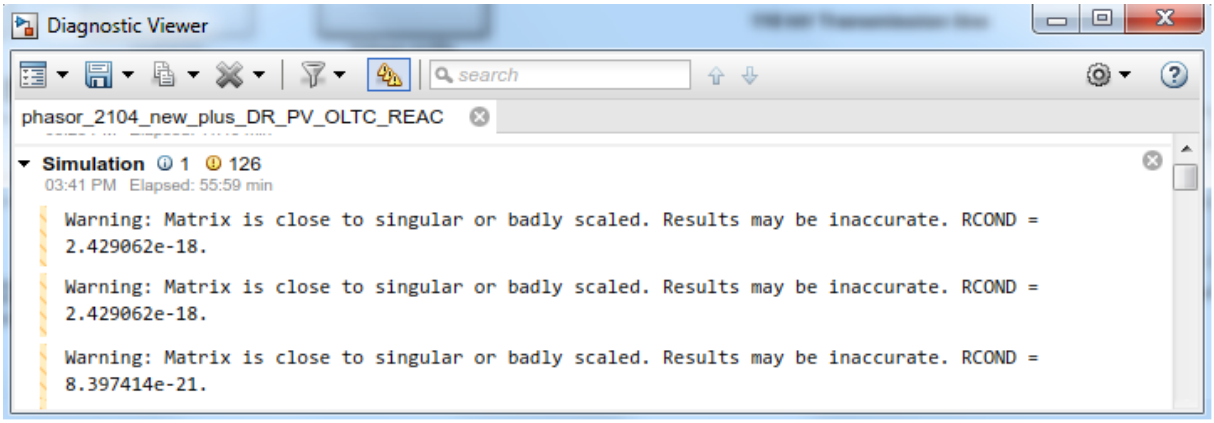

Figure 6.2. Singularity problem in Phasor model.

After the attempts to adopt the Discrete model to the needed requirements were failed, the decision was made to provide all the simulations in Phasor mode. Nevertheless, the created Discrete model can still be used for short time simulation of power system transients or other processes with high frequency. It includes the same elements of the power grid that are involved in this thesis.

Phasor models that will be used further in this thesis were also divided to represent the physical power grid and the model of this grid. The corresponding models were called “Detailed Phasor” and “Simplified Phasor”, respectively. The main difference between them

is that loads of Simplified Phasor are implemented as static loads while dynamic loads are designed for the Detailed Phasor. The diversity is also in the input parameters for the models. Parameters with artificial real-time variations are applied for the Detailed Phasor while average prognosis data – for the Simplified Phasor. The illustration of the Detailed Phasor model is presented in Figure 6.3.

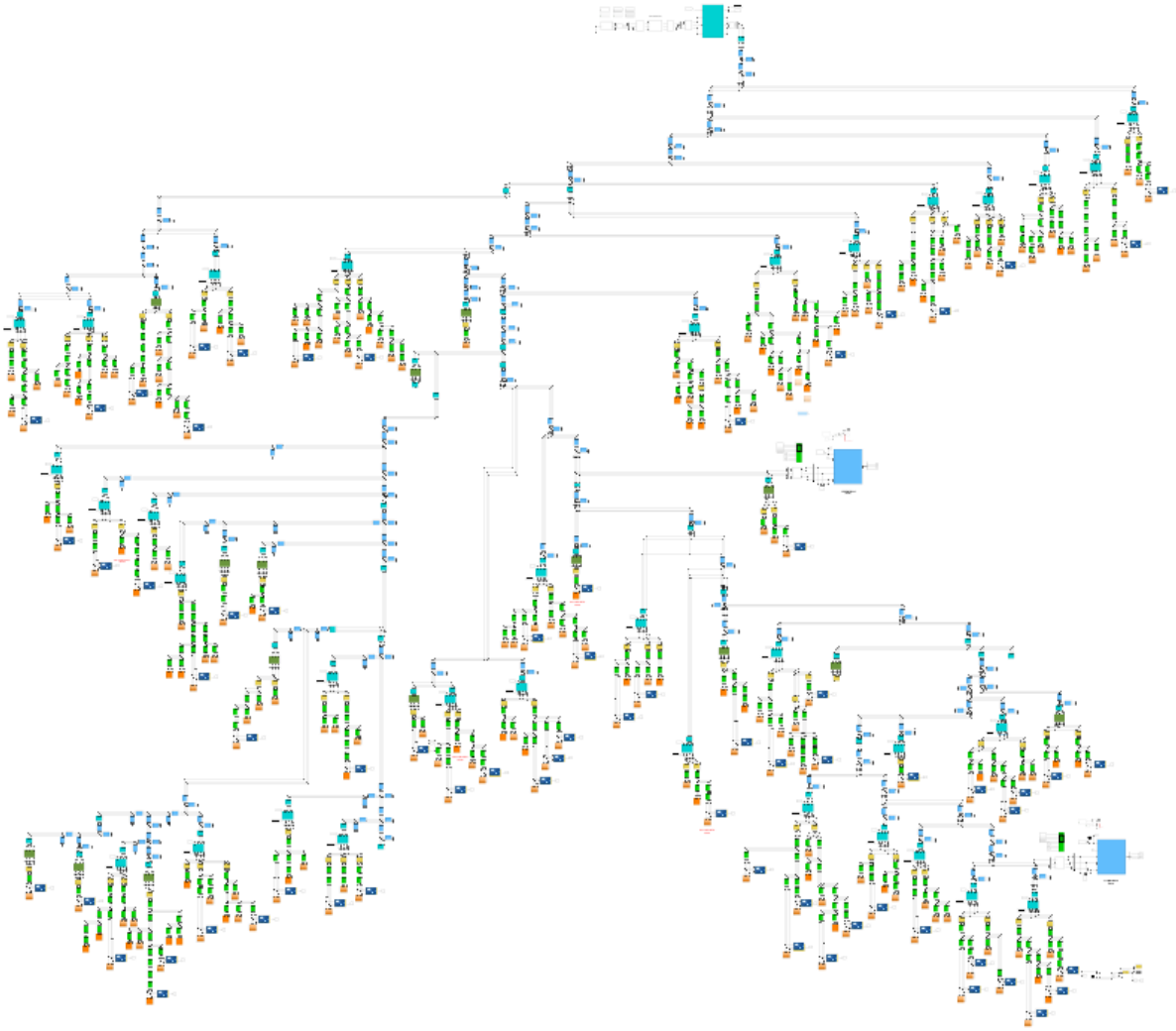

Figure 6.3. The Detailed Phasor model of the power grid in MATLAB®.

The electrical grid of the model is based on real data and represents a typical Finnish distribution system. It corresponds to a rural distribution network with radial configuration and consists of a 110 kV transmission system equivalent, supplying a 20 kV distribution substation. One LV feeder of 28.5 km length with imagined RDG units is connected to the 20 kV bus of the substation. The total feeder load varies from 100 kVA to 500 kVA at the power factor of 0.95_{ind}. The model allows describing power grid's power flow from the production to customers and can be used for wide range of research initiatives.

The simplified structure of the network without the presence of RDG units is displayed in Figure 6.4. The description of the elements is discussed explicitly further and is divided for that by two sections known as networks 110 and 20/0.4 kV.

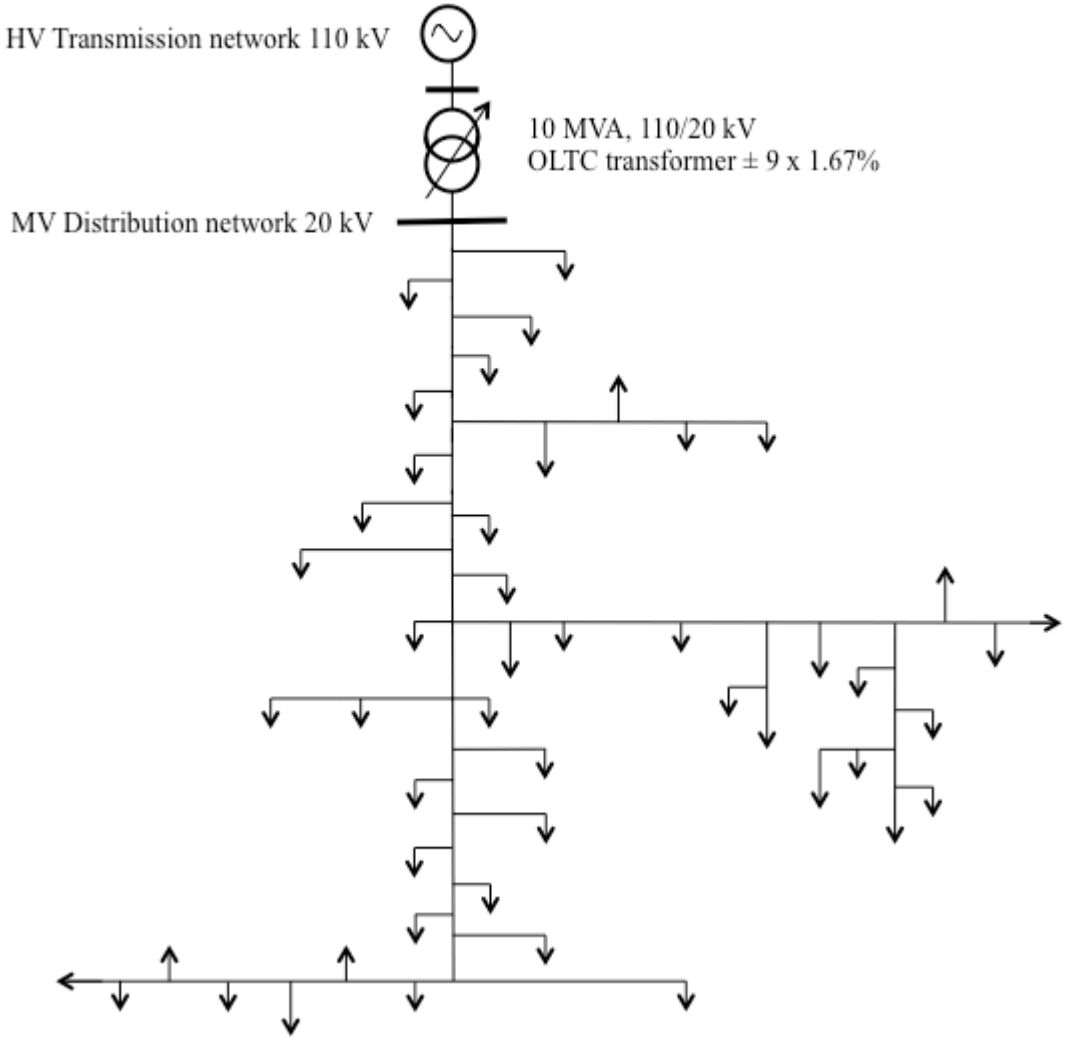

Figure 6.4. Simplified structure of the modeled network without the RDG units. **NOTE:** LV nodes are not presented, the structure is not scaled.

6.2 110 kV network

The main elements of this model's part are the electric source, PI section line, and OLTC regulating transformer as depicted in Figure 6.5. Furthermore, three-phase breakers labeled as Q_n and MV feeder of the substation are also illustrated in Figure 6.5.

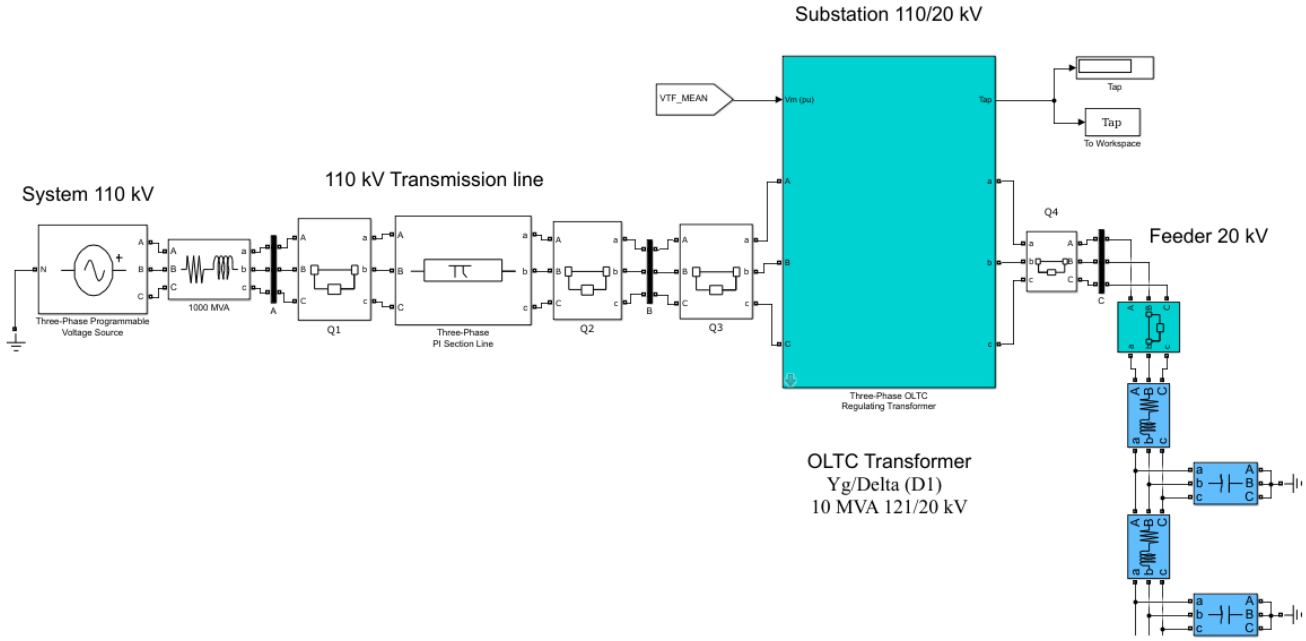

Figure 6.5. A network of 110/20 kV.

6.2.1 Electrical source

Three-phase voltage source block represents the rest of the HV power grid as 1000 MVA system. This block is implemented as a zero-impedance source and generates a three-phase sinusoidal voltage. The set parameters are the voltage amplitude, phase, and frequency. A three-phase series RLC branch models the inner impedance of the voltage source. Single resistor and inductor are employed for that purpose.

6.2.2 110 kV transmission line

The length of the modeled HV transmission line is 100 km. It is modeled by three-phase PI Section Line block. The line is represented by lumped parameters in a single π section as demonstrated in Figure 6.6.

The line positive - and zero - sequence parameters R, L, and C are specified to take into consideration the inductive and capacitive couplings between the three phase conductors, as well as the ground parameter [72].

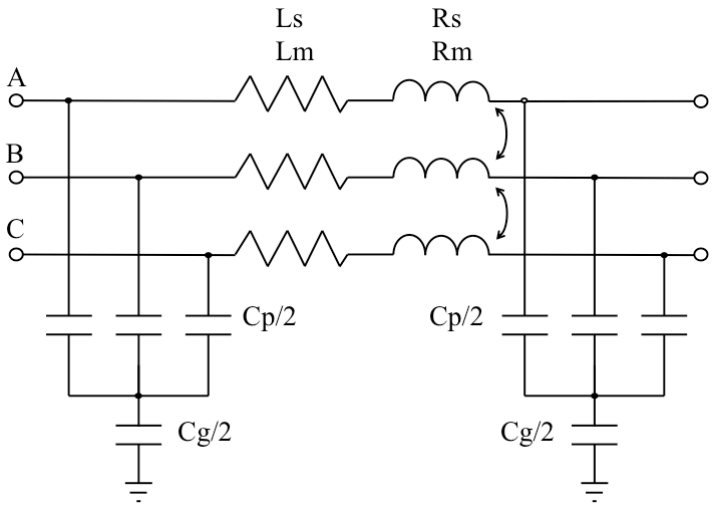

Figure 6.6. The equivalent circuit of the HV line [72].

6.2.3 Transformer 110/20 kV

The HV/MV OLTC regulating transformer rated 10 MVA, 110 kV/20 kV, Wye/Delta1 is implemented as a detailed model where all load tap changing switches and transformer characteristics are presented. The inner structure of the model is presented in Figure 6.7. The mechanism of OLTC is located on the primary winding and allows changing the HV/MV transformer's turn ratio by means of tapped winding that is connected in series with each 110 kV side phase winding. Ten OLTC switches including reversing switch provide a selection of 18 different taps besides the nominal ratio of the transformer. Each tap provides a voltage correction of ± 0.0167 per units or ± 1.67 % of nominal 110 kV voltage [73]. Consequently, a total of 19 tap positions can change a primary voltage from 0.85 per units (93.5 kV) to 1.15 per units (126.5 kV) by steps of 0.0167 per units (1.837 kV). It is possible to change the number of taps in this model as well as the voltage correction step. Initially, the model of the transformer had 8 taps, and one more was added to the model according to the instructions highlighted by red in Figure 6.7. The time of tap changing operation was also changed from 0.06 s to zero because when it previously led to short transients with high peaks that hampered the analysis of voltage variations. Voltage regulator part of the mechanism relates to the selection of further action that can be increasing or decreasing the tap position. OLTC control part is in charge of the switching mechanism operation. The reference voltage serves as an input signal for Voltage regulator part, and the output signal of the OLTC control part is the current tap position.

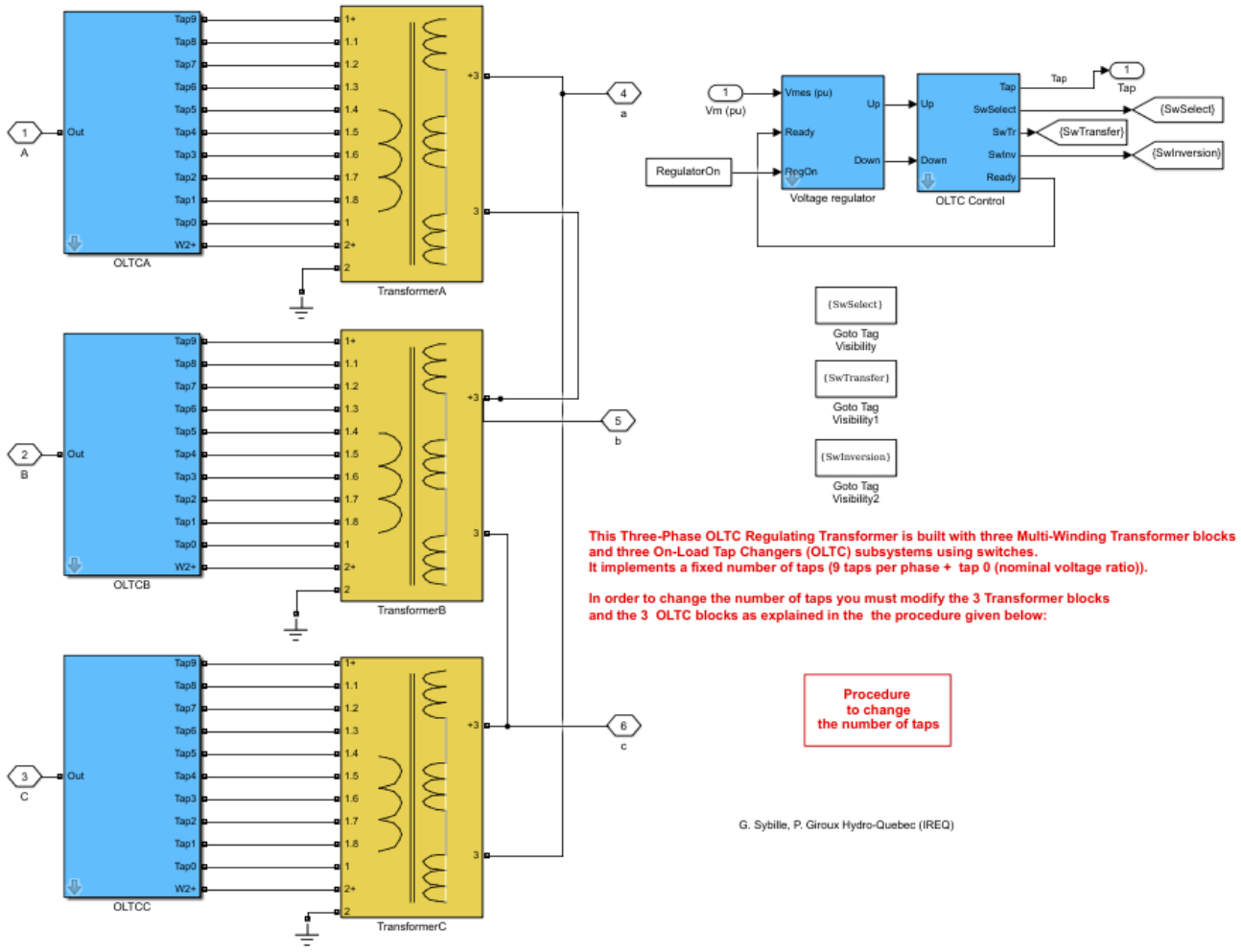

Figure 6.7. The implementation of OLTC mechanism.

6.3 Distribution networks 20/0.4 kV

Distribution networks of MV and LV are the main parts of this model because all of the conducted simulations relate to the voltage rise or variation problem appeared as a result of RDG units' installation in these networks. The typical representation of the MV/LV part without WTs is depicted in Figure 6.8. It is important to notice that some of the loads with very low consumption are modeled by a static load in Detailed Phasor. It did not affect the simulation results, but it helped to improve the singularity problem because the presence of all dynamic loads in the model sometimes led to crushing the MATLAB®.

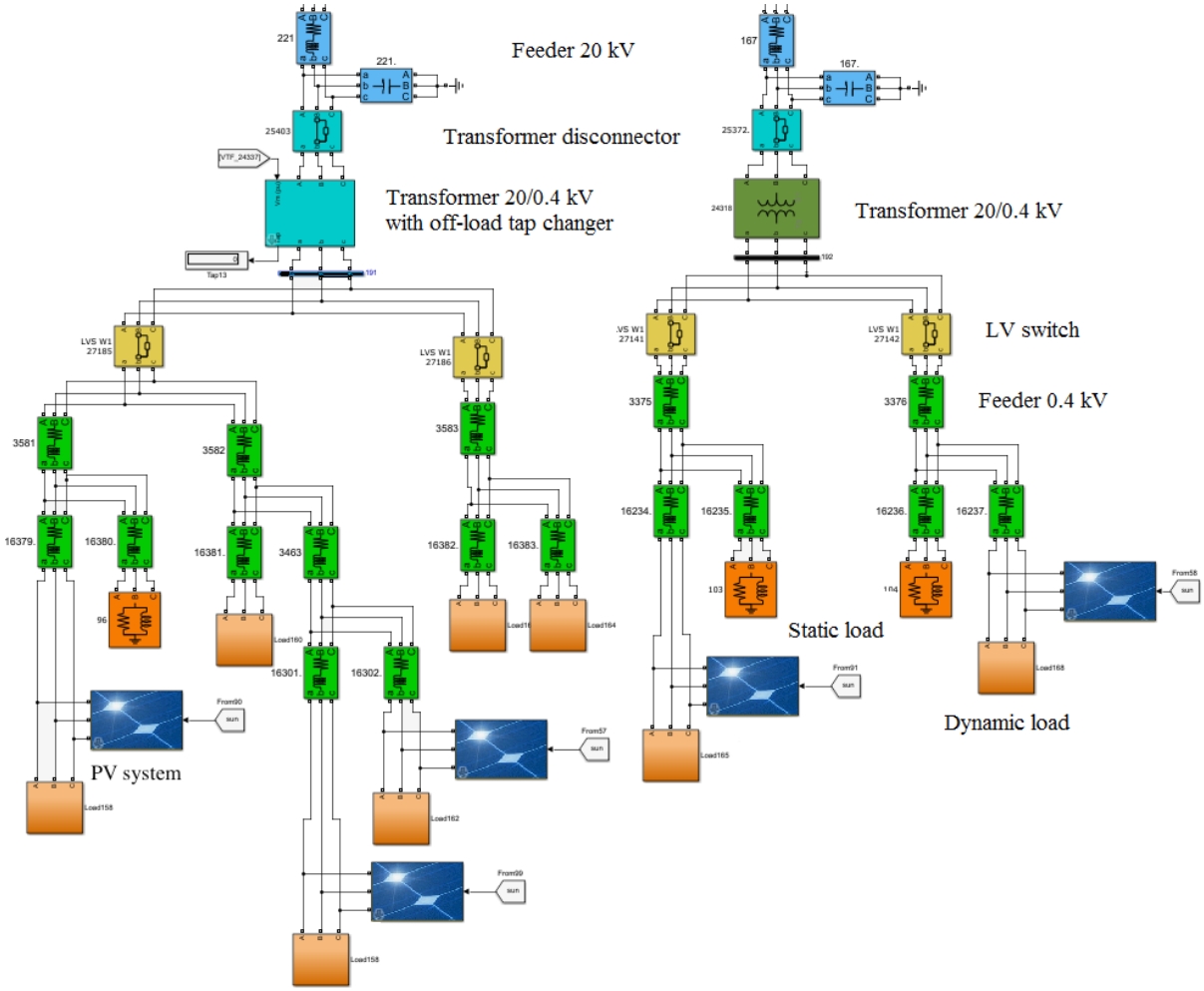

Figure 6.8. MV/LV part of the model without the presence of WT.

6.3.1 20 kV feeder and 0.4 kV networks

The model of MV lines is implemented as an ideal cable model (per unit length) including the skin-effect and dielectric losses in the model. The L, R, and C parameters presented in Figure 6.9 are the per unit length parameters for inductance, resistance, and capacitance, respectively.

Low voltage feeder has the same model as for the MV feeder but the capacitance is not taken into account for LV lines because of their low values. The scheme of the LV feeder's model is displayed in Figure 6.10.

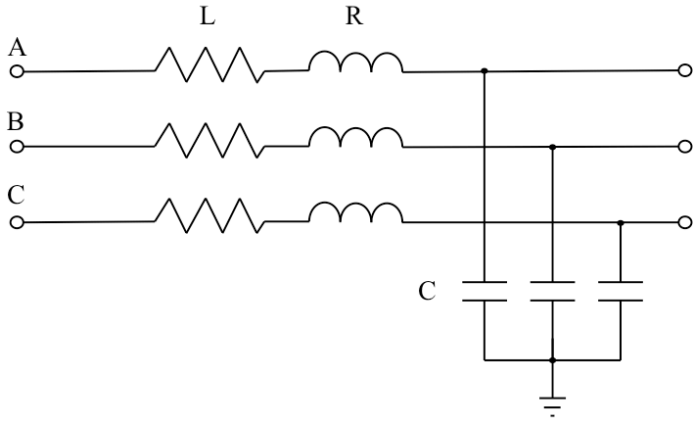

Figure 6.9. Ideal cable model (per unit length) for MV feeder.

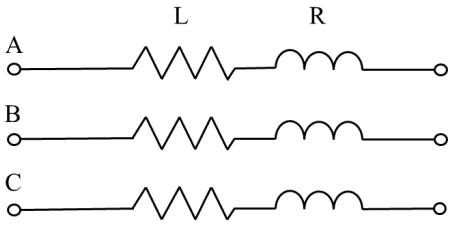

Figure 6.10. Ideal cable model (per unit length) for LV feeder.

6.3.2 Transformers 20/0.4 kV

The model contains 49 MV/LV transformers that are three-phase transformers with rated powers ranging tens-hundreds of kVAs, rated voltage 20 kV/0.4 kV and vector group Delta1-Wye. As it can be seen in Figure 6.8, the transformers are both with the off-load tap changer and with a constant ratio between the windings. They are highlighted by different colors in Figure 6.8. The transformers with off-load tap changer are implemented analogically with the HV/MV transformer, with some reconstructions: the tap changing mechanism is connected to the LV side (the off-load taps are normally located at the primary winding, but can be also placed at the secondary side [74]) and Voltage regulator part is turned off. The needed tap position is set manually in the model. Five or three off-load tap changers switches allow selection of four or two different taps with a voltage correction of ± 0.025 (± 2.5 %) per units or ± 0.05 (± 5 %) per units, respectively. However, for the most of the regulating transformers, the nominal ratio is used in simulations.

6.3.3 Wind turbine

A model of 1 MW wind turbine depicted in Figure 6.11 is used in the work. The WT with 575 V nominal AC output voltage is connected to the PCC through a 20/0.575 kV transformer.

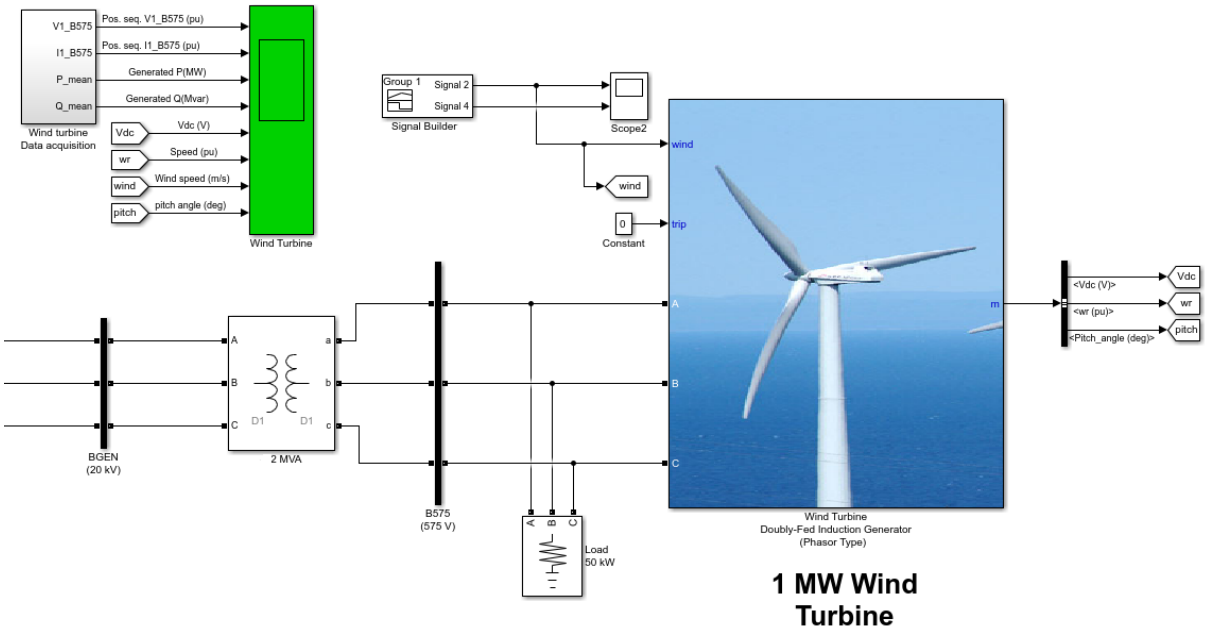

Figure 6.11. The model of WT in MATLAB®.

A doubly-fed induction generator (DFIG) is utilized for WT as illustrated in Figure 6.12. The DFIG technology optimizes the WT's speed, producing maximum mechanical energy for a given wind, and minimizes mechanical stresses on the turbine during gusts of wind. It consists of a wound rotor induction generator and an AC/DC/AC converter [75].

The induction generator converts the mechanical power of the wind to electrical power, and the stator and the rotor windings are used to transmit this power to the grid. The connection of WT to the 50 Hz grid is done through the stator winding, the AC/DC/AC converter feeds the rotor at a variable frequency. The AC/DC/AC converter can be divided into two parts that are known as the rotor-side (C_{rotor}) and the grid-side (C_{grid}) converters. The connection of three-phase rotor winding to C_{rotor} is carried out by slip rings and brushes, the three-phase stator winding is directly connected to the grid. To obtain an AC voltage from a DC voltage source the forced-commutated power electronic devices are exploited. A coupling inductor L separates C_{grid} from the grid.

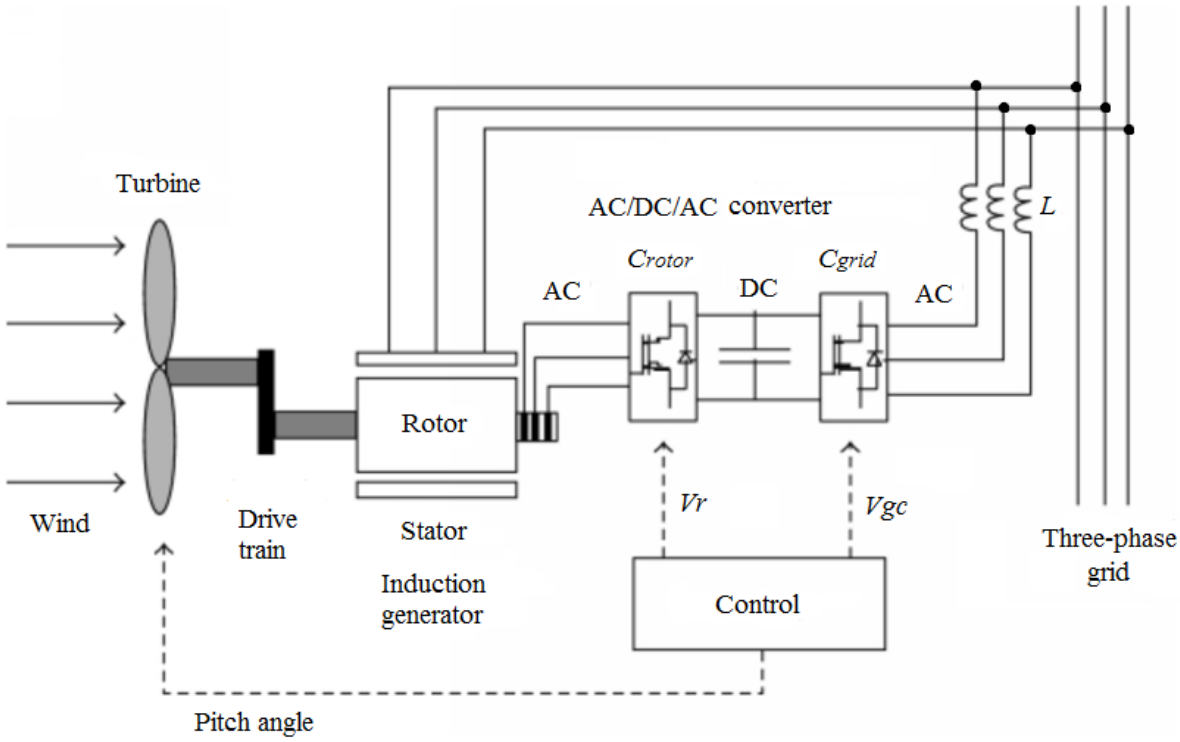

Figure 6.12. The WT and the DFIG system [75].

The purpose of the control system is to generate the pitch angle command and the voltage command signals V_r and V_{gc} for C_{rotor} and C_{grid}, respectively. This control system defines the output power of the WT, the DC bus voltage, and the reactive power or the voltage at the grid terminals. The capability of C_{rotor} and C_{grid} to operate with the reactive power is used to provide VAR or voltage control at the grid terminals and makes unnecessary the installation of the compensating devices. For the created model VAR control is chosen, allowing WT to operate with unity power factor.

The objective of the rotor-side converter is to regulate the WT's output power and the voltage at the point of connection to the grid. This is implemented by following a red curve of predefined power-speed characteristic named tracking characteristic for wind speeds ranging from 5 m/s to 16.2 m/s. This characteristic is displayed in Figure 6.13 and represents the ABCD curve placed on the mechanical power characteristics of the turbine. The corresponding mechanical power of the tracking characteristic is obtained by measuring the actual speed of the turbine and then used as the reference power for the power control loop [75]. The nominal power of the turbine is reached at and beyond point D.

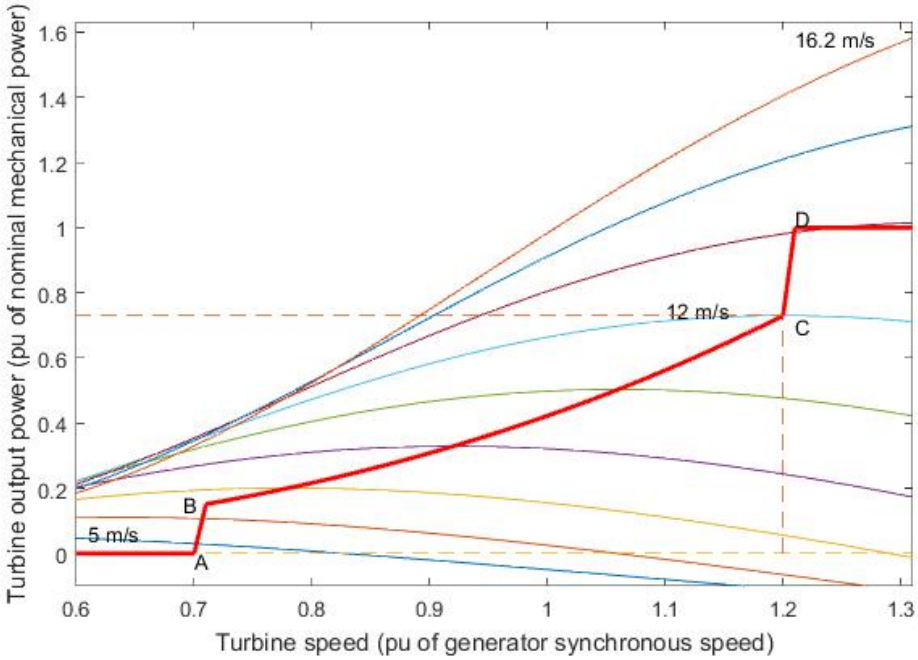

Figure 6.13. Tracking characteristic [75].

Signal Builder block provides time series of wind speed as an input to the WT's model. Constant wind speed is used for the Simplified Phasor, and sampled Gaussian noise is added to the Detailed Phasor.

6.3.4 Photovoltaic system

The model of the household PV system shown in Figure 6.14 is simplified and implemented as a negative dynamic load. It is connected to the LV network directly. The output energy of PV system is equal to the production of the size, efficiency, and input irradiance. The size of the PV array was chosen to be 10 m^2 with the 10 % efficiency of PV panels. In general case, the irradiance of 1000 kWh/m^2 will give 1 kWh of the electricity for each array. The input irradiance with the specified artificial shading for the PV system is provided by the means of Look up tables in MATLAB®. The output power is calculated in Irradiance data block and then transferred to the current. The real life structure of the PV systems is more complex. The example of household PV system's connection to the grid is demonstrated in Figure 6.15.

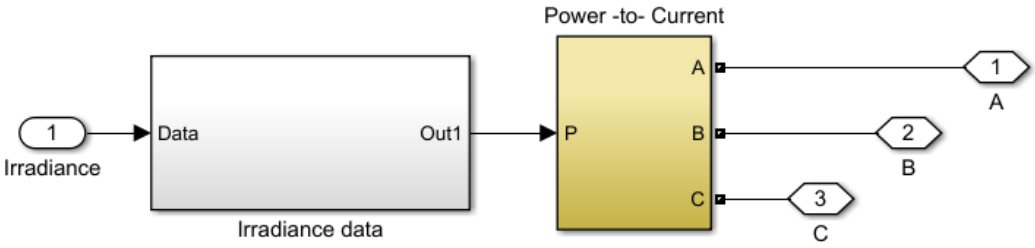

Figure 6.14. PV system structure in MATLAB®.

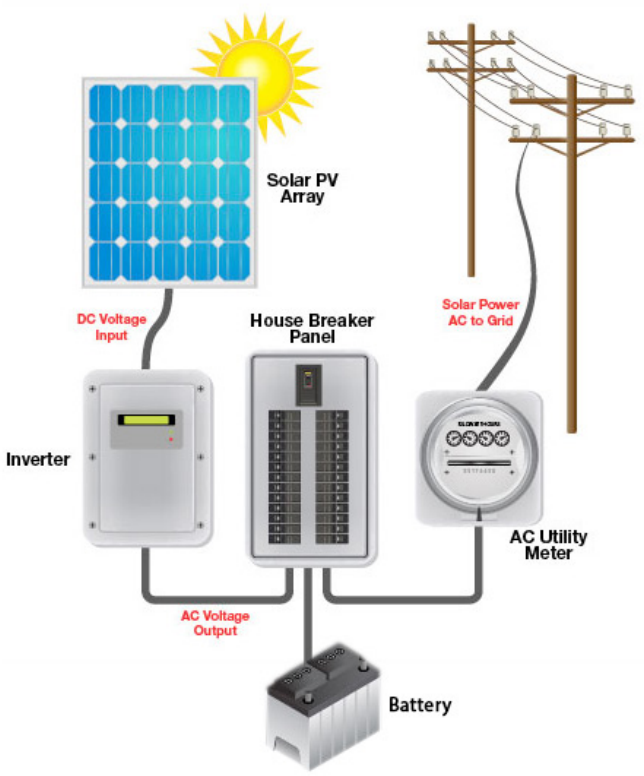

Figure 6.15. The connection of household PV system to the grid [76].

The energy of the sun is turned by the PV array to low voltage DC electricity and then converted by the inverter to AC voltage. If there is an excessive energy, it can be fed into the grid through the electric meter in reverse mode automatically or stored into the battery.

The output power of the real PV system is changing during the day and can vary significantly especially on a cloudy day as illustrated in Figure 6.16. The sharp peaks are appeared because of shading. However, the amount of generated power can also alter in several times during the year as it is shown in Figure 6.17.

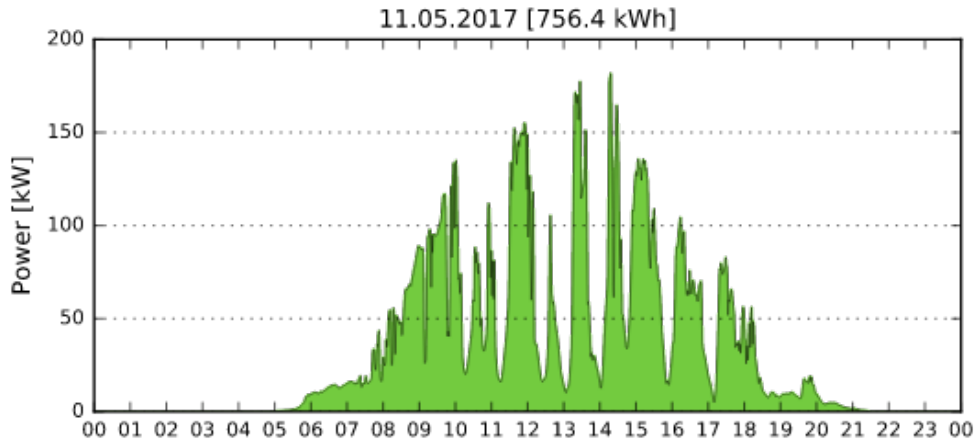

Figure 6.16. The generated power by the PV system during the day [77].

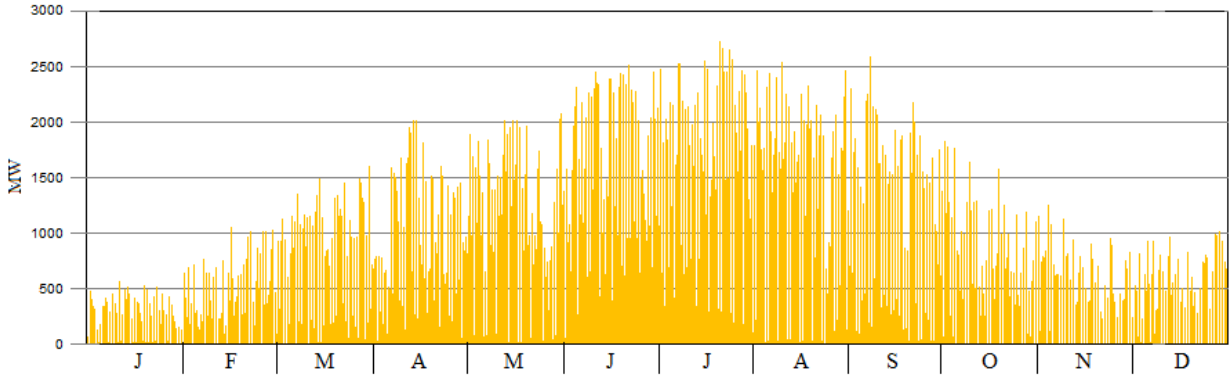

Figure 6.17. UK solar generation during the year, hourly data [78].

6.3.5 Electrical dynamic load

The dynamic load models are connected to LV network and are implemented based on load profiles of Finnish customers. The use of the hourly load profiles is possible because of a large amount of AMR's installations. The active power P and reactive power Q absorbed by the load are changed depending on the positive-sequence voltage V and load profiles data. P and Q vary as follows [79]:

$$P = P_{LOAD\_PROFILE} \cdot \left(\frac{V}{V_0} \right)^{np} \tag{6.1}$$

$$Q = Q_{LOAD\_PROFILE} \cdot \left(\frac{V}{V_0} \right)^{nq} \tag{6.2}$$

- V_0 is the initial positive sequence voltage;
- $P_{LOAD\_PROFILE}$ and $Q_{LOAD\_PROFILE}$ are the initial active and reactive powers at the initial voltage V_0;
- V is the positive-sequence voltage;
- *np* and *nq* are exponents controlling the type of the load (to get a constant impedance load, they are set as 2 in the model).

To define $P_{LOAD\_PROFILE}$ and $Q_{LOAD\_PROFILE}$ for the each user, the widespread load model among software applications of Finnish DNO was used [79]. It represents the expectation value $E[P(t)]$ and standard deviation $s_p(t)$ for the customer's hourly load as a linear function of the annual energy consumption W_a. The hourly load parameters with index series were calculated based on the following equations [80]:

$$E[P(t)] = \frac{W_a}{8760} \cdot \frac{Q(t)}{100} \cdot \frac{q(t)}{100} \tag{6.3}$$

$$s_p(t) = E[P(t)] \cdot \frac{s_{\%}(t)}{100} \tag{6.4}$$

- $Q(t)$ considers the model's seasonal variation with 26 two week indices;
- $q(t)$ takes into account the model's hourly variation for three different day's types (working day, Saturday and Sunday);
- $s_{\%}(t)$ is the index that defines a percentage of the average load.

The implementation of such dynamic load model in MATLAB® is presented in Figure 6.18 and is explained based on one of the utilized profiles. In this model $P_{LOAD\_PROFILE}$ is marked as *P0* in Figure 6.18 and the corresponding $Q_{LOAD\_PROFILE}$ is defined considering that the PF is equal to 0.95_{ind}.

P0 is calculated by multiplying several signals from demand response (marked as *DR* in Figure 6.18), Random number block and Constant value (*P20*). There is also the coefficient to the product of these signals.

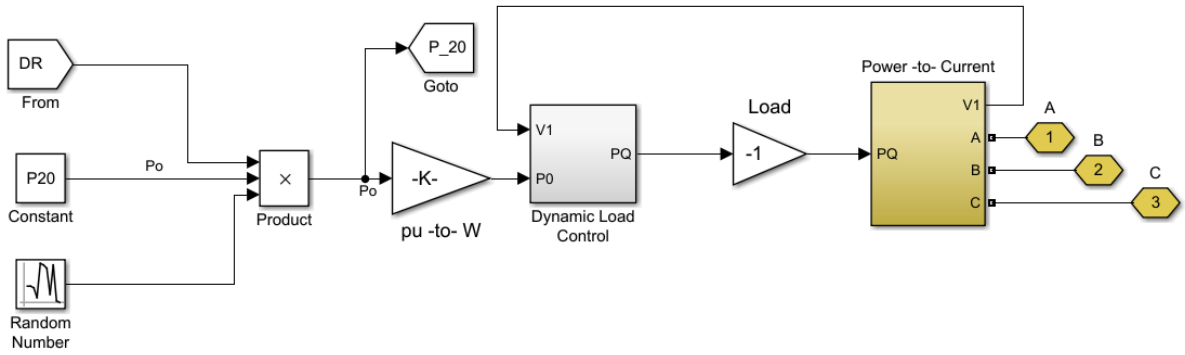

Figure 6.18. The dynamic load model in MATLAB®.

Constant value *P20* represents the total hourly profile index that includes both $Q(t)$ and $q(t)$ for a specific hour. To get the expectation value of average hourly consumption (50 % confidentiality) for a specific customer profile this hourly profile index is multiplied by the average power of a specific user.

The average power coefficient for a specific user is set in pu-to-W block and was calculated by dividing the annual consumption with a number of hours in a year (8760).

However, there are also two factors that have an impact on the load power. First one is the signal from DR that can decrease or increase the consumption and consequently the load. The second factor represents total hourly deviation index that is used to simulate the load changing caused by the customer's behavior. The Random Number block illustrated in Figure 6.19 that generates normally distributed random numbers is used to implement the deviation. It returns a sample of random numbers of a normal distribution with mean $\mu = 1$ as well as the corresponding variance σ^2 and sample time for a specific hour and a specific customer profile.

The probability density of the normal distribution is defined by 3-sigma rule explained in Figure 6.20. According to [81], about 68% of values are restricted by the frameworks of one standard deviation σ; about 95% of the values can be located at the distance of two standard deviations from the mean value, and about 99.7% of the values can be found within three standard deviations. Sample time for such variation is chosen based on the hypothetic behavior of end users and, in average, is equal to few minutes for different profiles.

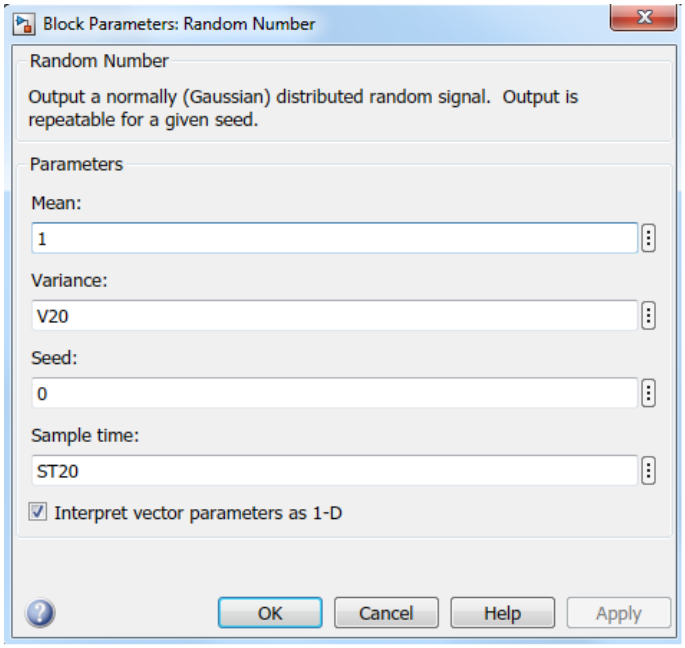

Figure 6.19. Random number block settings.

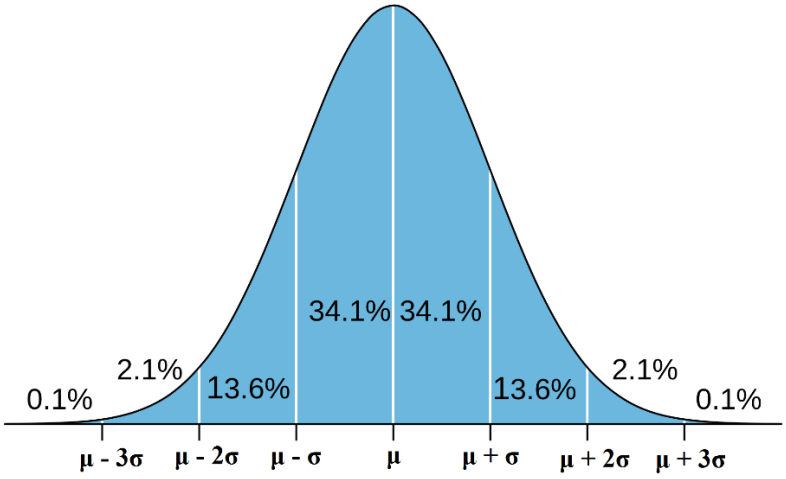

Figure 6.20. 3-sigma rule of normal distribution [81].

GoTo block P_20 is used to reduce the number of the model's calculations. It sends the production of DR signal, hourly profile index, and hourly deviation index for a specific profile. Thus, to calculate the input power for the others load within this profile the average load of a specific user is multiplied with the signal from GoTo block. It also gives possibilities for more flexible DR control, since the response time of the load and the amount of the load changing can be specified for every profile.

It is worth to mention that all parameters in the load model can be changed to investigate particular environment. To change the parameters it is necessary to specify the hour of the simulation and download the profiles data in MATLAB® workspace by a specific code. After that, there is a separate MATLAB® model where by using Look up tables it defines hourly profile indexes and hourly deviation indexes of different customer profiles and downloads them to the workspace. This process for a specific profile is elucidated in Figure 6.21. Sample time for each profile is set manually.

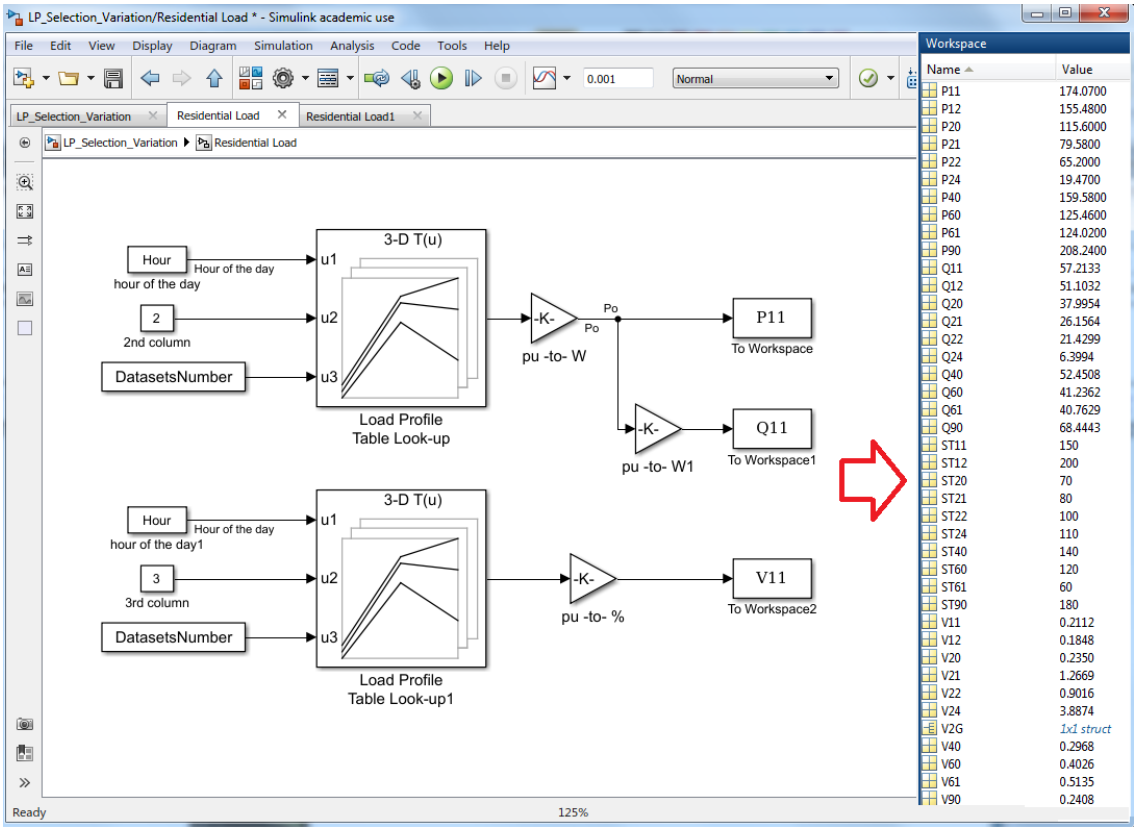

Figure 6.21. The process of defining the input parameters for the load.

The modeled region represents a rural area with typical loads as detached houses, stores, livestock and some manufacturing. There are ten load profiles used in the model for 285 customers. Among the modeled loads the most spread are detached houses with direct electrical heating and holiday houses. All profiles are described in Table 6.1. The hourly load and deviation curves of all profiles are illustrated in APPENDIX A.

Table 6.1. Description of used load profiles.

№	Customer group	Sener load profile	Description
1	11	I000110	Detached houses, direct electrical heating
2	12	I001120	Holiday's houses, conversion circuit
3	20	I000712	Livestock and dairy economy, housing is included
4	21	I000721	Meat production, housing is not included
5	22	I000711	Livestock and dairy economy, housing is not included
6	24	I000732	Plant production, housing is included
7	40	I810480	Manufacture of metal and mechanical engineering
8	60	I920623	Other retail trade
9	61	I920622	Department stores and market places
10	90	I910830	Hospitals and health care

6.4 Aggregated data of the model

The created simulation model has following aggregated data:

- Time domain - Phasor mode with variable time step;
- The network represents a typical Finnish distribution system (110/20/0.4 kV) with imagined RDG, where one 29 km feeder of 20 kV substation is modeled;
- The total feeder load vary from 100 kVA to 500 kVA at the power factor of 0.95_{ind};
- HV power grid is modeled by the three-phase programmable voltage;
- HV transmission lines are implemented by three-phase PI Section Line block;
- Ideal cable model is applied for MV and LV lines;
- The model contains 1 OLTC transformer (10 MVA, 110/20 kV, ± 9 x 1.67 %, Wye/ Delta1) and 49 off-load tap changer transformers (20 kV/0.4 kV, ± 5 (2 x 2.5) %, Delta1/ Wye) as well as the transformers with constant turn ratio;
- The dynamic load model is based on hourly load and deviation of 10 load profiles that are specified for 285 Finnish customers in LV network;
- The 1 MW wind turbine and household 1 kW PV systems working at unity power factor represent imagined RDG units.

6.5 Verification of the model

To validate the implementation of the model, voltage profile of the feeder from the real DMS600 obtained by the means of power flow simulation was compared to the voltage profile of the same feeder in implemented MATLAB® model with a static load for a specific hour. The chosen time parameters are 17th July (Monday) 2017 with time from 13:00 to 14:00 that almost corresponds to the minimum load conditions. The 3D voltage profiles are displayed below in Figure 6.22. Since the load is static and no disturbances are applied to the model, the voltages are stable during the simulated hour.

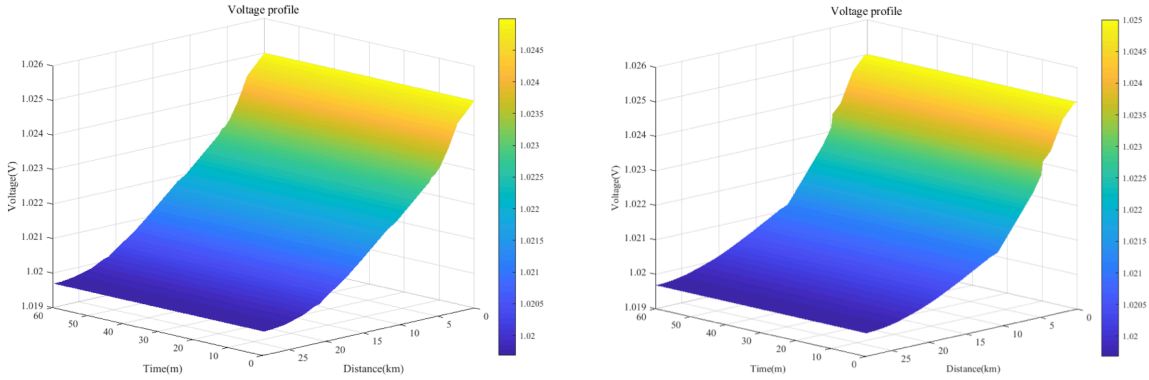

Figure 6.22. 3D voltage profiles of the feeder; Voltages here and later are according to the base MV network value (20 kV); The left is from the DMS600, the right - from the model.

The visualization of the voltage profiles is close to each other, but some diversity can be seen. It is noticeable in the middle of the feeder where voltages in the MATLAB® model are dropping a little bit more than in the DMS model. However, it could appear because of the slightly different measuring points of voltage along the feeder between the models in DMS and MATLAB®. The second reason is that the DMS power flow calculations consider more factors than it is done in the model, including the effect of other feeders connected to the substation. The zero point of the Distance axis corresponds to the supply point of the feeder at the substation as well as the farthermost point of the feeder is about 28.5 km. It is important to mention that the voltage descending from the substation to the end of the feeder as in conventional networks without DG. The voltage drop along the feeder is almost identical in both cases. The voltage drop from the real DMS600 is equal to 0.53 %, as well as it is equal to 0.5 % for the model that can be considered the same. Thus, despite some small diversity, the model can be used for further research.

6.6 Conclusions about chapter 6

The simulation model of the grid with RDG that allows investigating different network states and the effectiveness of developed dispersed voltage control algorithms was implemented in MATLAB® environment.

The accuracy of the model was verified by comparing the voltage profile of the feeder of the MATLAB® model with the voltage profile of the same feeder of the network based on data from the real DMS600 system for the predefined time.

7 SIMULATION ON VOLTAGE CONTROL ALGORITHMS

The purpose of this chapter is to investigate the effectiveness of developed dispersed voltage control algorithms on the created in MATLAB® simulation model of the power grid with RDG presented in the previous chapter. The effectiveness of the algorithms to mitigate voltage rise and fluctuation problem will be evaluated by the overvoltage time that they will be managed to decrease. The sections for every algorithm's simulation are built in the same manner. Initially, the network conditions and organization of the environment are discussed, then the results of simulations are illustrated and estimated.

7.1 Demand response algorithm

7.1.1 Network conditions and parameters

The reason for voltage rise and variation is a widespread installation of household PV systems and operation of the 1 MW WT in the end of the feeder at full capacity. Without the presence of the PV systems in the network, nominal power of WT creates an increase in voltage that is a bit more than 4 % limit defined by the rules [82]. However, the household PV systems add additional voltage rise in specified conditions. The location density of PV systems along the feeder is shown in Figure 7.1. The PV systems are installed for 69 customers normally distributed along the feeder that is corresponding to 23 % of all modeled customers.

The utilized irradiances with shading for minimum and maximum loads as a function of time are depicted in Figure 7.2. During the simulation time, the irradiance goes up from 100 to almost 1200 kWh/m^2 during minimum load/maximum generation or to almost 600 kWh/m^2 in the case of the maximum load/maximum generation. The wind curves with small deviation as a function of time are illustrated in Figure 7.3. The coefficient 0.95 is applied to the wind profile of minimum load/maximum generation conditions in comparison with maximum load/maximum generation. The selected parameters such as solar irradiance, shading, wind speed variations are created artificially based on the pure randomization within imaginary limits without the applying any statistical distributions. They were chosen to demonstrate the ability of voltage control methods to cope with possible disturbances. It is also valid for further input parameters applied for the simulations.

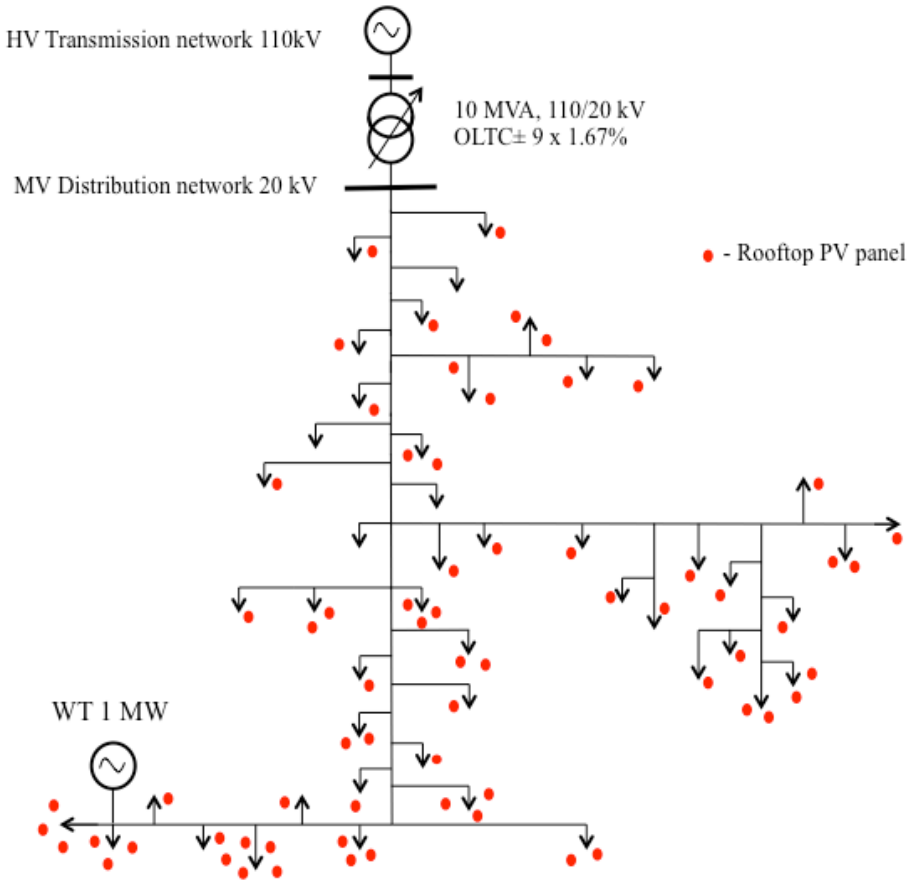

Figure 7.1. The location density of household PV systems.

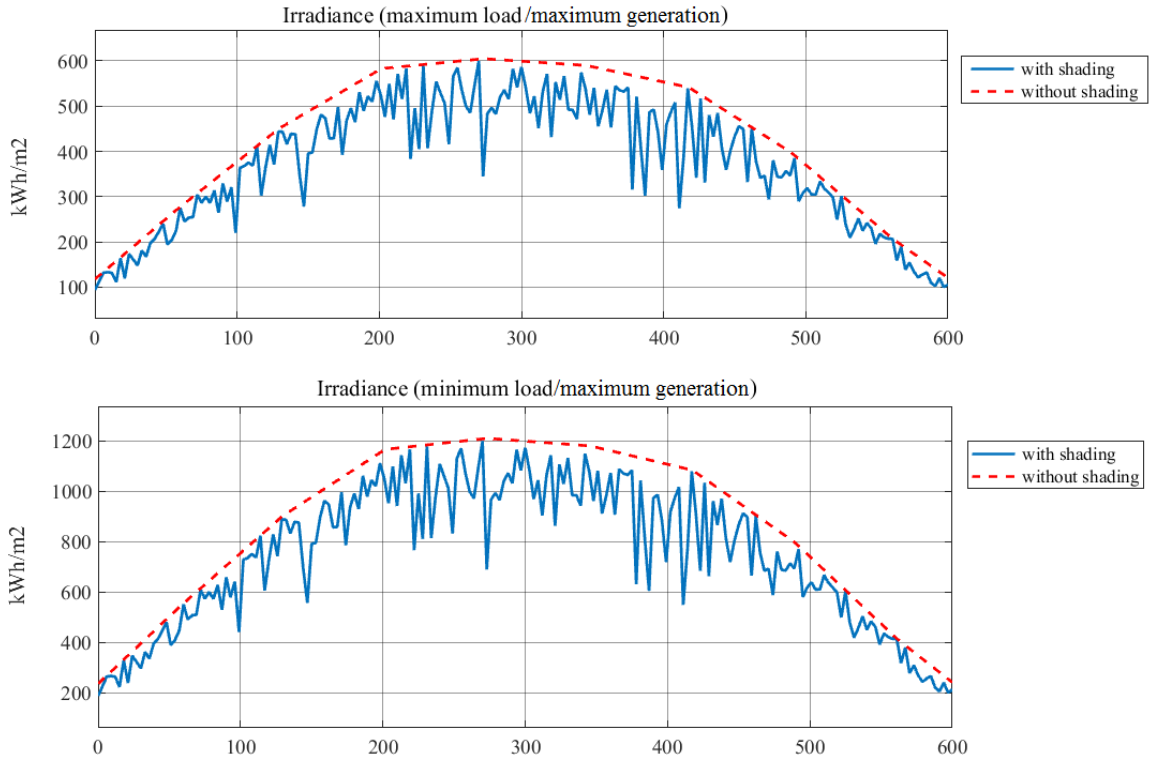

Figure 7.2. The irradiance for the model as a function of time (s).

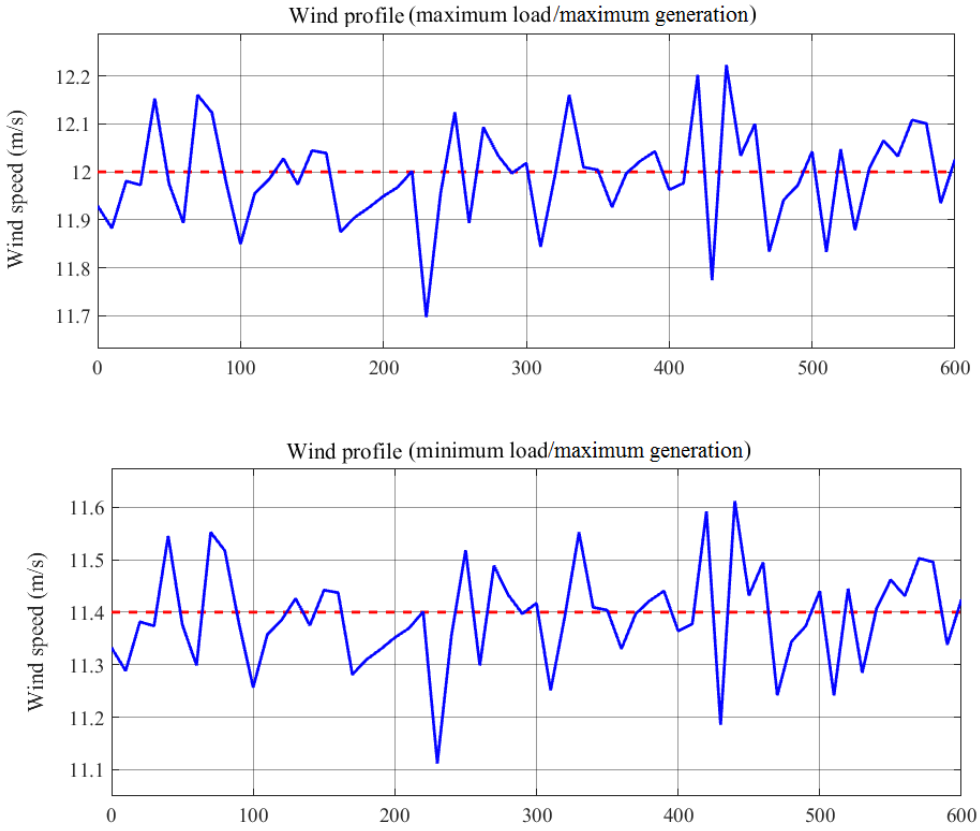

Figure 7.3. Wind profile for WT as a function of time (s).

7.1.2 MATLAB® simulation arrangements

Two MATLAB® models will be used for the environment of DR voltage control. The Detailed Phasor model emulates a real distribution network, and the second model is the prototype software of the real-time DR algorithm. The exchange of measurements and control signals is implemented by OPC standard. The data are maximum voltage and commands for the loads to alter its consumption. The data transfer is clarified in Figure 7.4. The delays in communication are set in DR control algorithm as 0.05 s and by means of OPC server's updating time, which is equal to 10 ms.

To create OPC communication Matricon OPC Server for Simulations and Testing was used. The process of the server development is depicted in Figure 7.5. In the server, new Alias group called DR was first created, and after that new alias elements known as DR and Vmax were added to this group. Then, Matricon OPC Explorer was used as a first OPC client to monitor the parameters in real-time as demonstrated in Figure 7.6.

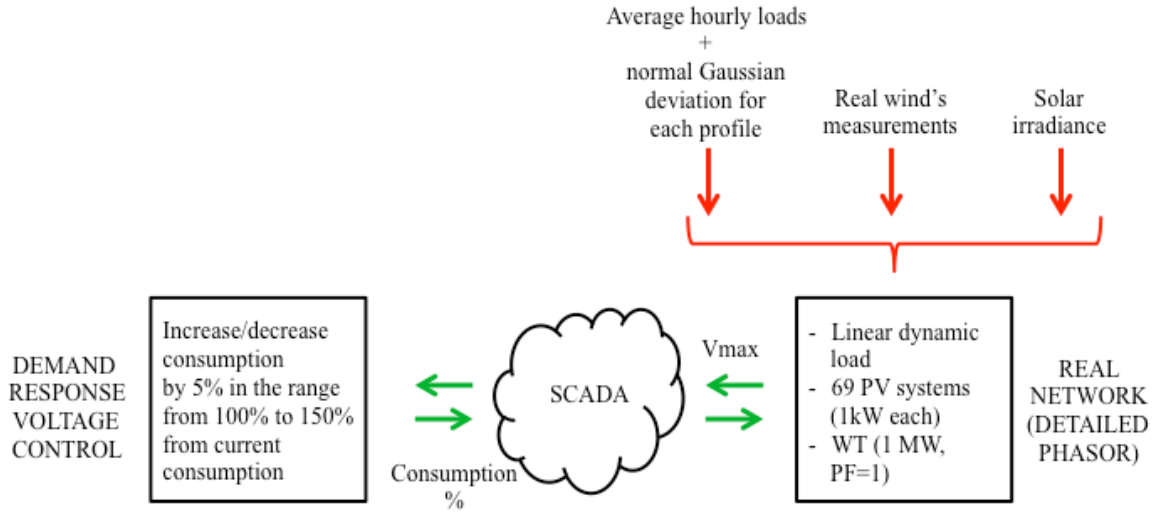

Figure 7.4. The simulation environment for DR control.

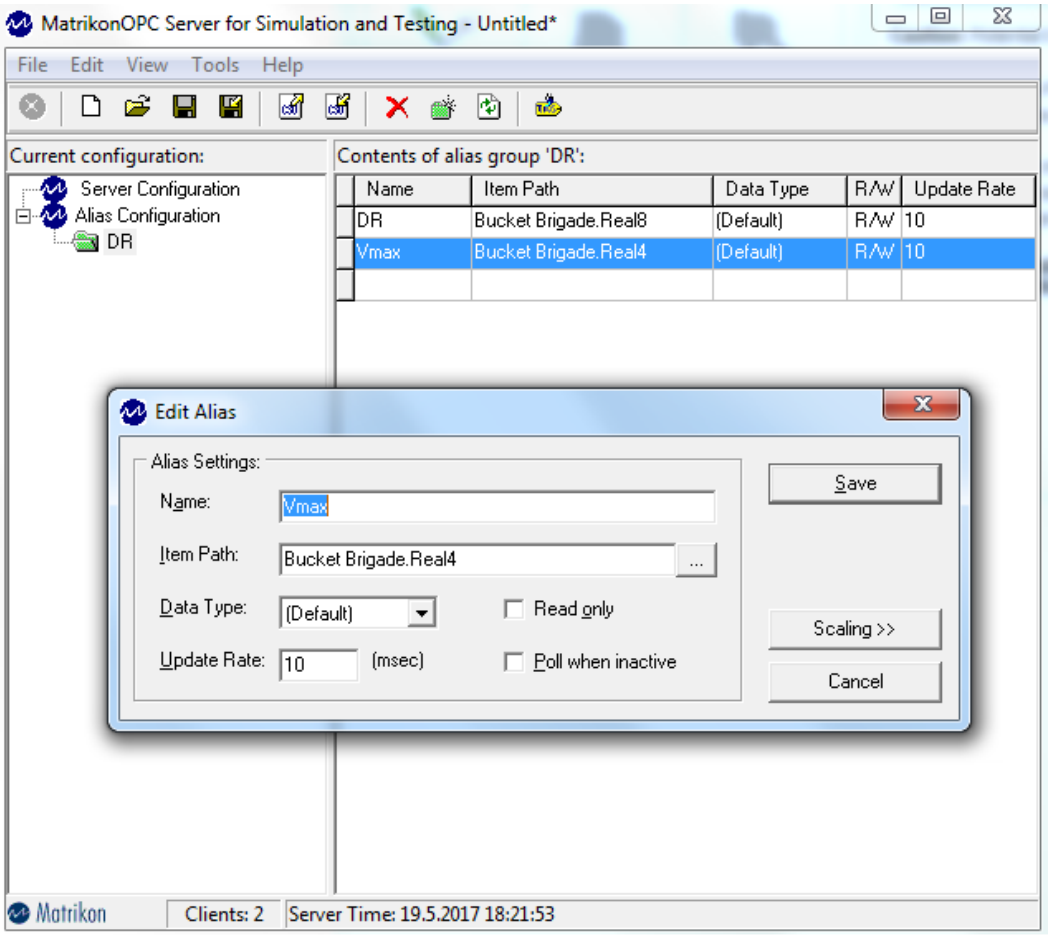

Figure 7.5. The process of the Alias configuration.

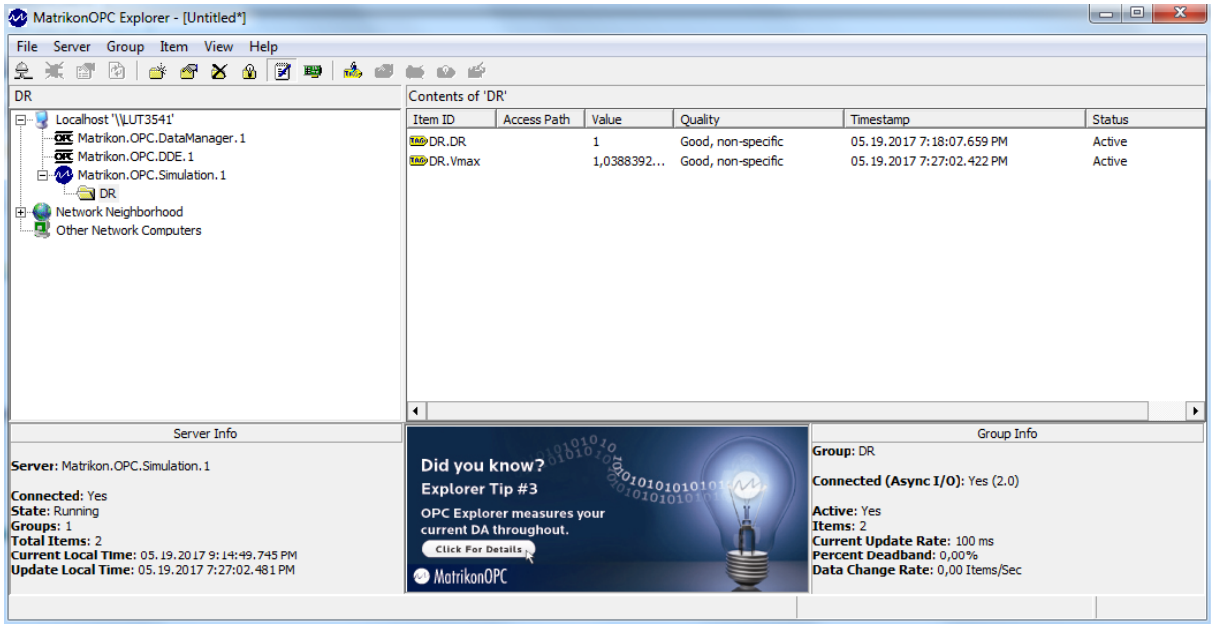

Figure 7.6. The OPC client.

The second OPC client is created by the means of OPC Toolbox™ that provides access to real-time data directly from MATLAB®. The organization structure of the MATLAB® model used to represent DR control with the employment of OPC Toolbox™ is described in Figure 7.7. The OPC Write block that is not presented in Figure 7.7 collects the data about voltage and writes them to the server. This information is then read by OPC Read Block and is fed to the DR control algorithm. The same model of communication with the use of OPC is organized for other simulations in this thesis, and the description of each case will be omitted.

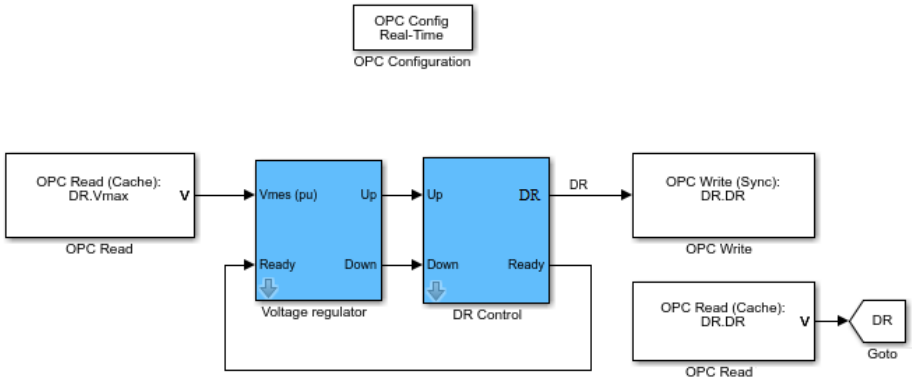

Figure 7.7. The structure of OPC communications in MATLAB®.

7.1.3 Simulation results

Case 1: maximum generation/minimum load, WT in the end of the feeder;

The maximum generation/minimum load conditions correspond to summertime when there is not too much load available for control, but the power generated by WT and household PV systems contributes to voltage rise and fluctuations. Power generation, as well as the voltage profile, highly depends on the wind fluctuations because of the significant WT's power. The effect of PV systems can be seen if compare the voltage profile of the feeder without PVs in the same conditions as illustrated in Figure 7.8. Yellow part corresponds to voltage rise because of active power generation of PV systems. According to the input irradiance, it contributes to 0.4 % of the voltage in maximum point. The effect of DR operation is marked by blue in Figure 7.9, and it is much less than the effect of PVs and corresponds to approximately 0.02 % of the voltage in maximum point.

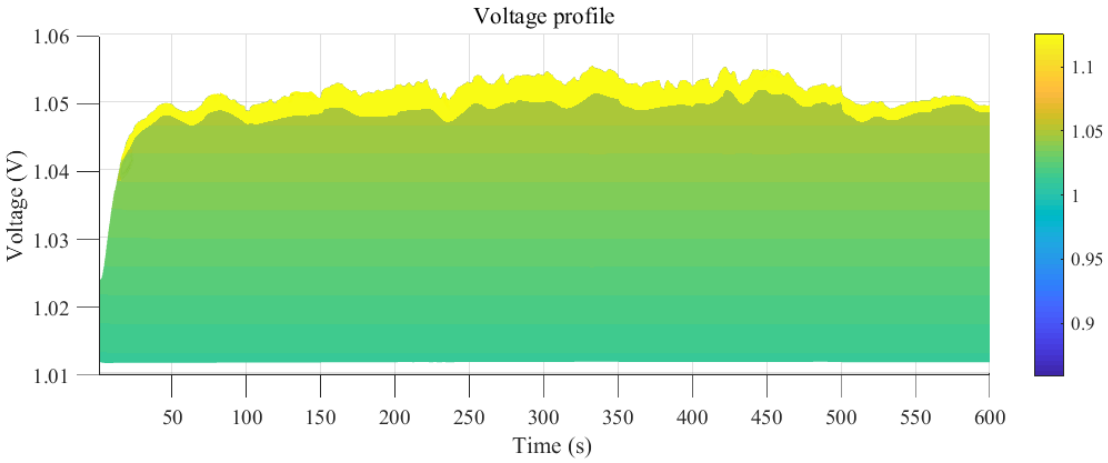

Figure 7.8. Voltage profile of the feeder with power injections from PVs (yellow).

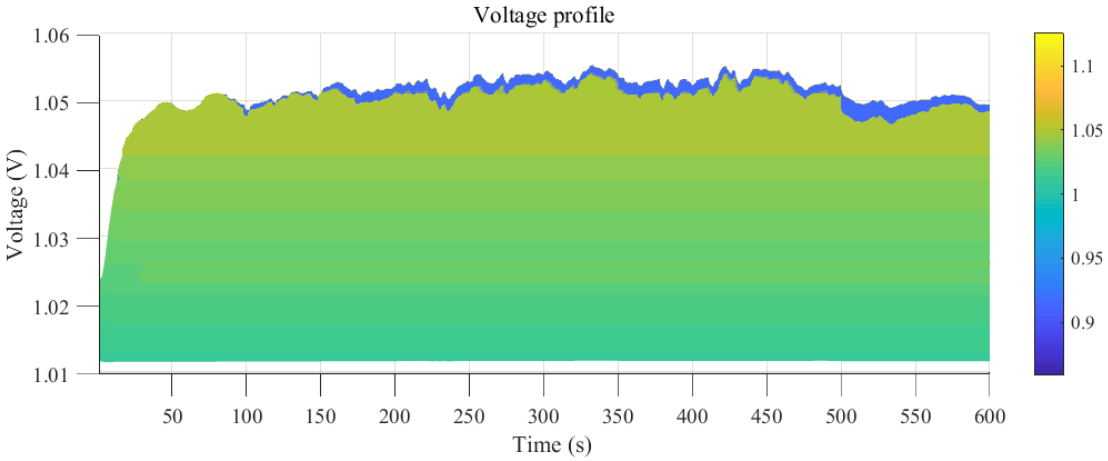

Figure 7.9. DR effect (blue) comparing with the feeder profile without DR.

Nevertheless, DR allowed reducing the overvoltage duration in 1.35 times from 470 s without DR control to 350 s with DR control. The operation of the algorithm is explained in Figure 7.10. The DR algorithm was activated 4 times and 60 % of the time was either increasing consumption or was at the maximum point.

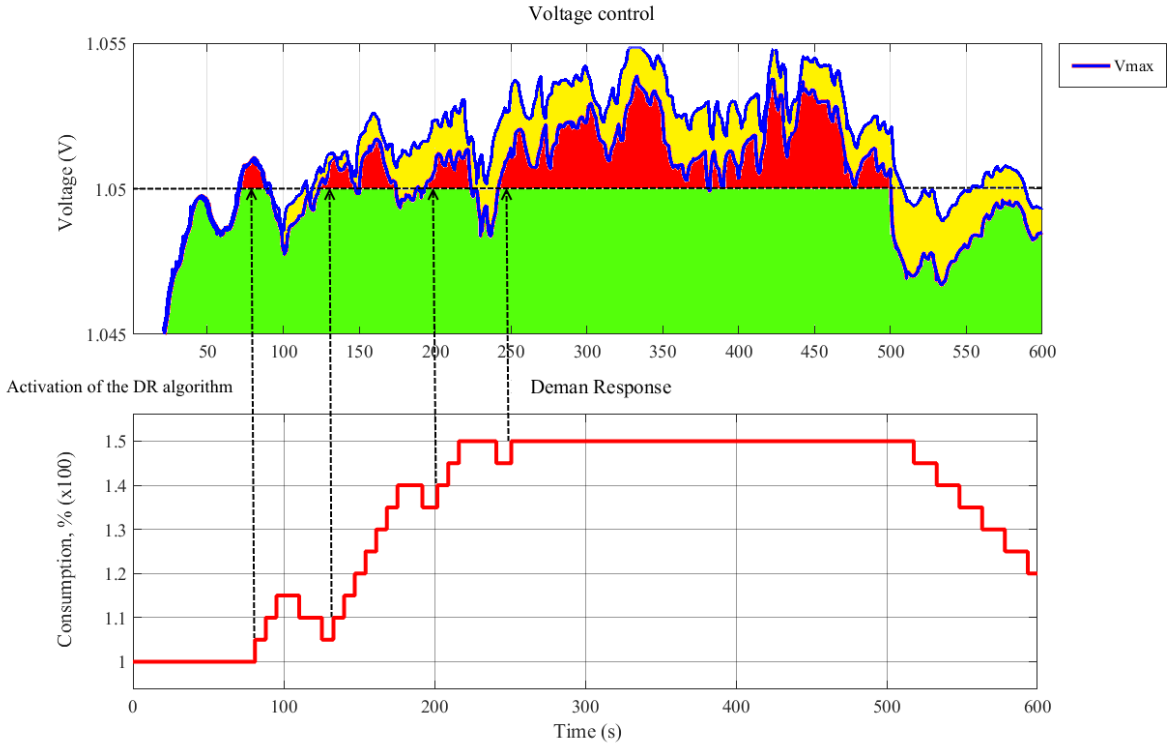

Figure 7.10. The operation of the DR algorithm.

It served well in the moment of small voltage rise as in the last 100 s of the simulation where about 50 s of overvoltage time were cut down to zero. In average, additional 30 % of consumption were involved for that purpose. However, DR could not return voltage in its tolerance range in the moments of maximum active power injection from WT and PV systems, despite the fact that the consumption was increased to the predefined maximum of 150 %.

The 3D voltage profile of the feeder with DR control is presented in Figure 7.11. In average, voltage rise is equal to 4.8 % from the point of the substation to the end of the feeder.

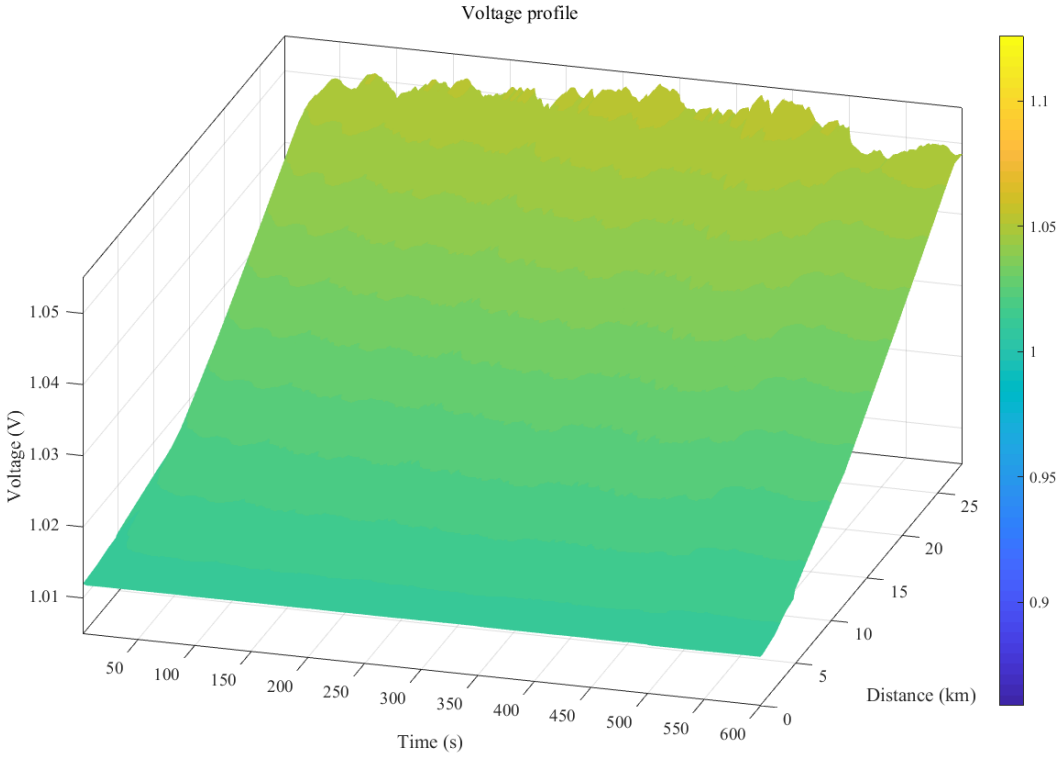

Figure 7.11. 3D representation of the feeder voltage profile with DR.

Case 2: maximum generation/maximum load, WT in the end of the feeder;

These conditions correspond to wintertime when maximum power injections for that period of time from household PV systems and WT led to voltage rise. The voltage rise because of the PV systems is illustrated in Figure 7.12 and is equal to approximately 0.2 % of nominal voltage. That is less than in the previous case because the irradiance was decreased. However, the effect of DR is noticed more. As it can be seen in Figure 7.13, at the point of 500 s it decreased the voltage by 0.7 % that is an ambitious result.

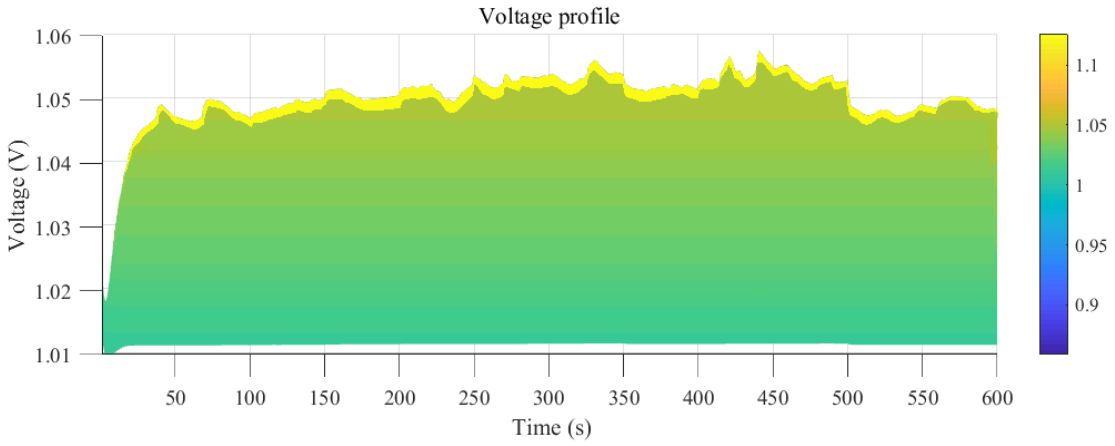

Figure 7.12. Voltage profile of the feeder with the effect of PV power generation (yellow).

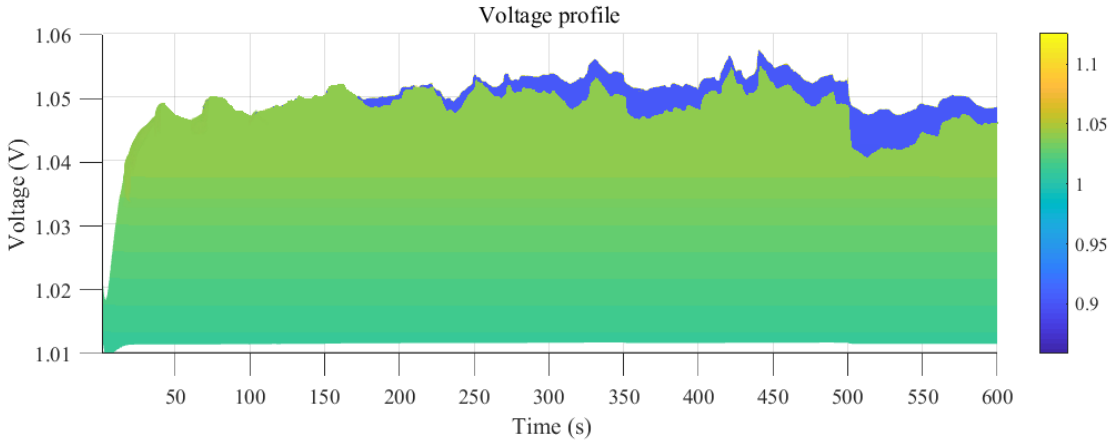

Figure 7.13. DR effect (blue) comparing with the feeder profile without DR.

If comparing the operation time of DR with the previous case, the operation time for the current case is lower, but the number of algorithm activations is more. As it can be seen from Figure 7.14, there were 6 activations of the algorithm, resulting in 40 % of the time when the load was increasing. However, the last activation could be erased by setting the delay before activation bigger or activating the algorithm by dynamic voltage value.

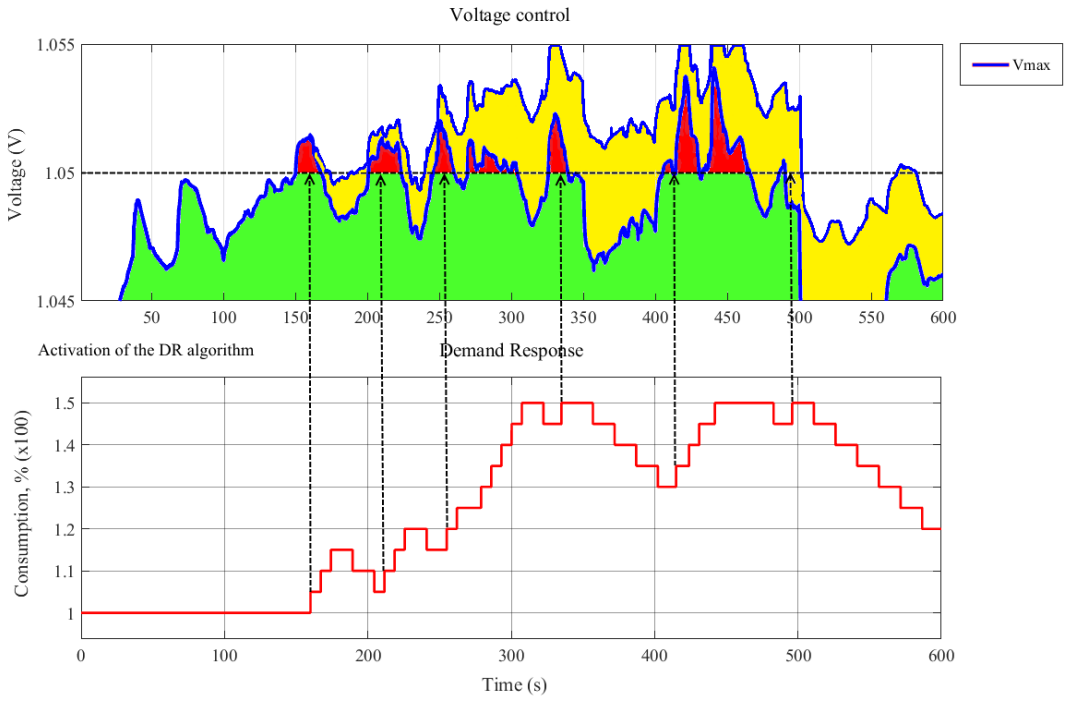

Figure 7.14. The operation of the DR algorithm.

Less operational time became possible because of the more balanced relation of generation and consumption in this period of time. Consequently, as it can be seen from Figure 7.14, the

average consumption enlargement of DR is lower, and it is equal about 120 % of the load. However, the effect of DR is more noticeable because of the large load available for control. The overvoltage duration was decreased in 1.9 times from 320 s to 170 s that is more effective than in the previous case. The 3D representation of the feeder with DR is displayed in Figure 7.15, and it has the same characteristics as in the first case.

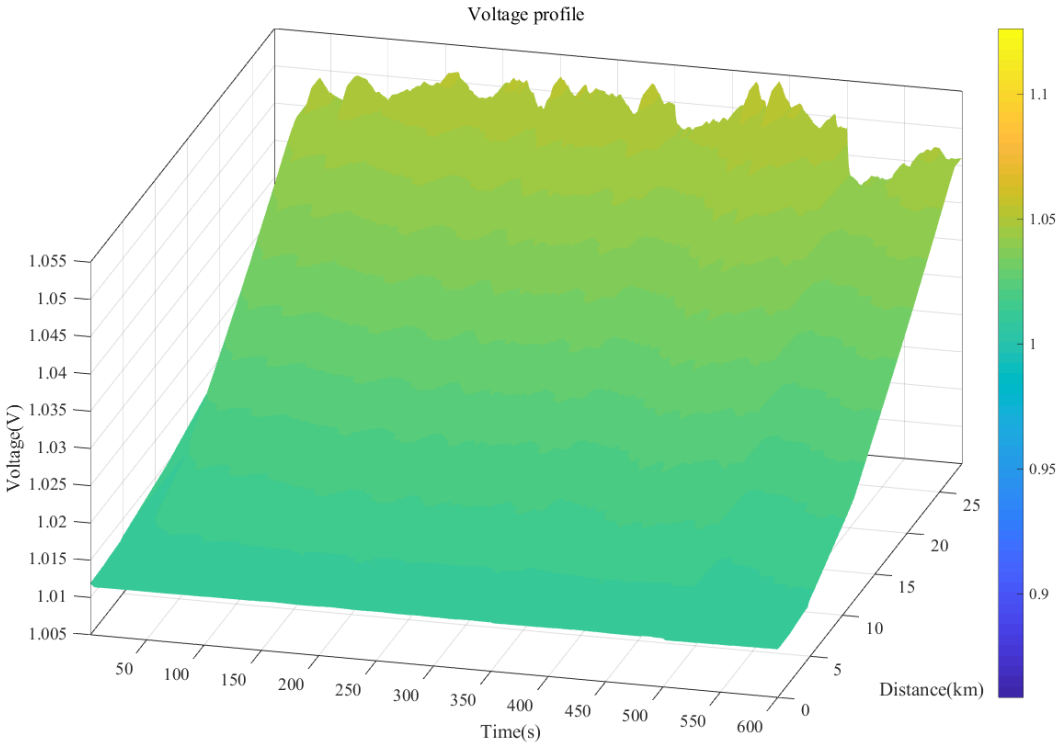

Figure 7.15. 3D representation of the feeder voltage profile with DR.

7.1.4 Conclusions on simulation results

Thus, in the most severe case with the location of WT in the end of the feeder, DR contributed to voltage support and allowed to reduce the duration of the voltage rise. According to the simulations, the available for the control load should be about 20-30 % of the current consumption. The system reserve electricity of existing controllable appliances could not be enough to achieve acceptable results, so DR needs more flexible resources in the grid for the qualitative operation. The situation will be enhanced when EESs, EVs, and other active resources start to play a significant role in grid operation. At that moment, it is obvious that including DR as a stand-alone method will not provide sufficient reliability for the voltage control, but it is definitely can be used as a supportive method. It can be utilized in coordination with main algorithms based on OLTC to decrease the number of tap changer's operations and deterioration of the taps as a consequence. It also can be involved in GC to

reduce unnecessary active power losses. As a result, including DR in voltage control algorithm will improve feasibility and reliability of RDG's dispatching.

7.2 Automatic voltage control algorithm

7.2.1 Network conditions and parameters

The simulation network contains two WTs located in the end and in the middle of the feeder as shown in Figure 7.16. The case will be investigated in minimum load/maximum generation conditions for both model-based and real-time AVC algorithm. The wind profile for both cases is demonstrated in Figure 7.17 and specified to investigate the operation of the method in case of stochastic power injections from WTs.

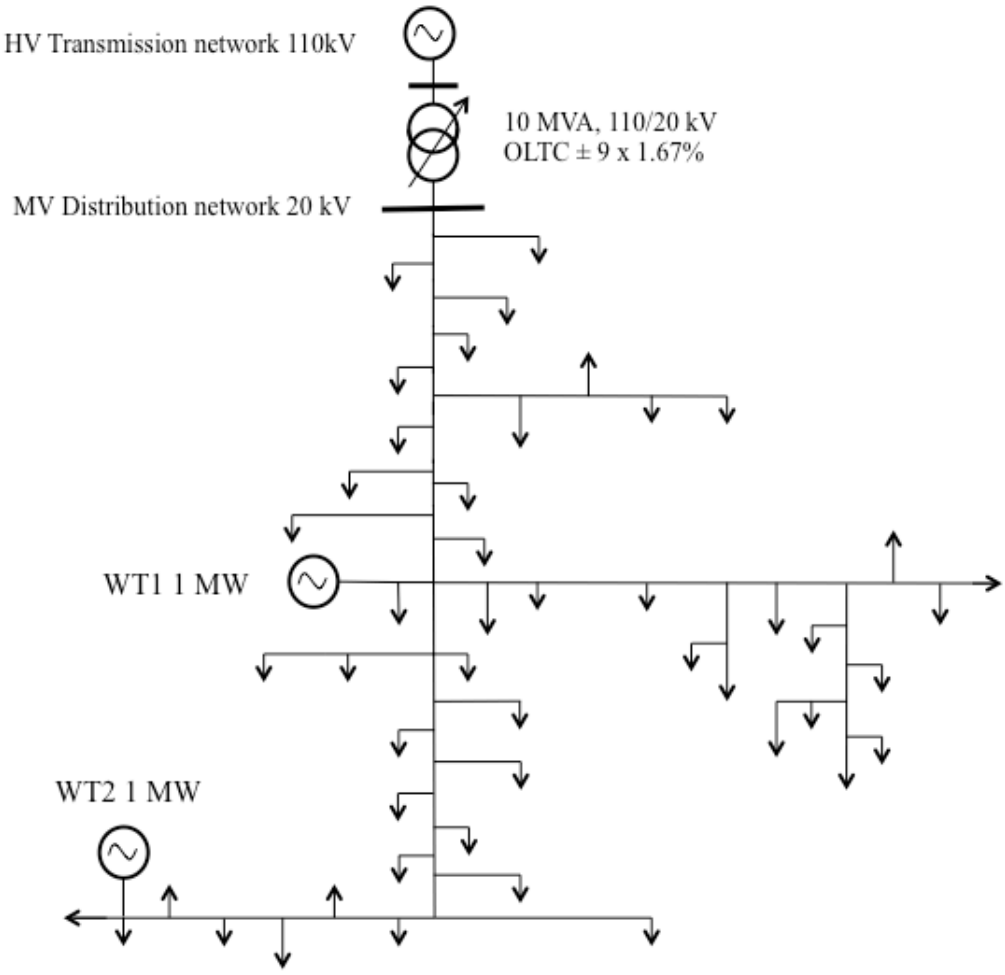

Figure 7.16. Simulation network.

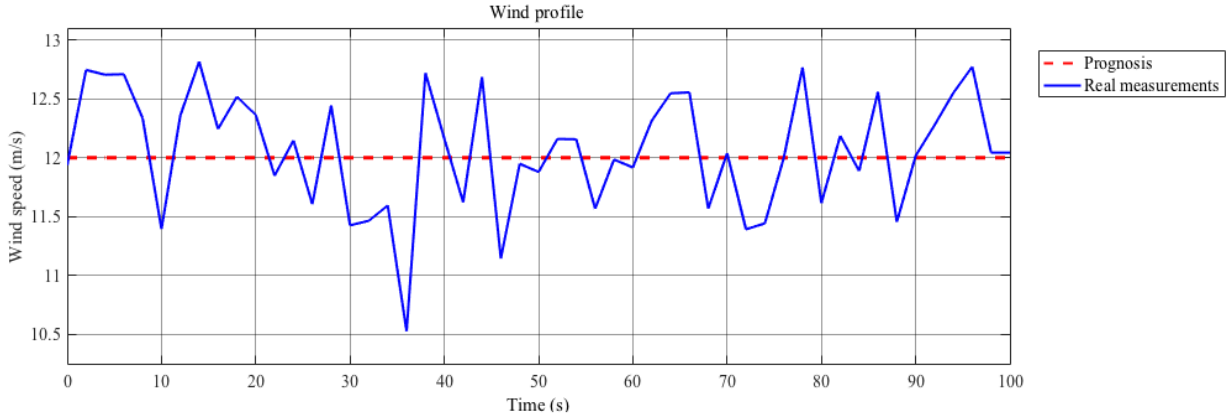

Figure 7.17. Wind profiles for AVC control.

7.2.2 MATLAB® simulation arrangement

The simulations are conducted in the MATLAB® simulation environment according to the simulation scheme elucidated in Figure 7.18. There are three MATLAB® models used in the simulations. The first model recreates a real distribution network (Detailed Phasor), the second model represents a DMS model (Simplified Phasor) and the third one is the prototype software of the real-time voltage control.

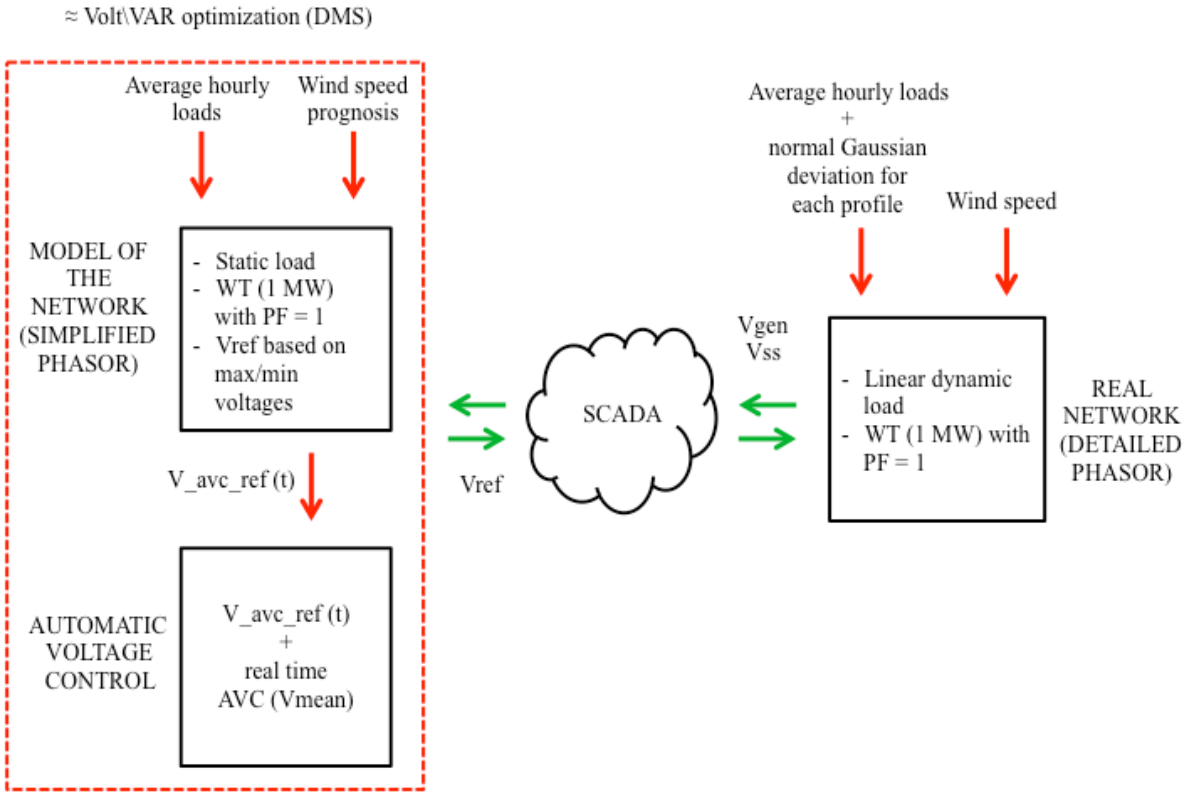

Figure 7.18. The simulation structure of VVC.

Data flows between the Detailed Phasor and the VVC are realized through a prototype of SCADA implemented by the means of OPC standard. Measurements signal from the simulated network are transferred to the server from where they are read by the AVC algorithm. The flow of control commands is done in the same way with the opposite direction. Data transfer between the AVC algorithm and DMS is realized using shared files as clarified in Figure 7.19. DMS writes a file with a reference voltage dependence that is read by the AVC during the simulation. Latency in SCADA communications is realized setting the updating time of OPC server to 10 ms.

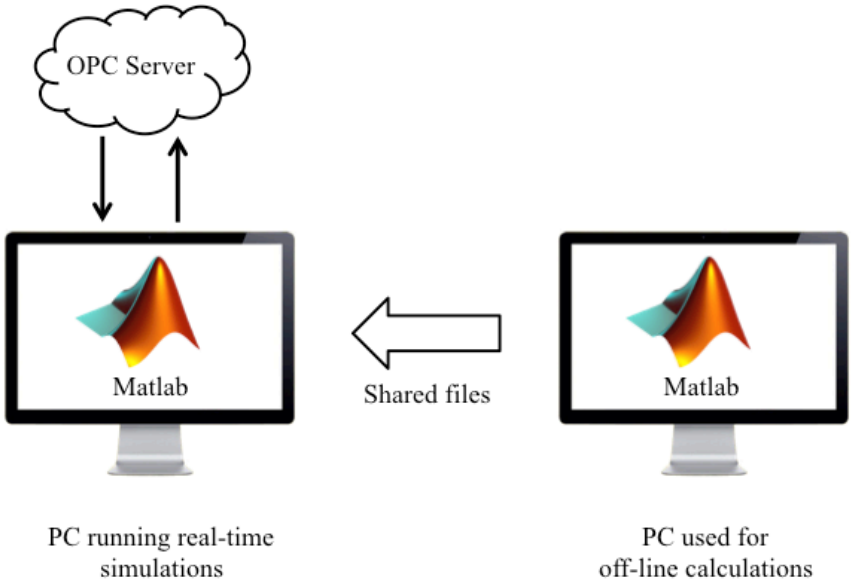

Figure 7.19. The communication structure of the simulation.

7.2.3 Simulation results

Case 1: Model-based AVC control

The simulation of Simplified Phasor model was first conducted to define input reference voltage signal for the voltage control algorithm. The corresponding curve of the reference voltage for that period of time was transmitted to the AVC part of the DMS and employed by the online part of AVC algorithm in the Detailed Phasor.

The voltage control algorithm of Simplified Phasor model used three tap changer operation to keep the voltages within the tolerance range, as it can be seen following the reference voltage in Figure 7.20. It is important to consider the fact that the operation of the WTs stated from

the beginning gradually rising the voltage in the feeder, resulting in this number of OLTC's operations. After the WTs stated to output nominal power (1 MW each) the AVC algorithm established final position of tap changer mechanism at the level of 3 taps. First two tap changing operations happened at the 14 s and 22 s. The last tap changing operation took place at 51 s. The obtained tap position is close to the optimum because it gives enough gap between the upper and lower limits that are equal to 1 % and 3 %, respectively.

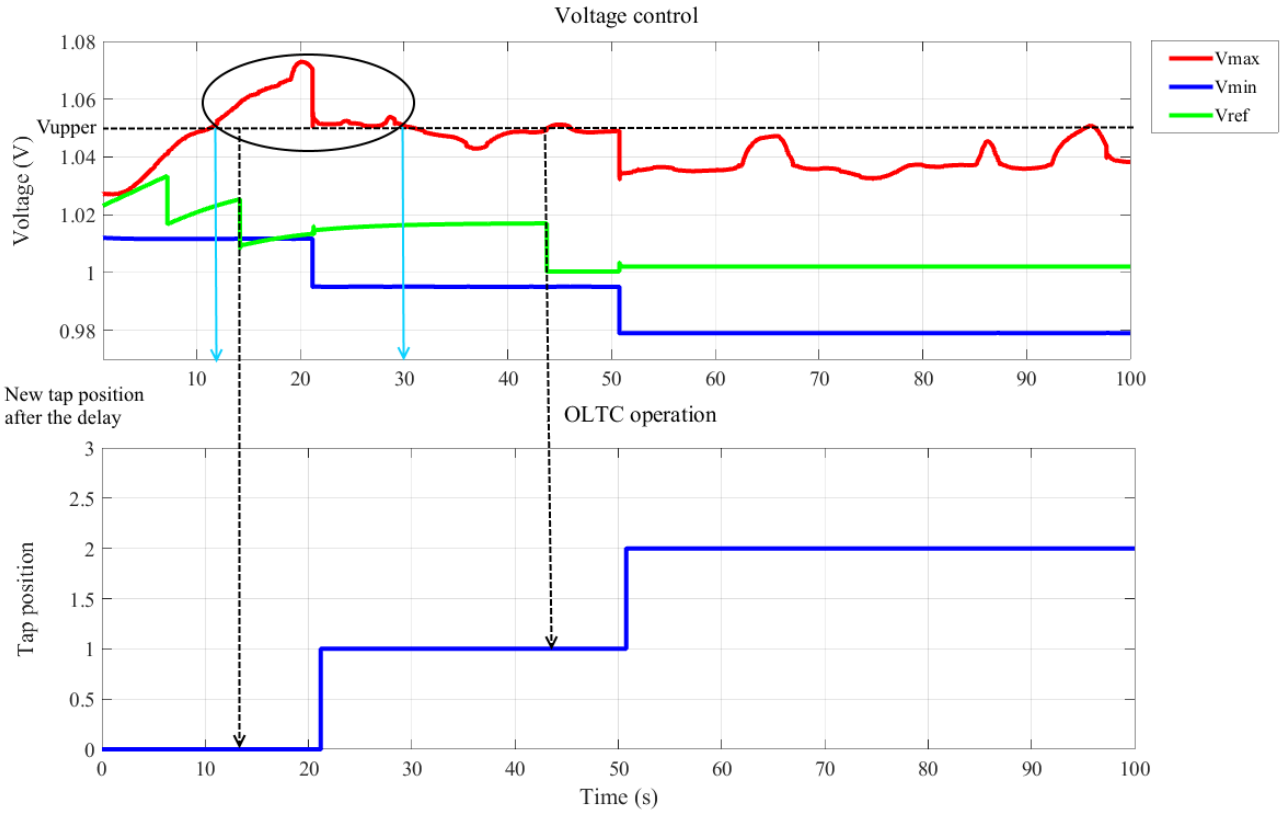

Figure 7.20. The results of Detailed phasor model simulations.

The results of Detailed phasor model testified that the algorithm applied one less number of tap changer's operations in comparison to Simplified Phasor model in spite of the stochastic behavior of the WTs. The first tap changing operation was ignored by the online control. The model-based reference voltage signal did not lead to the tap changer operation because of the DB between its signal's value and current mean value of real-time voltages. However, the DB was overcome when reference voltage decreased the second time. Ten seconds before this operation and about 8 s later, the maximum voltage exceeded the upper limit. The third decreasing of reference voltage provoked the second tap changing operation. It was right in time considering the following peaks at 65 s and 95 s.

The 2D and 3D representations of the feeder are illustrated in Figures 7.21 and 7.22, respectively. It is noticeable how the voltage profile was changed by the unstable power output of WTs. Figure 7.21 expresses a vivid characteristic of the voltage profile of the feeder with connected DG. The maximum point is at the place of large DG units' connection to the grid or at the substation in the case of the DG's absence or negligible power output. It is contrary to the traditional representations where maximum point is at the substation level. This information can be used for the networks' SE, and this is implemented in the real-time AVC algorithm.

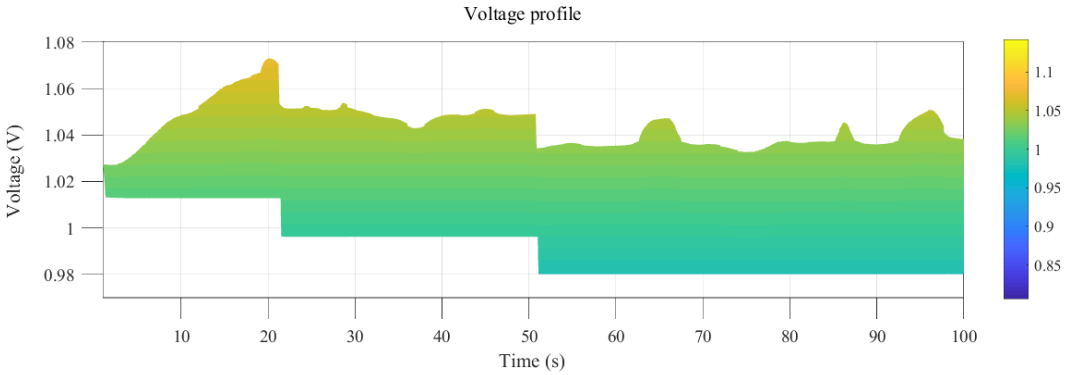

Figure 7.21. The 2D voltage profile of the Detailed Phasor model.

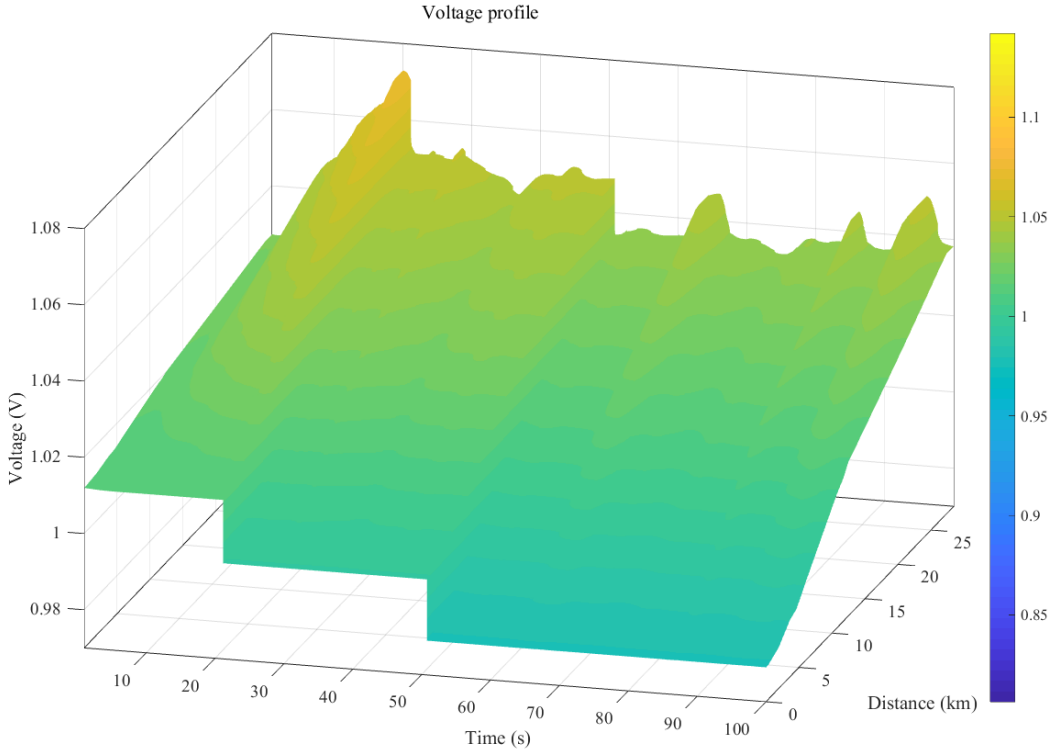

Figure 7.22. The 3D voltage profile of the Detailed Phasor model.

Case 2: Real-time AVC control

The same conditions as in the previous case were applied to the real-time algorithm to check it independent operation without the signal of the reference voltage from the Simplified Phasor. The illustration of the algorithm operation is described below in Figure 7.23.

Eventually, the simulation led to the same number of tap operations as with the reference voltage from the Simplified Phasor. Two tap changing operations were done in a row at 18 s and 25 s. Most of the time the second position of the tap was maintained. In such conditions, the overvoltage was kept during 14 s, and this is a bit better than in model-based control. As it is seen from Figure 7.23, the violation of upper voltage took place also at 96 s, but the algorithm was not activated because of the delay. That is a good strategy considering the stochastic operation of RDG. The 2D and 3D voltage profiles for this case are depicted below in Figures 7.24 and 7.25, respectively

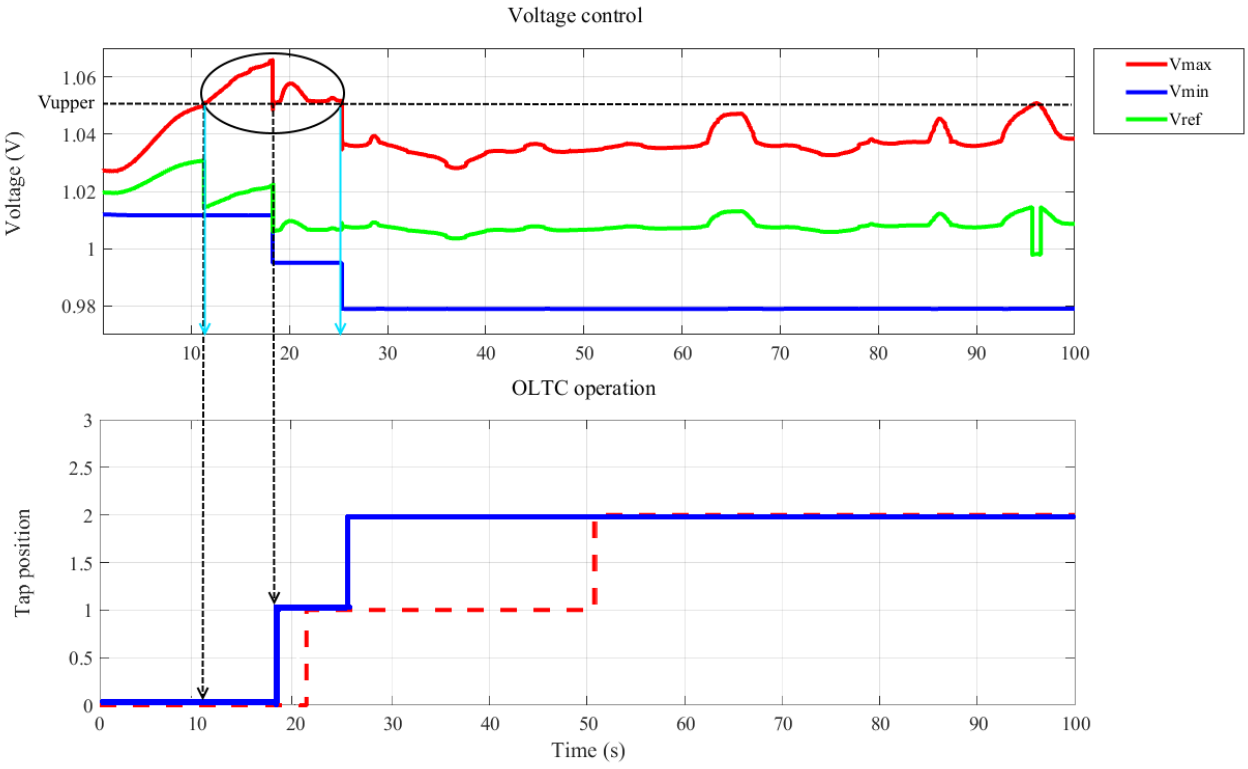

Figure 7.23. The operation of the OLTC mechanism without reference signal from the Simplified Phasor.

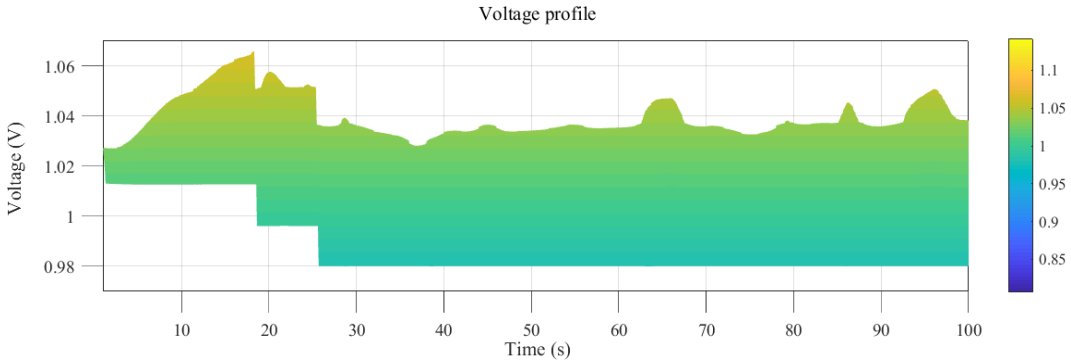

Figure 7.24. The 2D voltage profile of the Detailed Phasor model.

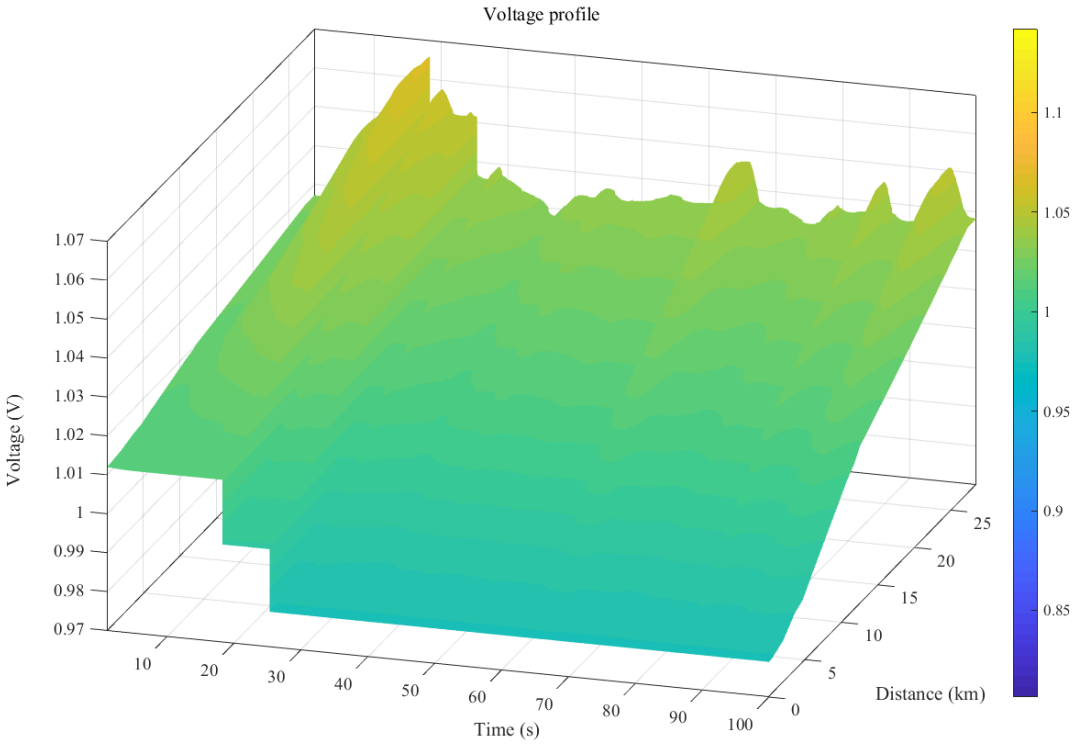

Figure 7.25. The 3D voltage profile of the Detailed Phasor model.

7.2.4 Conclusions on simulation results

Both AVC algorithms proved its reliability to operate in the networks with RDG. The simplicity of these algorithms allows utilizing them in existing networks without much investments and reconstructions. The problems of this method could be slow response time of OLTC's mechanism and its high degradation because of the frequent voltage variations caused by the power output of RDG units. However, the cooperation of this method with more fast one could reduce the employment of the OLTC's mechanism and improve voltage quality in the network. Such cooperation is researched in next section.

7.3 Cooperation of the real-time automatic voltage control with supportive methods

7.3.1 Network conditions and parameters

Two WTs and widespread installation of household PV systems were used to create the effect of voltage rise. The structure of this network is displayed in Figure 7.26. It is almost the same as was applied for DR algorithm with additional WT in the middle of the feeder. Wind profile for these conditions is illustrated in Figure 7.27.

The delay parameters were set in such way that first it gives an opportunity to a stand-alone operation of DR or RPC of PV systems, and if it is ineffective, then the AVC takes actions after 20 s delay. The rest of the settings for the algorithms are saved as described in chapter 5. MATLAB® simulation arrangements are the same, as they were applied for AVC and DR operations presented in Figures 7.18 and 7.4, respectively. The same arrangements as in the DR control are applied to the RPC.

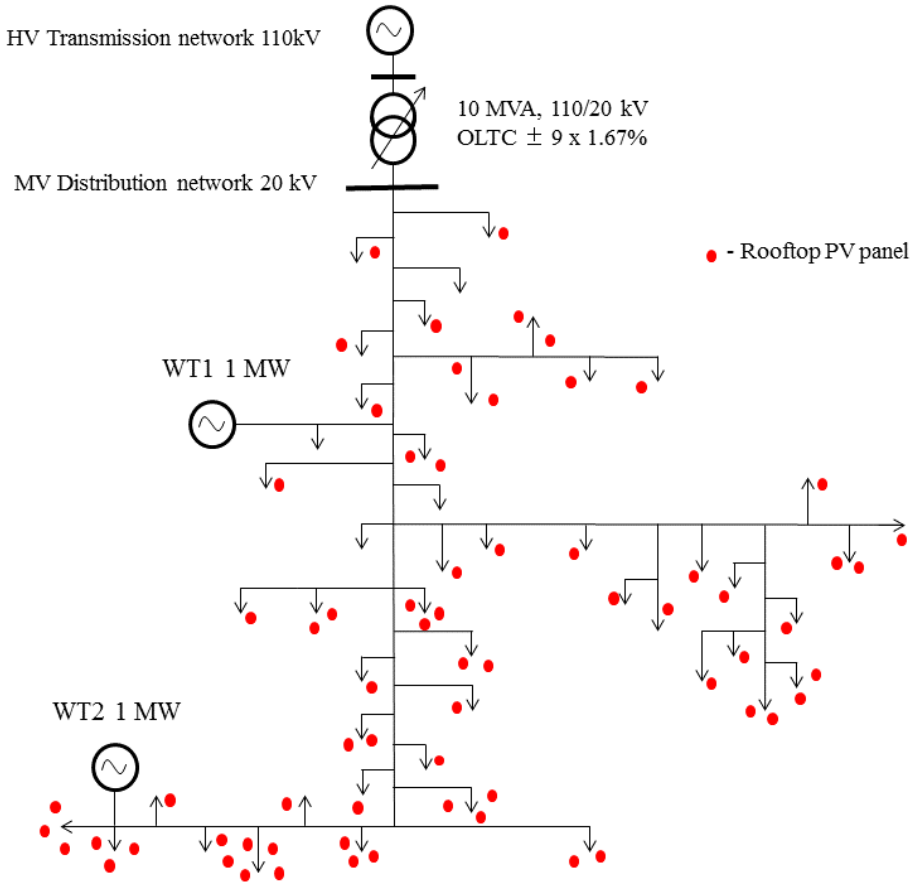

Figure 7.26. The network for the simulation of combined voltage control.

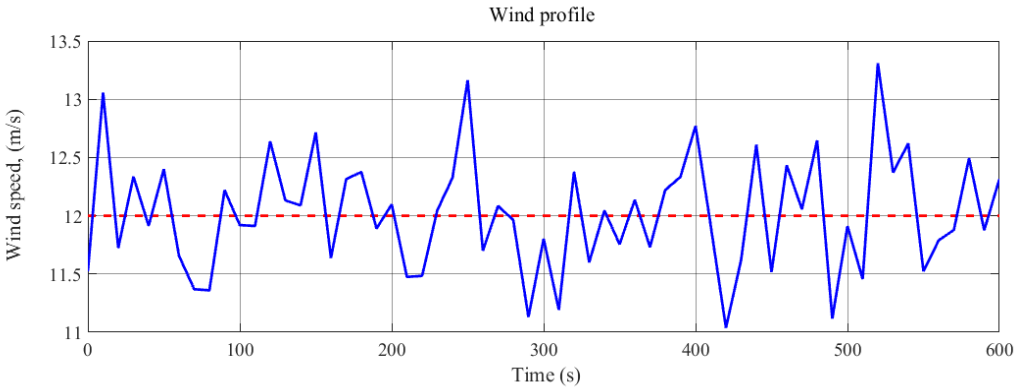

Figure 7.27. Wind profile for the simulation of combined method.

7.3.2 Simulation results

Case 1: Combined DR control and the real-time AVC algorithm

To compare the effect of DR support for the voltage control, the simulation of real-time AVC algorithm was first provided for the same conditions. Then the simulation with combined control took place. The results of such integrated voltage control are depicted in Figure 7.28.

The simulation without DR support led to three tap changer operations while only two operations were used for the combined voltage control, and this is the main effect of such control approach. The results depend most on the possible delay before the AVC operation. It is worth to notice that in the moments of small peak marked by the circles in Figure 7.28 the DR was activated and contributed to the fastest decrease of the voltage without the involving of tap changing. The average employment of the load was at the level of 115% during 75% of the simulation time.

The 2D and 3D voltage profiles of such control are demonstrated in Figure 7.29 and 7.30. The circled in Figure 7.28 points are easily distinguishable on the 3D profile.

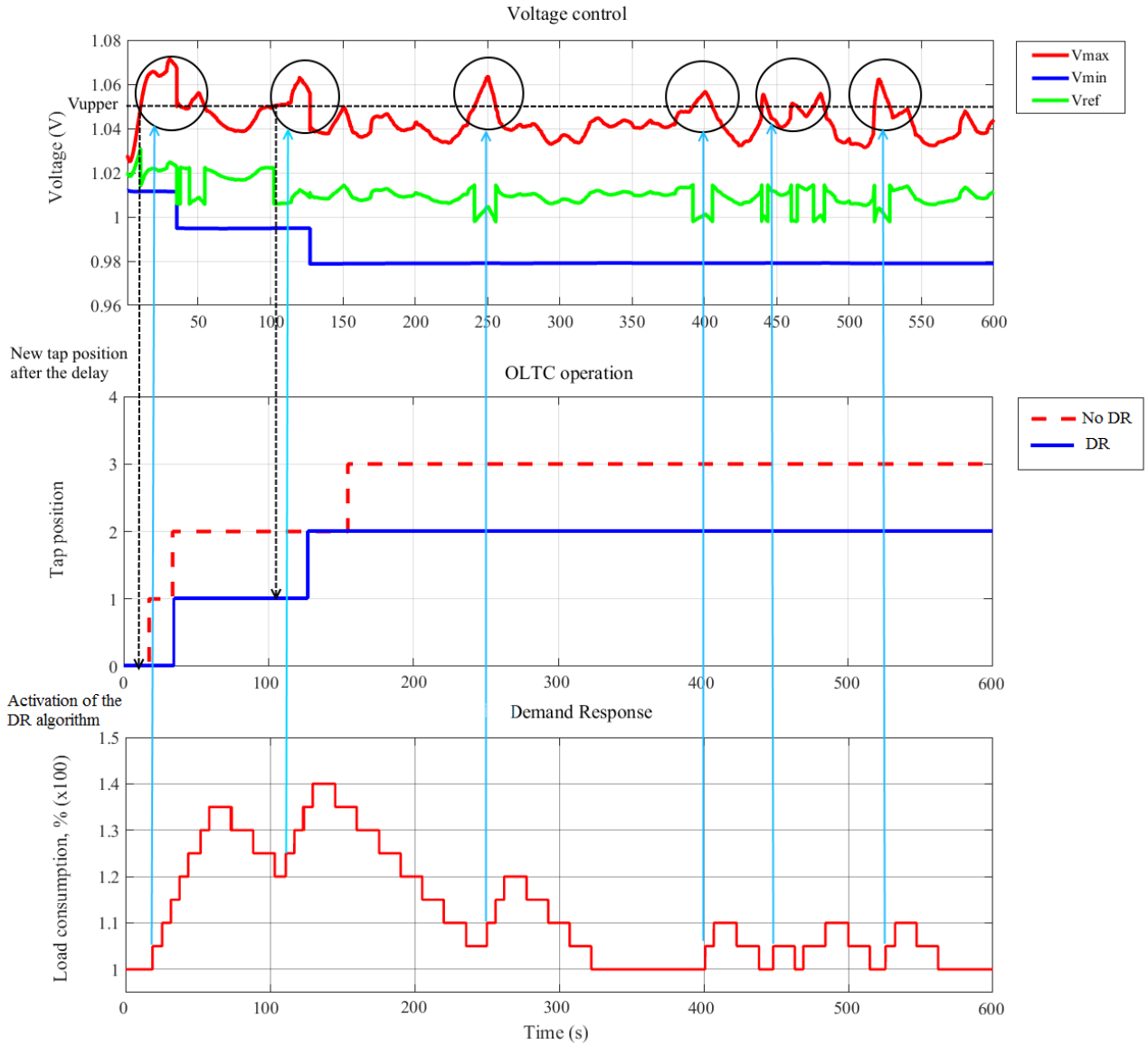

Figure 7.28. The operation of combined AVC and DR control.

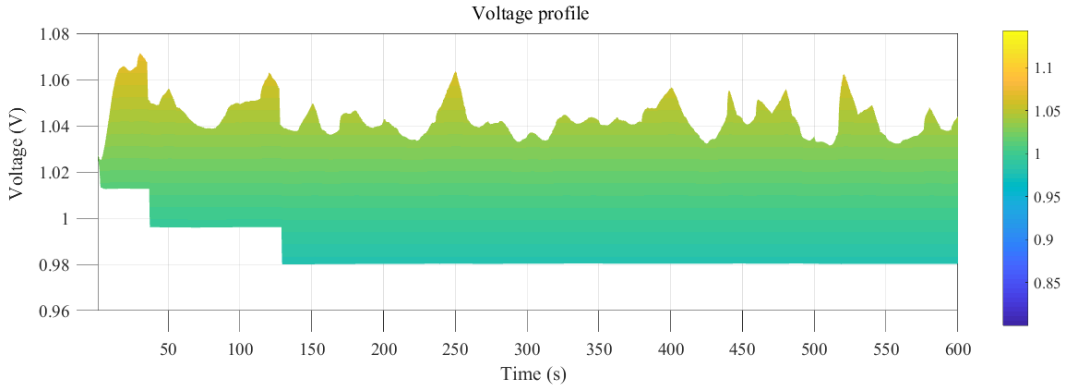

Figure 7.29. 2D profile of the feeder with combined real-time AVC and DR control.

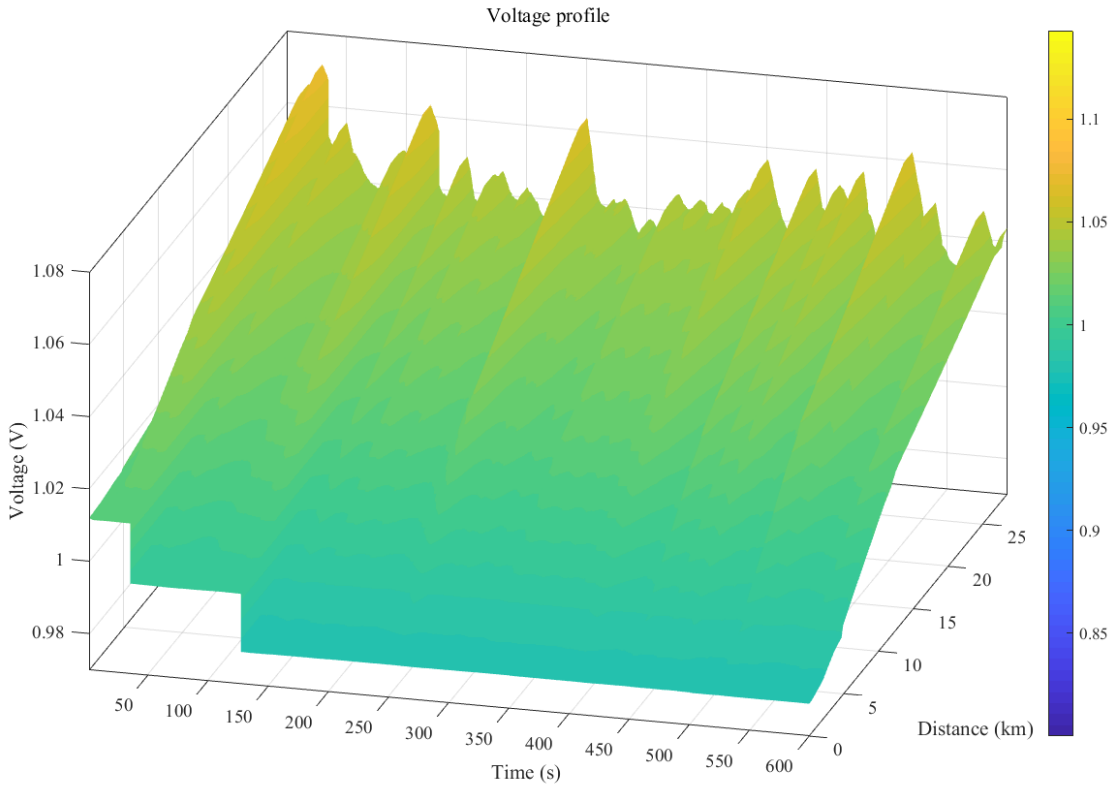

Figure 7.30. 3D profile of the feeder with combined real-time AVC and DR control.

Case 2: Combined RPC control and the real-time AVC algorithm

The effect of the reactive power control turned out to be less efficient than the contribution from DR control actions. As it can be seen from Figure 7.31, it could not decrease the number of tap changing operations comparing to stand alone AVC performance.

In this case, the most crucial moment happened during the period from 25 s to 50 s when RPC did not manage to decrease the voltage enough to prevent tap changing operation, as it has been done by DR control. Comparing this period with the same in DR control, the diversity in the voltage control capacity between RPC and DR became obvious. DR managed to decrease the voltage up to the tolerance range, while during the RPC it was close to the 1.064 per units.

The 2D and 3D voltage profiles of the feeder in such simulation conditions are depicted in Figure 7.32 and 7.33.

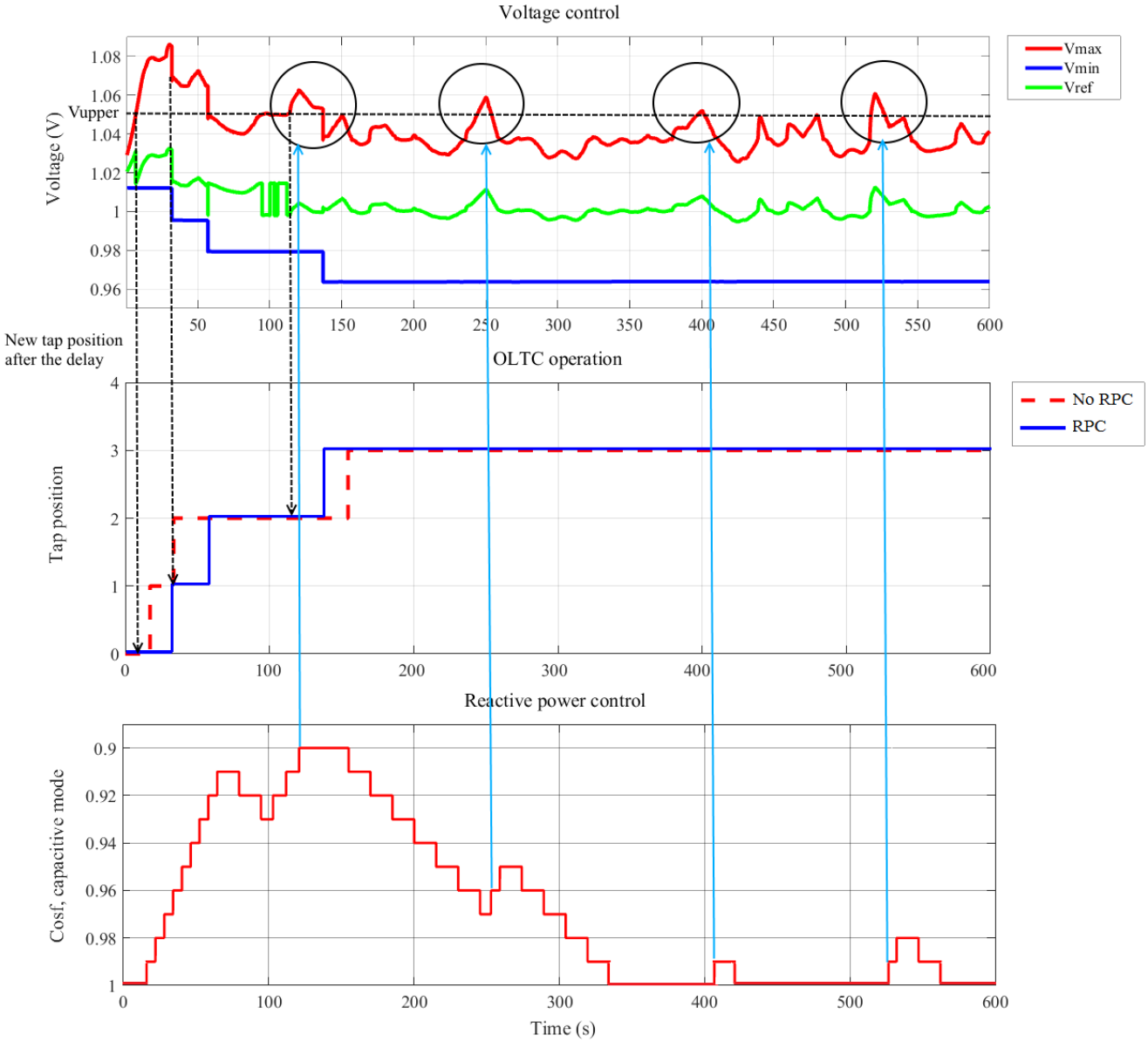

Figure 7.31. Combined RPC and real-time AVC control.

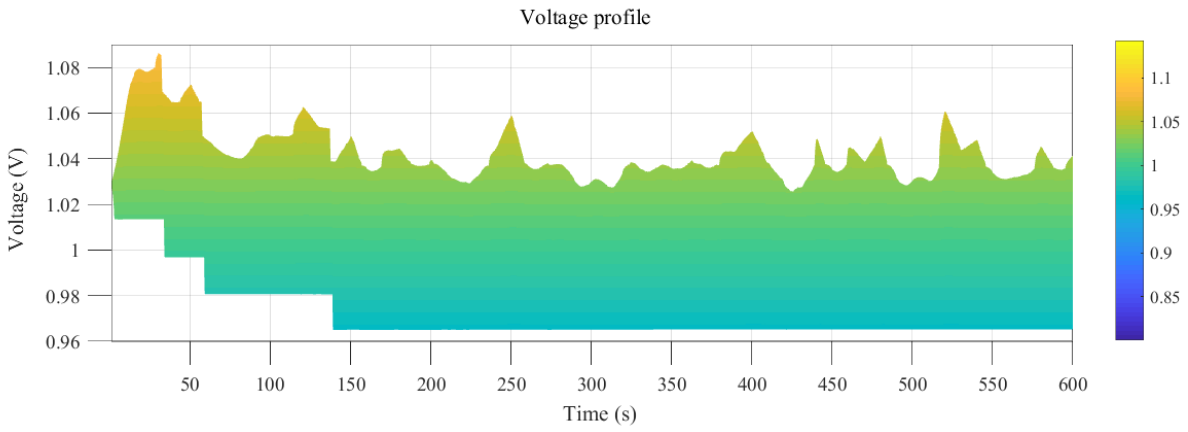

Figure 7.32. 2D profile of the feeder with combined real-time AVC and RPC control.

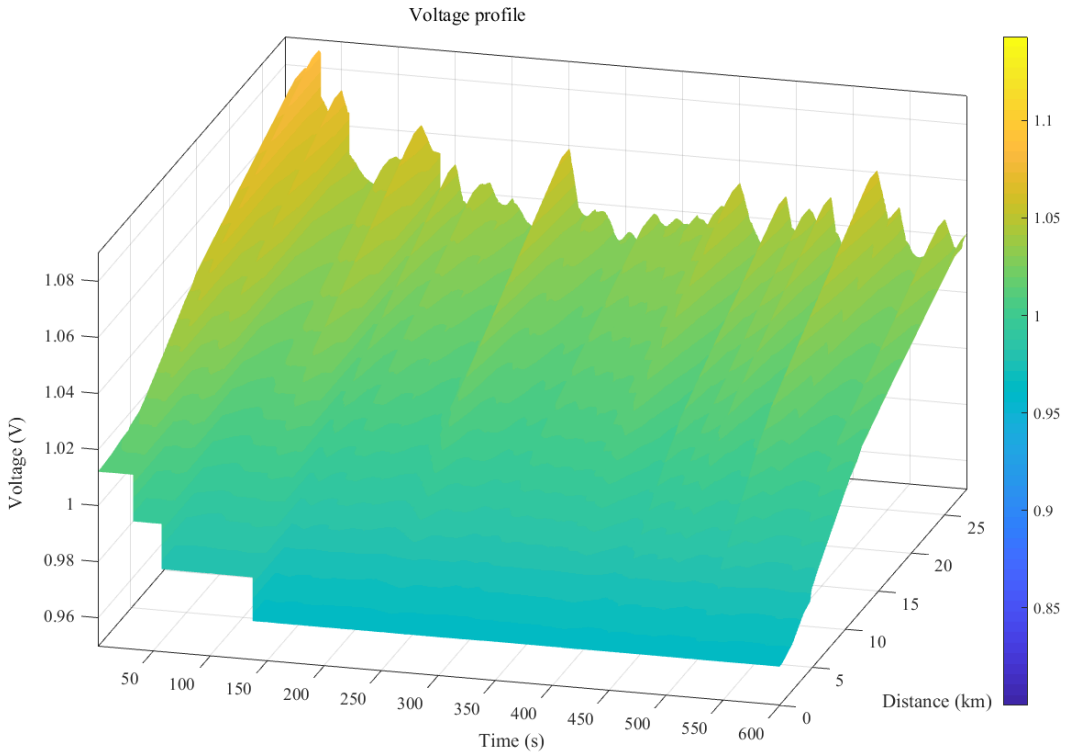

Figure 7.33. 3D profile of the feeder with combined real-time AVC and RPC control.

7.3.3 Conclusions on simulation results

The cooperation of DR and real-time AVC algorithms decreased the overvoltage time, but it led to a number of unwillingly voltage peaks. Although these spikes are not dangerous, considering that the limit voltage level was decreased more than it is necessary by requirements. However, they could be erased if activating the DR algorithm by dynamic changing of voltage with such volume of the load that corresponds to the speed of voltage rise. The cooperation of RPC of household PV systems algorithm and real-time AVC algorithm could be improved if introduce additional sources of reactive power in the control algorithm. Nevertheless, it still could be used to reduce the time of overvoltage or undervoltage periods in case of the small oscillations.

7.4 Conclusions about chapter 7

The reliability of the DR algorithm was tested, and its possibilities for voltage control are estimated. The obtained results testified that the 20-30 % of the current load should be available for proper voltage control by DR algorithm.

Two variations of designed AVC algorithm were researched in maximum generation/minimum load conditions. The algorithm can be used both together with the model

located in the DMS and independently utilizing only the real-time data. Both of the algorithms proved its reliability and capabilities to work in the networks with the RDG.

The combined operation of the real-time AVC with the supportive method in the face of DR was investigated. The cooperation of AVC and DR algorithms demonstrated its effectiveness, decreasing the number of tap changing operations comparing to stand-alone AVC algorithm operation in the same applied conditions.

The cooperation of RPC of household PV systems and AVC algorithms was examined. The effectiveness of the RPC algorithm did not allow reducing the number of tap changing operations because the available reactive power of PV systems was not enough to change the voltage significantly

For further development, AVC algorithm should be adopted to increased quantity of RDG units in the network and more developed structure of the network with more feeders connected to the substation. Then, it is needed to create a prototype unit for verification its operation at the real equipment.

For further approbation, DR and RPC algorithms could be implemented with the application of intelligent methods, and their operation could be investigated on real equipment connected to the created model.

8 SUMMARY AND CONCLUSIONS

In this thesis the impacts of DG on the voltage profile in a distribution network has been investigated under several possible scenarios. It is shown that the presence of DG complicates the operation of the distribution network by introducing new conditions: network elements start to operate in conditions of multidirectional supply; short-circuit currents alter its level and distribution; the appearance of power system swinging, asynchronous operation, and loss of main becomes possible. These conditions demand more comprehensive functionality for the DNOs to control energy generation and power flow. If they are accomplished, then the DG can contribute to the stability of centralized systems, participating in its integrated control as a supportive and main source of power.

An analysis of voltage quality in networks with DG was conducted. The existing voltage control equipment was designed to operate based on unidirectional power flow. However, these conditions should be revised with the appearance of DG. Voltage rise and rapid voltage fluctuations become the main problem because of the intermittent power injections of RDG. A literature review of voltage methods, which can be categorized in centralized and decentralized approaches, was carried out. The methods are based on variations of traditional means and employment of DG units as controlling elements for the voltage control.

A simulation model of the power grid with RDG in face of WTs and household PV systems was designed and implemented in the MATLAB® environment. The barriers to the implementation of the model such as the latency in communications, stochastic behavior of the load, time-domain implementation, and particularization of the model were solved. The results of the model's response confirm that the model operation can be considered close to the operation of the real power grid with RDG. The model is exploited for multiple simulations on dispersed voltage control.

The investigation of DR algorithm for voltage control was conducted by applying different conditions for simulation. Demand response algorithm allowed evaluating the approximate amount of load needed for proper voltage control, which according to the simulations should be about 20-30% of the current demand in the studied network. The obtained results indicated, that with the development of active resources as EESs and EVs, the amount of flexible load could be enough to utilize DR as one of the main tools for voltage control and to

contribute to more widespread penetration of DG. However, at the moment it could serve as a good supportive method.

The modernization of automatic voltage control algorithm was also examined, where the performance of model-based and real-time AVC control was compared in the conditions of stochastic operation of RDG. The algorithms proved its reliability and could be used both separately and together. They have its advantages as well as disadvantages. In the case of model-based AVC control, the main advantages are the more precise information about the state of the whole network as well as for the real-time control – the ease of the implementation and minimum of additional equipment's installation. The main problem for the AVC method is a possible large quantity of tap changer's operations that create short disturbances in the network and need more maintenance for tap changers. Also, the disadvantage of AVC is that the mechanism of OLTC is slow for rapid voltage fluctuations caused by RDG units. However, this could be solved by adding the assistance of supportive methods based on reactive or active power control to the AVC control.

The last assumption was validated by the combined control of real-time AVC algorithm with both DR and RPC algorithms. The operation of the DR control allowed decreasing the number of tap changing operations in comparison to stand–alone AVC control in the same conditions. Thus, it can contribute to the more safe exploitation of the OLTC's mechanism but with possible enlargement in the number of short voltage spikes that is not the best condition for the appliance of end users. This could be mitigated if the DR starts running controlling the speed of voltage rise rather than the voltage level. The effect of the RPC of the household PV systems was less efficient. The number of tap changing operations was the same because the reactive power of PV systems was not enough to control the voltage efficiently. The situation can be improved, adding large DG units with high output power to the RPC algorithm.

According to the obtained results, further ways of improvements and realization of developed algorithms are proposed. It is offered to enhance the AVC algorithm by its adaptation to a larger quantity of RDG units and more developed structure of the network. Then, a prototype unit of AVC algorithm's realization should be created to test this algorithm on a real equipment.

The algorithms of DR and RPC can be advanced by applying intelligent methods for their realization that could be then investigated on real equipment of end users (EVs, PV systems, EESs) connected to the created model. The utilization of intelligent algorithms can increase the efficiency of voltage control with the use of sensitivity analysis by affecting the specific amount of loads and/or PV systems that have the biggest effect on the appeared voltage rise.

The implemented work is dedicated only to a part of the problems appeared with the increased penetration of DG. The injection of such sources in the existing energy network in larger volume will lead to enlargement of power flow fluctuations in the distribution network and increasing problems in voltage control. It is necessary to mention that the appearance of such elements as RDG units, active consumers, EVs, and EESs presents enormous capabilities to the network operators for more efficient, flexible, and reliable power supply. The strategy of coordination of distributed sources through smart grids that are combining the two-way flow of electricity with the two-way flow of information is applied in the virtual power plants. In conditions of more precise information about distribution network's status and more developed communication infrastructure, the dispersed voltage control algorithms are gaining the advantage because they can consider the large volume of operational conditions of various distributed sources. However, the application of such technologies in real networks is still in developing phase and leaves opportunities for its analysis and investigation.

9 REFERENCES

[1] Owens, B. 2014. The Rise of Distributed Power, General Electric Company, [online document]. [Accessed 5 March 2017]. Available at http://www.ge.com/sites/default/files/2014%2002%20Rise%20of%20Distributed%20Power.pdf

[2] Lazard Company. 2016. Levelized cost of energy analysis, version 10.0, [online document]. [Accessed 11 May 2017]. Available at https://www.lazard.com/media/438038/levelized-cost-of-energy-v100.pdf

[3] Randall, T. 2015. Fossil Fuels Just Lost the Race Against Renewables: this is the beginning of the end, [webpage]. [Accessed 11 May 2017]. Available at https://www.bloomberg.com/news/articles/2015-04-14/fossil-fuels-just-lost-the-race-against-renewables

[4] Viawan, F. A. 2008. Voltage Control and Voltage Stability of Power Distribution Systems in the Presence of Distributed Generation, PhD dissertation, Chalmers University of technology, Department of Energy and Environment.

[5] Onisova, O.A. 2016. The enhancing of the power grids protection with the presence of small distributed power plants. PhD dissertation, Chuvashskiy state university, Department of power systems.

[6] Massa, G., Gross, G., Galdi, V., Piccolo A. 2016. Dispersed voltage control in Microgrids. *IEEE Transactions on Power Systems*, vol. 31, No. 5, september

[7] Ali, H., Dasgupta, D. 2012. Effects of Time Delays in the Electric Power Grid. In: Butts J., Shenoi S. (eds) Critical Infrastructure Protection VI. ICCIP 2012. IFIP Advances in Information and Communication Technology, vol 390. Springer, Berlin, Heidelberg, [online document]. [Accessed 11 May 2017]. Available at http://dl.ifip.org/db/conf/ifip11-10/iccip2012/AliD12.pdf

[8] Kulmana, A.,Repo, S., Jarventausta, P. 2012. Active voltage control – from theory to practice. CIRED Workshop – Lisbon, 29-30 May 2012, Paper 215, [online document]. [Accessed 2 June 2017]. Available at http://www.cired.net/publications/workshop2012/pdfs/CIREDWS2012_0215_final.pdf

[9] Bayod Rújula, A.A., Mur Amada, J., Bernal-Agustín, J.L., Yusta Loyo, J.M., Domínguez Navarro, J.A. 2005. Definitions for Distributed Generation: a revision.

Department of Electrical Engineering Centro Politécnico Superior, University of Zaragoza, *RE&PQJ*, vol. 1, No.3, March

[10] Purchala, K., Belmans, R., Exarchakos, L., Hawkes, A.D. Distributed generation and the grid integration issues, [online document]. [Accessed 2 June 2017]. Available at https://www.eusustel.be/public/documents_publ/WP/WP3/WP%203.4.1%20Distributed%20generation%20and%20grid%20integration%20issues.pdf

[11] Jadhava, S., Harchandania, R. 2015. Grid Interfacing Technologies for Distributed Generation and Power Quality Issues - A Review. *International Journal of Innovative and Emerging Research in Engineering*, vol. 2, Issue 3

[12] Microgrid. Wikipedia. [webpage]. [Accessed 11 May 2017], Available at https://en.wikipedia.org/wiki/Microgrid

[13] Stennikov, V.A., Voropai, N.I. 2015. The centralized and distributed generation is not an alternative but integration. [online document]. [Accessed 11 May 2017], Available at http://energystrategy.ru/projects/Energy_21/4-2.pdf

[14] Cummings, M. 2016. Distributed generation – what are the benefits. Energy Alabama, [webpage]. [Accessed 11 May 2017]. Available at https://alcse.org/distributed-generation-benefits/

[15] Idelchik, V.I. 1989. Electrical power systems. Moscow: Energoatomisdat.

[16] Sikorski, T., & Rezmer, J. 2015. Distributed Generation and Its Impact on Power Quality in Low-Voltage Distribution Networks, Power Quality Issues in Distributed Generation, Dr. Jaroslaw Luszcz (Ed.), InTech, DOI: 10.5772/61172. [Accessed 11 May 2017]. Available at https://www.intechopen.com/books/power-quality-issues-in-distributed-generation/distributed-generation-and-its-impact-on-power-quality-in-low-voltage-distribution-networks

[17] Thong, V.V., Driesen, J., Belmans, R. 2007. Using DG for ancillary service and secure operation of power systems. 19th International Conference on Electricity Distribution. Paper 0308. Vienna, 21-24 May 2007. [online document] [Accessed 11 May 2017]. Available at http://www.cired.net/publications/cired2007/pdfs/CIRED2007_0308_paper.pdf

[18] Belyaev, A.V. 2014. Some features of relay protection and automation of small-scaled energy sources. *Releishik*. – № 4(20), p. 40-47.

[19] Ashley-Edison. Mains Voltage Supply Problems - Symptoms, Causes & Solutions. [webpage].[Accessed 9 March 2017]. Available at https://www.ashleyedison.com/voltage- problems-805/

[20] Sonel. 2015. Influence of voltage deviation, [webpage]. [Accessed 5 March 2017]. Available at http://www.sonel.ru/ru/biblio/article/quality-voltage/influence-deviation-voltage/printable.php

[21] Lakervi, E., Holmes, E. J. 1995. Electricity Distribution Network Design, 2nd ed. London, UK: The Institution of Electrical Engineers, 1995, 325 p.

[22] Pacific gas and electric company. Power quality in your home. How to ensure the life and reliable operation of your home electronics. [online document]. [Accessed 5 March 2017]. Available at https://www.pge.com/includes/docs/pdfs/about/news/outagestatus/powerquality/pq_home.pdf

[23] State Farm. Are Power Surges Damaging Your Electronics?, [webpage]. [Accessed 5 March 2017]. Available at https://www.statefarm.com/simple-insights/residence/are-power-surges-damaging-your-electronics

[24] Effects of voltage fluctuations on electrical equipment. 2011, [webpage]. [Accessed 5 March 2017]. Available at http://www.powerqualityworld.com/2011/09/effects-voltage-fluctuations.html

[25] 2007. *Voltage characteristics of electrity supplied by public distribution networks*, European Standard EN 50160:2007.

[26] Melhem, Z. (ed.) 2013. Electricity transmission, distribution and storage systems. Oxford: Woodhead Publishing Series in Energy 38.

[27] Masters, C.L. 2005. Voltage rise, the big issue when connecting embedded generation to long 11 kV overhead lines. *IEEE Power Engineering Journal* 16(1): 5–12.

[28] Kulmala, A. 2014. Active Voltage Control in Distribution Networks Including Distributed Energy Resources, PhD dissertation, Tampere University of Technology.

[29] 2011. AMR measurement data of Finnish customers. One week load profile of detached houses with direct electrical heating. SLY-load profiles 2011.05.02.

[30] 2017. Smart Grid course BL20A1600. Lappeenranta University of Technology.

[31] Xiangdong, Z., Gray, P.A., and Lehn., P.W. 2016. New Metric Recommended for IEEE Standard 1547 to Limit Harmonics Injected Into Distorted Grids. *IEEE Transactions on Power Delivery*, vol. 31, No. 3, june 2016

[32] Jenkins, N.,Ekanayake, J.B. and Strbac, G. 2010. Distributed Generation. The Institution of Engineering and Technology IET Renewable energy series.

[33] Khan, U. N. Distributed Generation and Power Quality. IEEE Power Engineering Society [online document]. [Accessed 5 March 2017]. Available at

http://eeeic.org/proc/papers/38.pdf

[34] Golovanov, N., Lazaroiu, G. C., Roscia, M. and Zaninelli, D. 2013. Power Quality Assessment in Small Scale Renewable Energy Sources Supplying Distribution Systems. *Energies* 2013, *6*, 634-645; doi:10.3390/en6020634

[35] Ramos, S. C. 2014. Optimization of the operation of a Distribution Network with Distributed Generation using Genetic Algorithm, Master's thesis, Polytechnic University of Catalonia.

[36] Bignucolo, F.,Caldon, R., Prandoni, V. 2008. Radial MV networks voltage regulation with distribution management system coordinated controller. Article in Electric Power Systems Research

[37] The power grids course. Lectured by Prof. Shvedov G.V. 2014. Moscow Power Engineering Institute.

[38] Bernáth, F., Mastný, P. 2014. Distributed Generation and Voltage Control in Distribution Network, Reactive power control of power sources. Proceedings of the 2014 15th International Scientific Conference on Electric Power Engineering (EPE), 12-14 May, Prague, Czech Republic.

[39] Pilo, F., Pisano, G., and Soma, G. G. 2009. Advanced DMS to manage active distribution networks, *IEEE Bucharest PowerTech*, pp. 1-8.

[40] Kupzog, F., Brunner, H., Pruggler, W., Pfajfar, T., and Lugmaier, A. 2007. DG DemoNet - Concept - A new Algorithm for active Distribution Grid Operation facilitating high DG penetration. *5th IEEE International Conference on Industrial Informatics,* 23-27 June, Vienna, Austria, *vol.* 2, pp.1197-1202.

[41] Zhou, Q., Bialek, J. W. 2007. Generation curtailment to manage voltage constraints in distribution networks. *IET Generation, Transmission & Distribution,* vol. 1 (3), pp. 492-498.

[42] Dothinka, R., Ashish, P. A. 2016. Online Coordinated Voltage Control in Distribution Systems Subjected to Structural Changes and DG Availability. *IEEE Transactions on Smart Grid*, vol. 7, No. 2, pp.580-591.

[43] Senjyu, T., Miyazato, Y., Yona, A., Urasaki, N., and Funabashi, T. 2008. Optimal Distribution Voltage Control and Coordination With Distributed Generation. *IEEE Transaction on Power Delivery,* vol. 23, No.2, pp.1236-1242.

[44] Thornley, V., Hill, J., Lang, P., and Reid, D. 2008. Active network management of voltage leading to increased generation and improved network utilization. *IET-CIRED Seminar on SmartGrids for Distribution*, 23-24 June, pp. 1-4.

[45] El Moursi, M. S., Bak-Jensen, B., and Abdel-Rahman, M. H. 2011. Coordinated Voltage Control Scheme for SEIG-Based Wind Park Utilizing Substation STATCOM and ULTC Transformer. *IEEE Trans on Sustainable Energy,* vol. 2, No.3, pp. 246-255.

[46] Nguyen, P. H., Myrzik, J. M. A., and Kling, W. L. 2008. Coordination of voltage regulation in Active Networks. *IEEE/PES Transaction and Dist Conference and Exposition*, pp. 1-6.

[47] Multi-agent system. Wikipedia. [web-page]. [Accessed 11 May 2017]. Available at https://en.wikipedia.org/wiki/Multi-agent_system

[48] Ausavanop, O., Chaitusaney, S. 2011. Coordination of dispatchable distributed generation and voltage control devices for improving voltage profile by Tabu Search. 8th 76. International Conference on Electrical Engineering/ Electronics,Computer, Telecommunications and Information Technology (ECTI-CON), 17-19 May, Khon Kaen, Thailand, pp. 869-872.

[49] Morin, J., Colas, F., Grenard, S., Dieulot, J-Y., Guillaud, X. 2016. Coordinated predictive control in active distribution networks with HV/MV reactive power constraint. PES Innovative Smart Grid Technologies Conference Europe (ISGT-Europe), 9-12 October, pp. 1-6.

[50] Elnashar, M., Kazerani, M., El Shatshat, R., and Salama, M. M. A. 2008. Comparative evaluation of reactive power compensation methods for a stand-alone wind energy conversion system. IEEE Power Electronics Specialists Conference, 15-19 June, Rhodes, Greece, pp. 4539- 4544.

[51] Öztürk, A., Kenan, D. Investigation of the Control Voltage and Reactive Power in Wind Farm Load Bus by STATCOM and SVC, International Conference on Electrical and Electronics Engineering - ELECO 2009, 5-8 November, pp. I-61- I64.

[52] Sansawatt, T., O'Donnell, J. B., Ochoa, L. F. and Harrison, G. P. 2009. Decentralised Voltage Control for Active Distribution Networks, Proc. 44th International Universities' Power Engineering Conference (UPEC), 1-4 September, pp. 1- 5.

[53] Sansawatt, T., Ochoa, L.F., Harrison G.P. 2010. Decentralised Voltage and Thermal Management to enable more Distributed Generation Connection. CIRED Workshop, 7-8 June, Lyon, France, pp. 1-4.

[54] Hiscock, J., Hiscock, N., Kennedy, A., 2007. Advanced Voltage Control for Networks with Distributed Generation. 19th International Conference on Electricity Distribution, 21-24 May, Vienna, Austria, pp. 1-4.

[55] Dela Torre, L.J.C., Pedrasa, M.A. 2016. Decentralized voltage control for distribution networks with high penetration of distributed generators. Innovative Smart Grid Technologies - Asia (ISGT-Asia), 28 November -1 December, pp. 636-641.

[56] Golden, R., Paulos, B. Curtailment of Renewable Energy in California and Beyond. Crossmark. [online document]. [Accessed 11 May 2017]. Available at http://www.powermarkets.org/uploads/4/7/9/3/47931529/calif_curtailment_as_published.pdf

[57] Sansawatt, T., Ochoa, L.F., Harrison, G.P. 2010. Integrating Distributed Generation Using Decentralised Voltage Regulation. IEEE PES General Meeting, 25-29 July, Minneapolis, USA, pp. 1-6.

[58] Zillmann, M., Yan, R., Saha, T. K. 2011. Regulation of Distribution Network Voltage Using Dispersed Battery Storage Systems: A Case Study of a Rural Network. IEEE Power and Energy Society General Meeting, 24-29 July, San-Diego, USA, pp. 1-8.

[59] Farag, H. E. Z., El-Saadany, E. F., Seethapathy, R. 2012. A Two Ways Communication- Based Distributed Control for Voltage Regulation in Smart Distribution Feeders. *IEEE Trans. Smart Grid,* vol. 3, pp. 271-281.

[60] Ugranli, F., Ersavas, C., Karatepe, E. 2011. Neural network based distributed generation allocation for minimizing voltage fluctuation due to uncertainty of the output power. International Symposium on Innovations in Intelligent Systems and Applications (INISTA), 15- 18 June, pp. 415-419.

[61] Ling, L., Xiangjun, Z., Ping, Z., Yunfeng, X., Guopin, L. 2008. Optimization of Reactive Power Compensation in Wind Farms Using Sensitivity Analysis and Tabu Algorithm. IEEE Industry Applications Society Annual Meeting, 5-9 October, pp. 1-5.

[62] Antoniadou–Plytaria, K. E., Kouveliotis–Lysikatos, L. N., Georgilakis, P. S., and Hatziargyriou, N. D. Distributed and Decentralized Voltage Control of Smart Distribution Networks: Models, Methods, and Future Research. DOI 10.1109/TSG.2017.2679238, *IEEE Transactions on Smart Grid*

[63] Saric, A.T., Rankovic, A. 2012. Load reallocation based algorithm for state estimation in distribution networks with distributed generators. *Electric power sysytems research* vol. 84, Issue 1, March 2012, pp. 72–82.

[64] Roytelman, I., Wee, B.K., Lugtu, R.L. 1995. Volt/V AR control algorithm for modern distribution management system, *IEEE Transactions on Power Systems*, vol. 10, No 3, pp. 1454 – 1459.

[65] Demand response. [web-page]. [Accessed 11 May 2017]. Available at https://energy.gov/oe/services/technology-development/smart-grid/demand-response

[66] Hreinsson, K., Scaglione, A., Vittal, V. 2016. Aggregate load models for demand response: Exploring flexibility. Signal and Information Processing (GlobalSIP), 2016 IEEE Global Conference on Signal and Information Processing (GlobalSIP), 7-9 Dec. 2016, Washington, DC, USA

[67] He, Y., Petit, M. 2016. Valorization of Demand Response for Voltage Control in MV Distribution Grids with distributed generation. IEEE International Energy Conference (ENERGYCON 2016) 4-8 April 2016, p 1611

[68] Huseinagic, I. 2015. Modern Distribution Management System and Voltage VAR Control. Southeast Europe Journal of Soft Computing. vol. 4, No.2 September 2015 - ISSN 2233 – 1859.

[69] Vasudevan, K., Atla, C.S.R., and Balaraman, K. Improved state estimation by optimal placement of measurement devices in distribution system with ders, In Power and Advanced Control Engineering (ICP ACE), 2015 International Conference on, pages 253–257, Aug 2015.

[70] Toghroljerdi, H. & Østergaard, S.J. 2016. Methods and Strategies for Overvoltage Prevention in Low Voltage Distribution Systems with PV. *IET Renewable Power Generation*, 11(2), 205 – 214. DOI: 10.1049/ietrpg.2016.0277

[71] Kulmala, A., Repo S. and Järventausta, P. Using statistical distribution network planning for voltage control method selection. in Proc. IET Conf. on Renewable Power Generation, Sept. 2011.

[72] Three-phase PI section line. [web-page]. [Accessed 11 May 2017]. Available at https://se.mathworks.com/help/physmod/sps/powersys/ref/threephasepisectionline.html

[73] Distribution Transformers. ABB Power Technology Products. [online document] [Accessed 11 May 2017]. Available at http://ocw.uniovi.es/pluginfile.php/5422/mod_resource/content/1/Cat%C3%A1logo%20transformadores%20ABB.pdf

[74] Tap Changing Transformer. Your electricial home. 2011. [web-page]. [Accessed 11 May 2017]. Available at http://www.yourelectrichome.com/2011/08/tap-changing-transformer.html

[75] Wind Turbine Doubly-Fed Induction Generator (Phasor Type). [web-page]. [Accessed 11 May 2017]. Available at

https://se.mathworks.com/help/physmod/sps/powersys/ref/windturbinedoublyfedinductiongeneratorphasortype.html#bqs2x4j

[76] Solar PV Residential Grid Tie Energy System – Alternate Energy Company. [web-page]. [Accessed 18 May 2017]. Available at http://alternateenergycompany.com/grid-tie-systems/solar-pv-residential-grid-tie-energy-system/

[77] LUT Solar Total. [web-page]. [Accessed 18 May 2017]. Available at http://www.lut.fi/green-campus/alykas-sahkoverkko-smart-grid/tuotantolukemia

[78] Andrews, R. 2016. Hinkley Point C or solar; which is cheaper? [web-page]. [Accessed 18 May 2017]. Available at http://euanmearns.com/hinkley-point-c-or-solar-which-is-cheaper/

[79] Three-phase dynamic load. [web-page]. [Accessed 18 May 2017]. Available at https://se.mathworks.com/help/physmod/sps/powersys/ref/threephasedynamicload.html

[80] Mutanen, A., Ruska, M., Repo, S., and Järventausta, P. 2010. Customer Classification and Load Profiling. Method for Distribution Systems. [online document]. [Accessed 11 May 2017]. Available at https://webhotel2.tut.fi/units/set/research/inca-public/tiedostot/Kansainvaliset_julkaisut/INCA_clustering_artikkeli_draft.pdf

[81] Three-sigma rule. [web-page]. [Accessed 18 May 2017]. Available at https://en.wikipedia.org/wiki/68%E2%80%9395%E2%80%9399.7_rule

[82] IEEE 1547. 2011. IEEE Standard for interconnecting Distributed Resources with Electrical power systems// Institute of Electrical and Electronics Engineers.

APPENDIX A. LOAD PROFILES

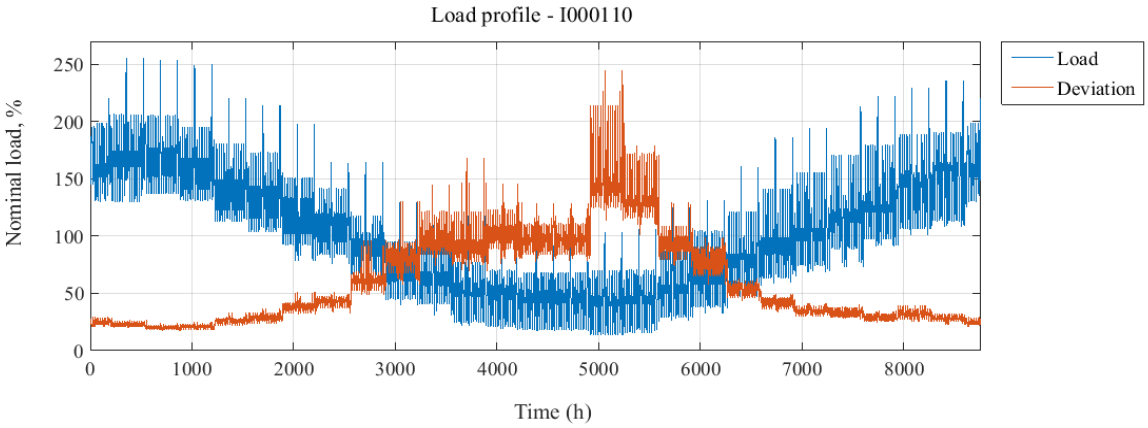

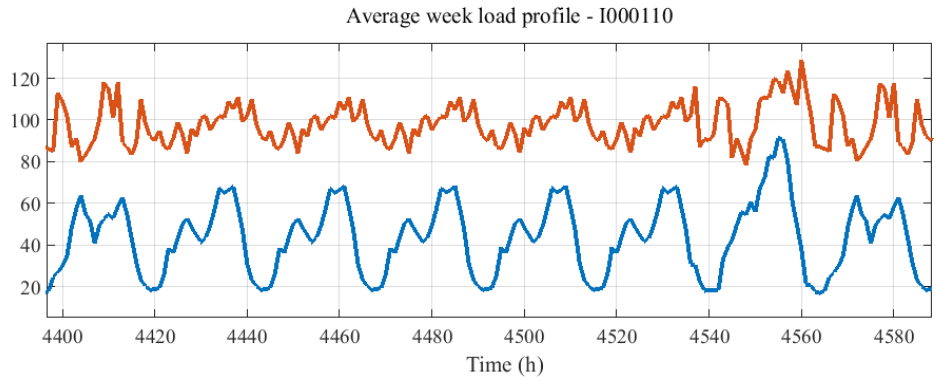

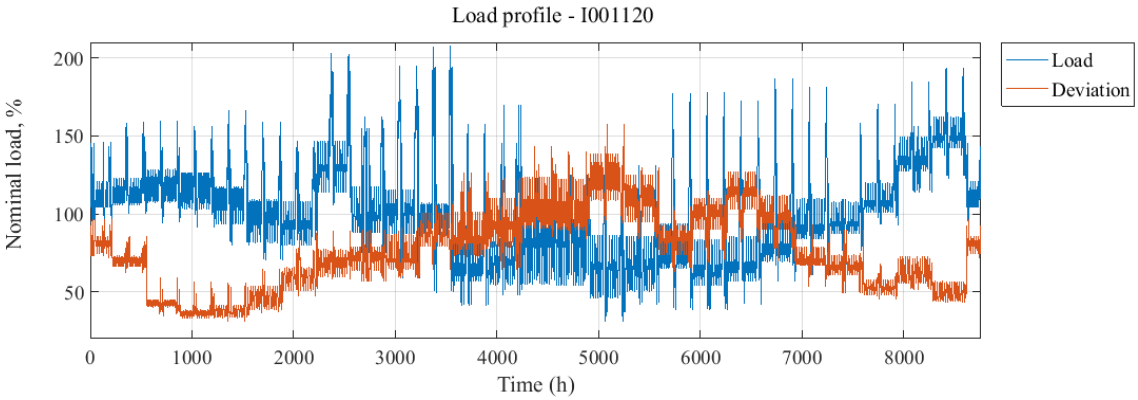

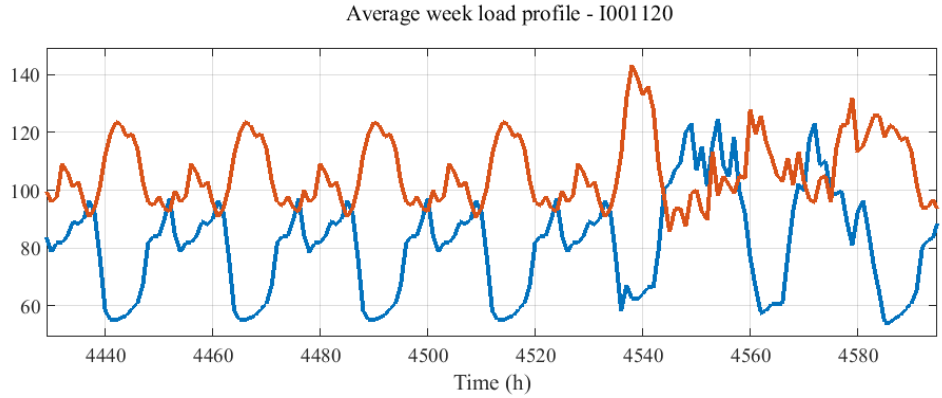

APPENDIX A. LOAD PROFILES (continues)

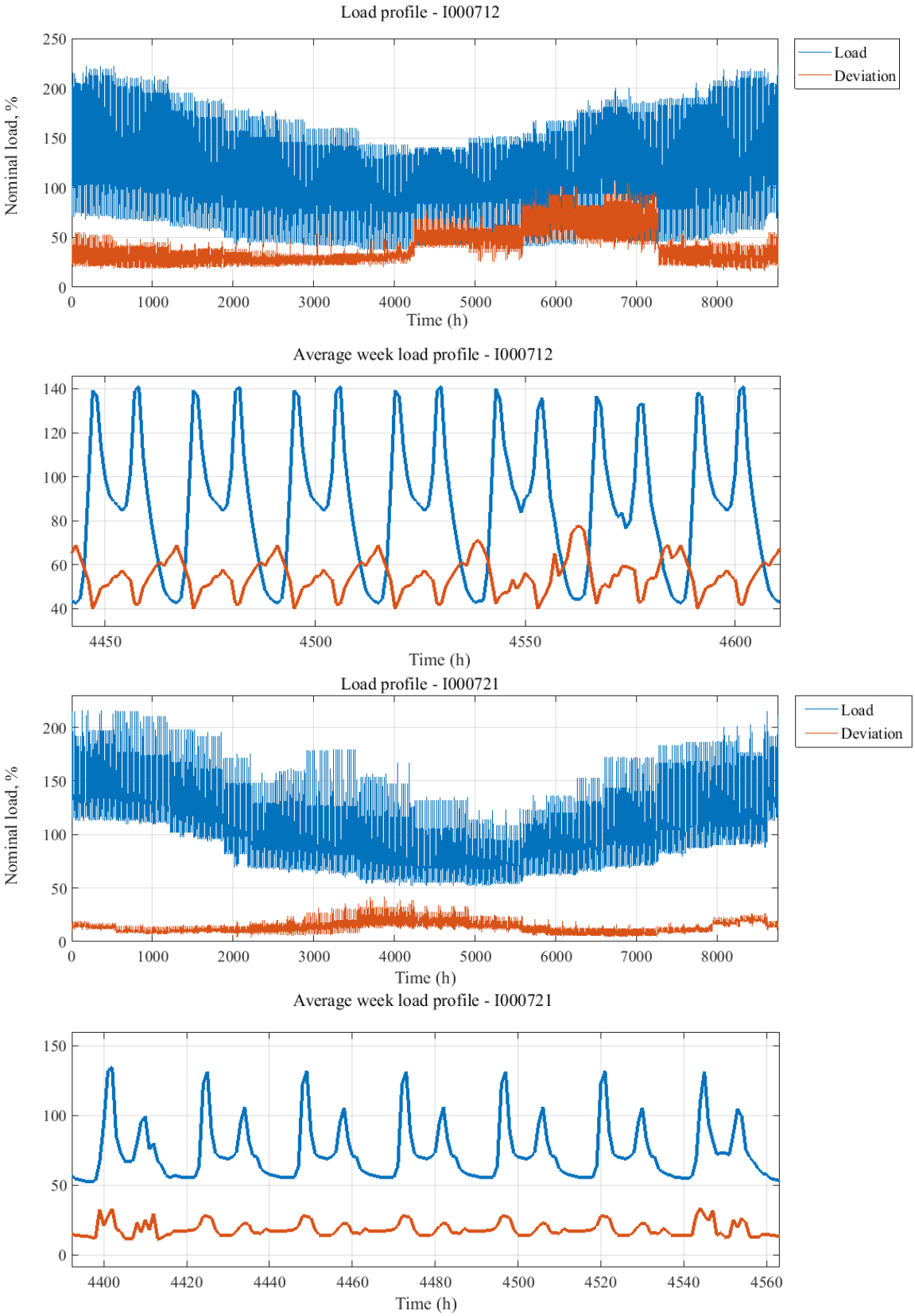

APPENDIX A. LOAD PROFILES (continues)

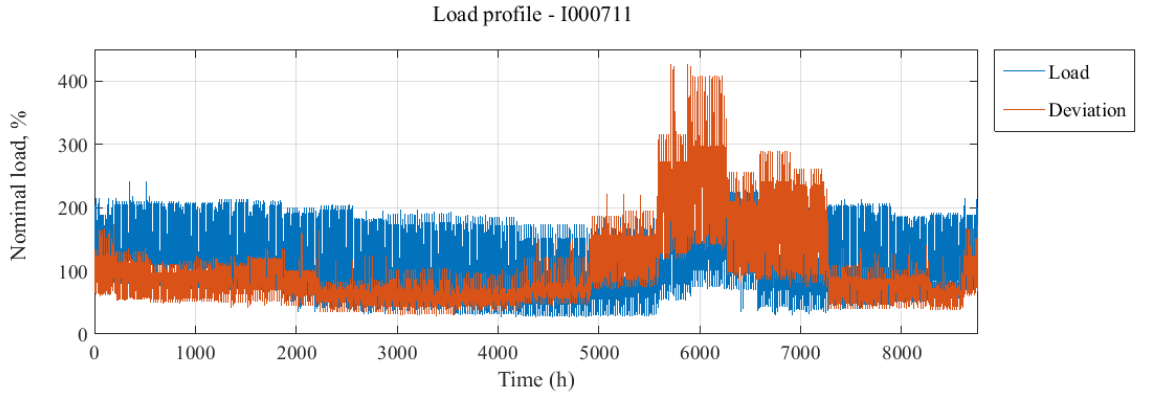

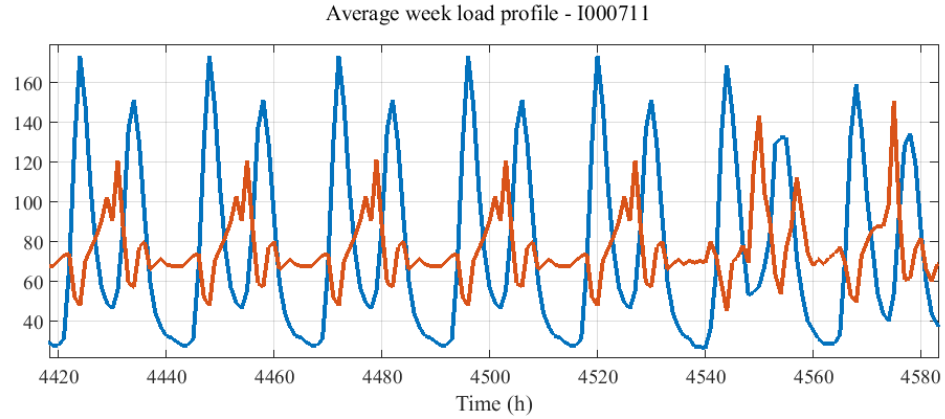

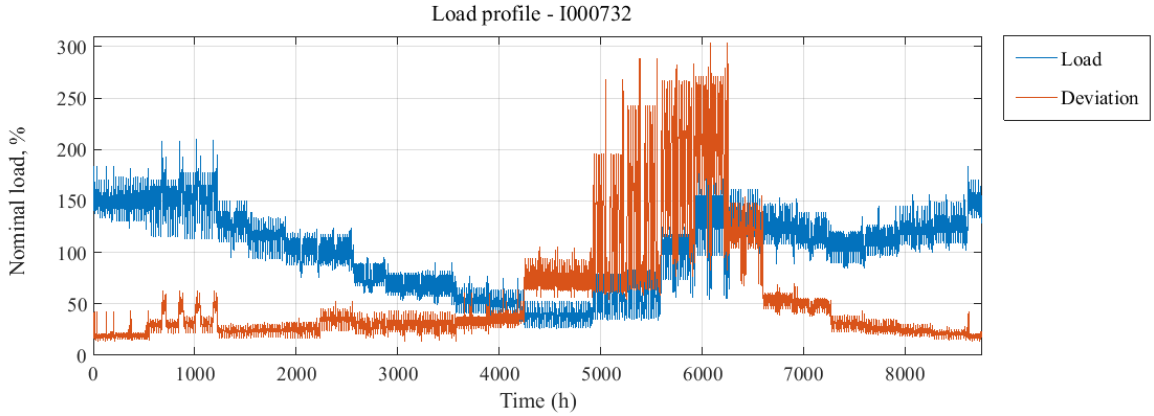

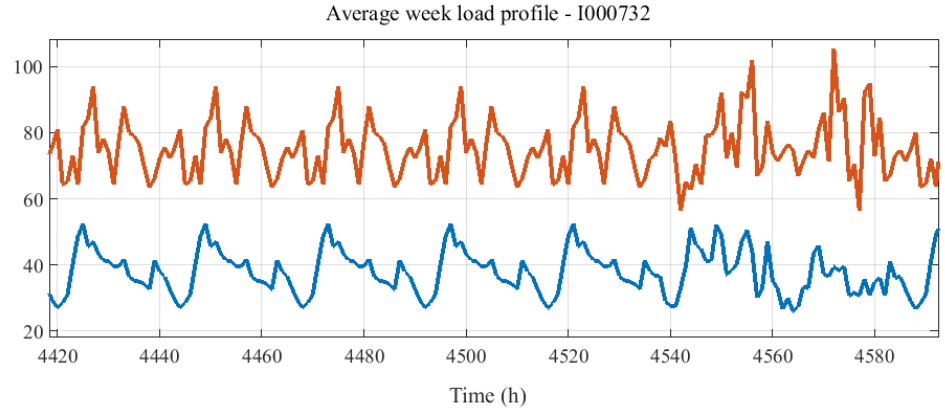

APPENDIX A. LOAD PROFILES (continues)

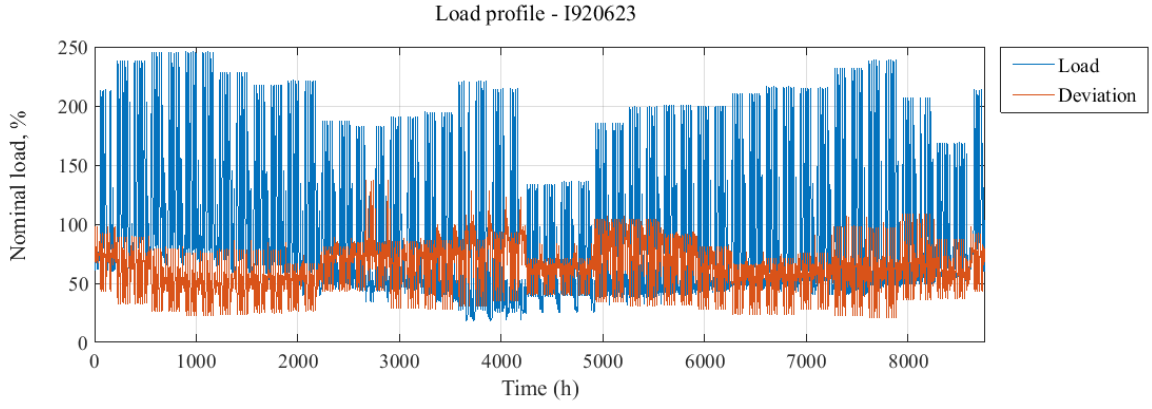

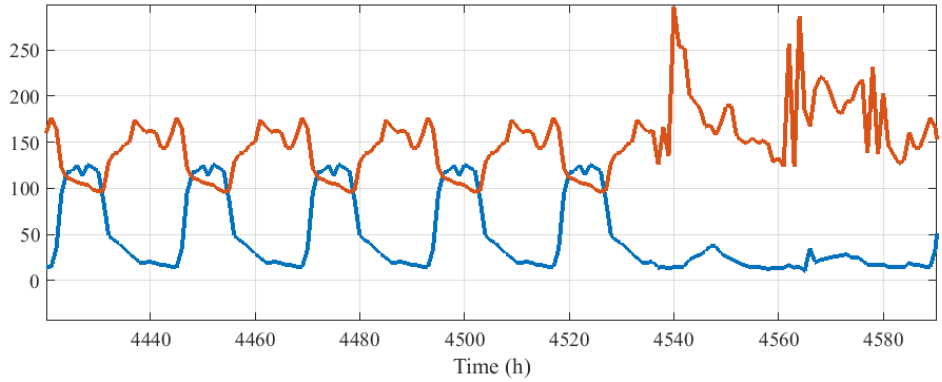

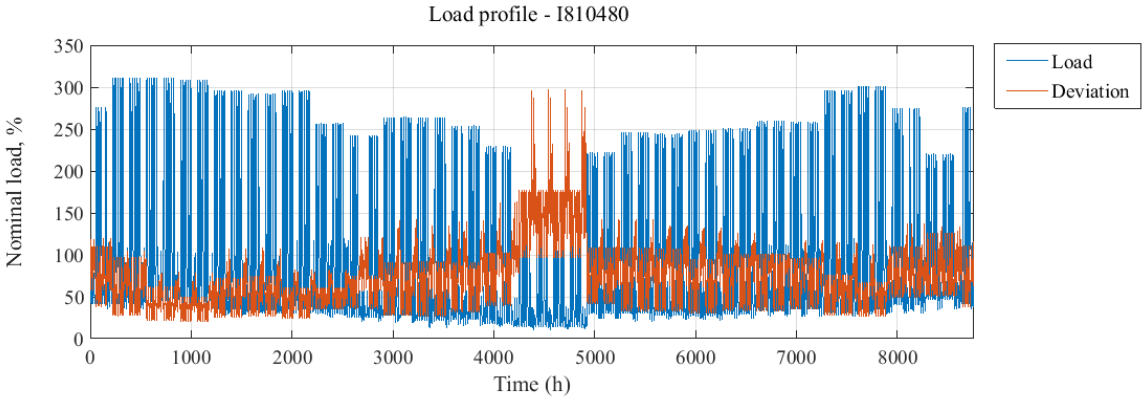

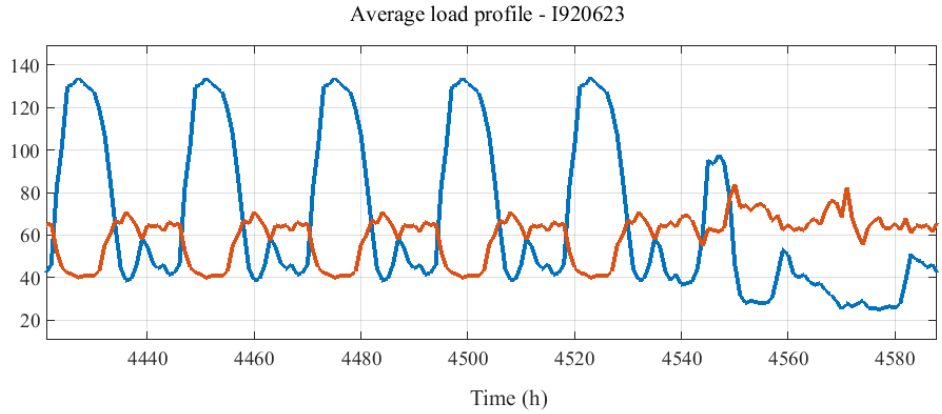

APPENDIX A. LOAD PROFILES (continues)